UNIVERSIDADE FEDERAL DO RIO GRANDE DO SUL
INSTITUTO DE CIÊNCIA E TECNOLOGIA EM ALIMENTOS
PÓS-GRADUAÇÃO EM CIÊNCIA E TECNOLOGIA DE ALIMENTOS

MODELAGEM, SIMULAÇÃO E OTIMIZAÇÃO DE CULTIVOS AUTOTRÓFICOS DE *Pseudoneochloris marina* EM FOTOBIORREATORES *AIRLIFT*

Carolina Ferrer Gonçalves

Porto Alegre,
2019

Carolina Ferrer Gonçalves

MODELAGEM, SIMULAÇÃO E OTIMIZAÇÃO DE CULTIVOS AUTOTRÓFICOS DE *Pseudoneochloris marina* EM FOTOBIORREATORES *AIRLIFT*

Tese apresentada ao Programa de Pós-Graduação em Ciência e Tecnologia de Alimentos como requisito para obtenção do título de Doutora em Ciência e Tecnologia de Alimentos.

Orientadora: Profª. Drª. Rosane Rech

Porto Alegre,
2019

CIP - Catalogação na Publicação

Gonçalves, Carolina Ferrer
MODELAGEM, SIMULAÇÃO E OTIMIZAÇÃO DE CULTIVOS AUTOTRÓFICOS DE *Pseudoneochloris marina* EM FOTOBIORREATORES AIRLIFT / Carolina Ferrer Gonçalves. -- 2019.
113 f.
Orientador: Rosane Rech.

Tese (Doutorado) -- Universidade Federal do Rio Grande do Sul, Instituto de Ciência e Tecnologia de Alimentos, Programa de Pós-Graduação em Ciência e Tecnologia de Alimentos, Porto Alegre, BR-RS, 2019.

1. ácidos graxos . 2. carotenoides. 3. cultivo em batelada. 4. cultivo contínuo. 5. modelagem matemática. I. Rech, Rosane, orient. II. Título.

Elaborada pelo Sistema de Geração Automática de Ficha Catalográfica da UFRGS com os dados fornecidos pelo(a) autor(a).

AGRADECIMENTOS

À Deus pela vida e por todo aprendizado que tenho recebido nesta jornada acadêmica.

À minha família pelo apoio, dedicação, conselhos, suporte, compreensão e carinho durante toda minha vida. Amo vocês.

Aos meus tios, Vera e Edgard, e primos, Igor e Gisele pelo amparo e todo carinho.

Às minhas amigas-irmãs Mauren, Juliana e Maíra por todo amor e amizade sempre.

Aos meus amigos do Laboratório de Bioengenharia, em especial à Tania, Lenon, Mariel e Carla pelo convívio diário, amizade e fundamental contribuição científica para execução desse trabalho.

À minha orientadora Pr.ª Dr.ª Rosane Rech pela orientação, ensinamentos, seriedade, amizade, paciência e incentivos que contribuíram para meu crescimento profissional e pessoal.

Aos iniciantes científicos, em especial a Daniela por toda ajuda no laboratório para realização deste trabalho.

À Universidade Federal do Rio Grande do Sul e professores do PPGCTA, pelos auxílios e ensinamentos recebidos durante esses anos. Aos funcionários, à estrutura física e técnica dos Laboratórios do Instituto de Ciência e Tecnologia de Alimentos pela disponibilidade para concretização deste trabalho.

Ao CNPQ e à CAPES pelo financiamento da pesquisa.

Agradeço a todas as pessoas e amigos que direta ou indiretamente colaboraram para a realização deste trabalho.

RESUMO

As microalgas são micro-organismos fotossintéticos que podem fixar o CO_2 de diferentes fontes e sob condições adequadas de cultivos são capazes de produzir carboidratos, proteínas, lipídeos e compostos de valor agregado como ácidos graxos e carotenoides de interesse para a área de alimentos. Na fase inicial deste trabalho, a partir de análise de rDNA foi feita a identificação filogenética da cepa de microalga verde que apresentou 96 % de similaridade para *Pseudoneochloris marina* quando comparada as sequências depositadas no GenBank. A partir da identificação da microalga foram realizados testes preliminares para ajuste da concentração de nitrogênio ($NaNO_3$) no meio de cultura dos cultivos em processo descontínuo (batelada). A maior concentração de biomassa (2,02 ± 0,21 g L^{-1}) foi obtida com 450 mg L^{-1} de $NaNO_3$. Esta condição foi definida e aplicada nos experimentos subsequentes. Além da concentração de nitrogênio, a influência dos parâmetros externos, temperatura e intensidade luminosa, foram avaliados na produção e composição da biomassa de *P. marina*. A maior produtividade de biomassa (0,26 g L^{-1} d^{-1}) foi obtida nas culturas a 28 ºC e 252 e 364 µmol m^{-2} s^{-1}. Os carboidratos foram os compostos de reserva acumulados em maior concentração pelas células de microalga. O teor de proteínas foi reduzido quando cultivadas em maior temperatura e intensidade luminosa. O aumento da intensidade luminosa afetou negativamente o conteúdo de carotenoides e lipídeos. A partir da identificação e quantificação dos carotenoides e ácidos graxos presentes na biomassa obteve-se como majoritários a luteína e β-caroteno, e C16:0, C18:2n-6 e C18:3n-3, respectivamente. Quando cultivadas a 20 ºC, obteve-se a menor proporção ω6:ω3 (1,6) na produção de ácidos graxos. Nesta etapa mostrou-se o potencial de cultivo da microalga *P. marina* para produção de produtos como carotenoides e ácidos graxos poli-insaturados. Na segunda etapa foi realizada a modelagem matemática para os cultivos de *P. marina* nos processos em batelada, batelada repetida e contínuo. Cinco modelos matemáticos foram analisados para descrever o crescimento celular e consumo de nitrogênio de cultivos em batelada. Os resultados mostraram que o modelo ModNXmax apresentou os maiores coeficientes de correlação para predição das culturas. Ainda foram desenvolvidos modelos matemáticos para descrever a formação dos produtos: carotenoides, proteínas e lipídeos. Os modelos CP2 e CP3 apresentaram melhor predição para carotenoides e proteínas, o modelo Luedeking-Piret apresentou R^2 igual a 0.99 para produção de lipídeos. Na terceira etapa deste trabalho, a partir dos resultados obtidos na modelagem das culturas, foram realizadas simulações de crescimento celular e consumo de nitrogênio para os processos em batelada-

repetida e contínuo. O volume ótimo para renovação de meio nos cultivos em batelada repetida a cada 48 h e a taxa de diluição no processo contínuo foi 1,4 L e 0,46 d^{-1}, respectivamente. A produtividade de biomassa em ambas as culturas superou os valores preditos na simulação resultando em 0,56 ± 0,06 g L^{-1} d^{-1} para culturas em batelada repetida e 0,66 ± 0,04 g L^{-1} d^{-1} para o processo contínuo. Observou-se aumento na produção de proteínas e carotenoides (all-*trans*-violaxantina, all-*trans*-*α*-caroteno e β-caroteno) quando comparados aos cultivos em batelada. Os cultivos contínuos apresentaram aumento na produção de ácidos graxos poli-insaturados e ω3 (ácido linolênico). Assim, os cultivos resultaram em uma relação ω6:ω3 de 1,4, sendo considerada apropriada, uma vez que por recomendação da FAO/WHO estima que o consumo desses ácidos graxos tenha razão inferior a 10. Os cultivos contínuos de microalga *P. marina* integrados com fermentadores de cerveja para fixação de CO_2 biológico apresentaram resultados satisfatórios. O suprimento de CO_2 a partir de fermentação de cerveja em ambas as relações entre os volumes de fotobiorreator:fermentador para fixação/produção de CO_2 avaliadas foram suficientemente adequadas para manter o crescimento celular, bem como o perfil e quantidade de produtos formados de acordo com os resultados prévios obtidos para o sistema contínuo com CO_2 de cilindro.

Palavras-chave: ácidos graxos, carotenoides, cultivo em batelada, cultivo contínuo, modelagem matemática.

ABSTRACT

Microalgae are photosynthetic microorganisms that can fix CO_2 from different sources and, under proper cultivation conditions, are capable of producing carbohydrates, proteins, lipids and value-added compounds such as fatty acids and carotenoids with significance to the food area. In the first step of this work, the green microalgae strain was subjected to rDNA analysis and phylogenetic identification, and presented 96 % of similarity to *Pseudoneochloris marina* when compared as sequences deposited in GenBank. After the identification of the microalga, preliminary tests were performed to adjust the nitrogen concentration ($NaNO_3$) of the cultures in batch process. The highest biomass concentration (2.02 ± 0.21 g L^{-1}) was achieved with 450 mg L^{-1} of $NaNO_3$. This condition was applied in subsequent experiments. In addition to the nitrogen concentration, the influence of the external parameters, temperature and light intensity were evaluated in the production and composition of *P. marina* biomass. The highest biomass productivity (0.26 g L^{-1} d^{-1}) was achieved in the cultures at 28 °C and 252 and 364 μmol m^{-2} s^{-1}. Carbohydrates were the reserve compounds accumulated at high concentrations by microalgae cells. The protein content was reduced when *P. marina* was grown at high temperature and light intensity. The increase in light intensity showed a negative effect in the content of carotenoids and lipids. Lutein and β-carotene, and C16:0, C18:2n-6 and C18:3n-3, respectively, were identified as the major components of the identification and quantification of the carotenoids and fatty acids present in the biomass. The lowest ω6:ω3 (1.6) ratio was observed at 20 °C. This step of the study showed the potential of *P. marina* for the production of carotenoids and polyunsaturated fatty acids. During the next step, the mathematical modeling was performed for the *P. marina* cultures in the batch processes, repeated and continuous batch. Five mathematical models were analyzed to describe cell growth and nitrogen consumption of batch cultures. The results showed that the ModNXmax model presented the highest correlation coefficients. Mathematical models have also been developed to describe the formation of products: carotenoids, proteins and lipids. The CP2 and CP3 models showed better prediction for carotenoids and proteins. The Luedeking-Piret model presented $R^2 = 0.99$ for lipid production. In the last step of this work, from the models were used to simulate cell growth and nitrogen consumption in repeated-batch and continuous processes aiming to maximize biomass productivity. The optimum renewal volume for the repeated-batch cultures using 48-h intervals and the dilution rate for the continuous process were 1.4 L and 0.46 d^{-1}, respectively. The biomass yield in both cultures exceeded predicted values by the simulations, resulting in 0.56 ± 0.06 g $L^{-1}d^{-1}$ for repeated-batch cultures and 0.66 ± 0.04 g $L^{-1}d^{-1}$ for the continuous

process. There was an increase in the production of proteins and carotenoids (all-*trans*-violaxanthin, all-*trans*-α-carotene and β-carotene) when compared to batch cultures. Continuous cultures showed increased production of polyunsaturated fatty acids and ω3 (linolenic acid). Thus, the cultures resulted in an ω6:ω3 ratio of 1.4. Finally, the continuous culture of *P. marina* was integrated to beer fermenters. The CO_2 supply from beer fermentation in both photobioreactor:fermenter volume ratios tested (2.5:1 and 5:1) were adequate to maintain cell growth, as well as the profile and amount of products formed according to the results obtained for the continuous system with cylinder CO_2.

Key-words: batch cultivation, carotenoids, continuous cultivation, fatty acids, mathematical modeling.

LISTA DE FIGURAS

CAPÍTULO 3 e 4

CAPÍTULO 5, 6 e 7

LISTA DE TABELAS

CAPÍTULO 5, 6 e 7

SUMÁRIO

1 INTRODUÇÃO

As microalgas são microrganismos fotossintéticos que podem fixar o CO_2 de diferentes fontes, como processos industriais, CO_2 atmosférico, e na forma de carbonatos solúveis. As microalgas têm recebido atenção neste cenário, devido às suas taxas de crescimento mais rápidas e maior eficiência fotossintética se comparada às plantas terrestres. As microalgas são microrganismos capazes de produzir quantidades significativas de compostos intracelulares como proteínas, carboidratos e lipídeos. Além dessas macromoléculas, as microalgas podem sintetizar compostos como carotenoides e ácidos graxos poli-insaturados com alto valor agregado que apresentam propriedades bioativas e benefícios a saúde humana quando consumidos na dieta alimentar (MATA; MARTINS; CAETANO, 2010; COSTA; MORAIS, 2014).

A adequação das condições de cultivo como temperatura, pH, fonte de nitrogênio e uso de CO_2, visam a redução de custos de processo e o aumento da produção de biomassa, além de auxiliar na proteção do meio ambiente resultando na obtenção de compostos de interesse industrial. Os regimes de cultivos de microalgas em batelada repetida e contínuo propiciam elevada produtividade de biomassa quando comparadas ao processo em batelada. Além disso, são operacional e economicamente mais vantajosas em escala industrial (SYDNEY et al., 2010; ANJOS et al., 2013; CHEAH et al., 2015).

A modelagem matemática é uma ferramenta útil para compreender o comportamento cinético de crescimento de microalgas, o consumo de substratos, a formação de produtos e otimizar os parâmetros cinéticos do processo em escala laboratorial sob determinadas condições nutricionais e ambientais. A modelagem é capaz de prever com precisão o comportamento de crescimento de microalgas e oferece uma base confiável para modelar operações de aumento de escala. A predição de crescimento celular e consumo de substratos baseiam-se em modelos clássicos como Droop e Monod sob condições fotoautotróficas e heterotróficas de cultivos. Além disso, o modelo Luedeking-Piret é amplamente utilizado para predizer a formação de produtos (associado e não-associado ao crescimento celular) (MONOD, 1949; LUEDEKING; PIRET, 1959; DROOP, 1968; ADESANYA et al., 2014; HE et al., 2016; KUMAR et al., 2016; SACHDEVA et al., 2016).

A utilização de gases residuais de processos industriais tem se tornado de interesse e cada vez mais aplicável, uma vez que permite a redução dos custos de processo gerados

pelos meios de cultivos e auxiliam na compensação das emissões de carbono ao ambiente. Diversos estudos utilizam CO_2 da queima de combustíveis fósseis e alguns utilizam CO_2 de processos fermentativos como fonte de carbono para o crescimento de microalgas objetivando a produção de biocombustíveis, sendo assim, importante investigar o uso de CO_2 para a produção de compostos de interesse para a indústria de alimentos (FERREIRA et al., 2012; CHAGAS et al., 2015; VAZ; COSTA; MORAIS, 2016).

A partir do conhecimento das condições ambientais e nutricionais ótimas dos cultivos de microalgas aliado a modelagem matemática e simulação dos processos de cultivo bem como a formação de produtos intracelulares é possível otimizar os processos tecnológicos de cultivos de microalgas. Neste sentido, cultivos contínuos de microalgas com uso de CO_2 de fermentação alcóolica de cerveja se torna de interesse industrial por ser uma fonte de carbono inorgânico de qualidade e alta pureza visando o aumento da produtividade de biomassa e obtenção de produtos de alto valor agregado como proteínas, carotenoides e ácidos graxos poli-insaturados.

2 OBJETIVOS

2.1 Objetivo Geral

O objetivo do trabalho consiste em avaliar as condições de cultivo, otimizar a produção de biomassa e biocompostos, bem como a modelagem matemática e simulação de cultivos autotróficos de *Pseudoneochloris marina* em fotobiorreatores *airlift* sob diferentes regimes de processo.

2.2 Objetivos Específicos

- Determinar o efeito de diferentes condições de cultivo – concentração de nitrogênio, luz e temperatura – sobre a cinética de crescimento e formação de proteínas, lipídeos e carotenoides por *P. marina*;
- Identificar e quantificar o perfil lipídico e de carotenoides obtidos nos cultivos da microalga;
- Avaliar diferentes modelos cinéticos para descrever o cultivo de microalga em processo de batelada;
- Otimizar matematicamente cultivos em batelada-repetida e contínuos, e validar experimentalmente o resultado da otimização;
- Avaliar o uso de CO_2 de fermentação de cerveja por *P. marina* em cultivos contínuos: integrar o fotobiorreator a um processo de fermentação de cerveja estudando a relação volume de fotobiorreator:fermentador.

3 REVISÃO BIBLIOGRÁFICA

3.1 Microalgas: *Pseudoneochloris marina* (*Chlorophyta*)

As microalgas estão presentes em diversos ecossistemas. São organismos descendentes das primeiras formas de vida fotossintética e apresentam papel regulador da biosfera do planeta. Estima-se a existência de mais de 50.000 espécies, porém o número de espécies identificadas e estudadas concentra-se em torno de 30.000. As microalgas fazem parte de um grupo heterogêneo de microrganismos fotossintetizantes, que tem a capacidade de desenvolver-se rapidamente em condições adversas devido a sua estrutura celular simples. As cianobactérias (*Cyanophyceae*) são procarióticas enquanto as algas verdes (*Chlorophyta*) e diatomáceas (*Bacillariophyta*) são eucarióticas (MATA; MARTINS; CAETANO, 2010).

A espécie *Pseudoneochloris marina* foi identificada por análise ultraestrutural e molecular (DNA) realizadas por Watanabe et al. (2000) a partir de uma cepa de *Neochloris* sp. que apresentou características morfológicas, moleculares e condições de crescimento distintos das espécies anteriormente identificadas. Quanto a classificação filogenética, *Pseudoneochloris marina* (Figura 3.1), são microalgas marinhas verdes (*Chlorophyta*) pertencentes a classe das *Ulvophyceae* que possuem células vegetativas uninucleadas, unicelulares, esféricas e o tamanho das células variável entre 3 µm e 20 µm dependente do estágio de desenvolvimento. Conforme o estágio de ciclo de vida, as células vegetativas apresentam formação e perda de zoósporos e aplanosporos biflagelados que participam do processo de reprodução assexuada. A classe *Ulvophyceae* de forma geral, foi objeto de poucas revisões e classificações em nível de gênero na última década e a composição da biomassa dessas algas é pouco explorada (BAUDELET et al., 2017).

Figura 3.1 – *Pseudoneochloris marina* (× 1000). (O autor, 2019)

Na literatura, não existem publicações anteriores aos resultados obtidos neste trabalho acerca do potencial biotecnológico de *P. marina* para produção biomassa. Conforme pesquisa realizada utilizando a base de dados Scopus (Figura 3.2), em que foram utilizadas as palavras-chave *Pseudoneochloris e Pseudoneochloris marina*, resultou apenas no trabalho de identificação filogenética descoberta por Watanabe e colaboradores no ano 2000. Contudo, essa espécie é parte do filo *Chlorophyta* que extensivamente têm-se investigado estratégias de cultivo e aumento de escala por serem fontes renováveis de produtos de alto valor para a área de alimentos, farmacêutica, energética e outras (COSTA; MORAIS, 2013; BAUDELET et al., 2017).

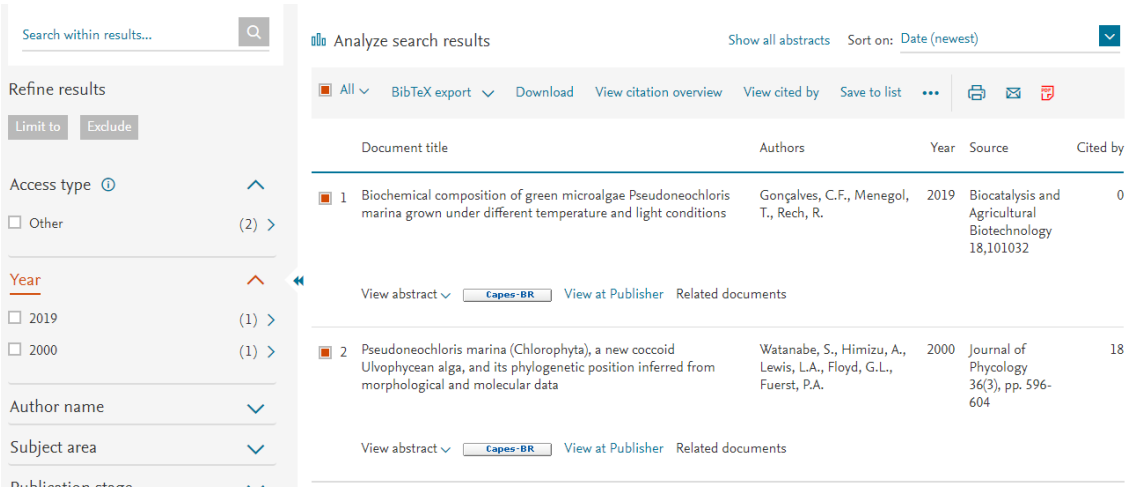

Figura 3.2 – Resultado da pesquisa pelas palavras-chave "*Pseudoneochloris"* e "*Pseudoneochloris marina*" na base de dados Scopus. (acesso dia 27/02/2019 às 17:34h).

As microalgas, em particular *Chlorophyta*, tornaram-se microrganismos de importância tecnológica devido à capacidade de adaptação de seu metabolismo em resposta as condições ambientais, sistemas de cultivos e pela diversidade de metabólitos produzidos que são de interesse industrial. A biomassa das microalgas é essencialmente composta por carboidratos, proteínas e lipídeos. Além destes compostos, estes microrganismos são capazes de produzir moléculas bioativas de alto valor agregado como carotenoides, polissacarídeos, ácidos graxos, vitaminas e minerais (MATA; MARTINS; CAETANO, 2010; COSTA; MORAIS, 2014).

3.2 Fotossíntese e fixação de CO_2 por microalgas

A fotossíntese é um processo físico-químico no qual microrganismos fotossintetizantes, como as microalgas, sintetizam carbono orgânico por meio do carbono inorgânico, utilizando a energia solar e liberando oxigênio na atmosfera. A reação global da fotossíntese (Equação 3.1) envolve duas etapas: fase clara (fotoquímica) onde há absorção de energia luminosa para produção de ATP a partir de ADP e fosfato; e a fase escura (química) em que o ATP se liga com o CO_2 formando compostos orgânicos, também conhecida como fixação de carbono (MASOJÍDEK et al., 2013).

$$6CO_2 + 12H_2O + energia\ luminosa \rightarrow C_6H_{12}O_6 + 6O_2 + 6H_2O \quad (3.1)$$

A fixação biológica de CO_2 é considerada uma tecnologia sustentável ambientalmente a longo prazo. O CO_2 da atmosfera é convertido em biomassa por microrganismos autótrofos quando associado ao fornecimento de nutrientes em condições adequadas de crescimento. Em comparação com outras matérias-primas vegetais, microalgas apresentam inúmeras vantagens na fixação de CO_2 e obtenção de biocompostos de interesse industrial. Dentre elas, estão inclusas a alta eficiência fotossintética para conversão em diversos produtos, alta taxa de reprodução, adaptação em diversos ecossistemas, não competitividade com a área de alimentos e planejamento de projetos em escala industrial (ZENG et al., 2011).

A fixação de carbono pelas microalgas é efetuada por meio da via metabólica conhecida como ciclo de Calvin-Benson-Bassham (Figura 3.3), em que enzimas presentes nestes organismos catalisam reações que incorporam átomos de carbono provenientes do CO_2. Na reação central de fixação de carbono, um átomo de carbono inorgânico é convertido em carbono orgânico. O CO_2 dissolvido combina-se com a ribulose-1,5-bifosfato e água resultando em duas moléculas de 3-fosfoglicerato. Esta reação de fixação é catalisada no estroma cloroplástico pela ribulose-bifosfato-carboxilase. A reação é energeticamente favorável devido à reatividade do composto ribulose-1,5-bifosfato rico em energia, em que cada molécula de CO_2 é adicionada. Porém, para produzir um suprimento suficiente de ribulose-1,5-bifosfato, é necessária uma série de reações que consomem grandes quantidades de NADPH e ATP (JAJESNIAK et al., 2014).

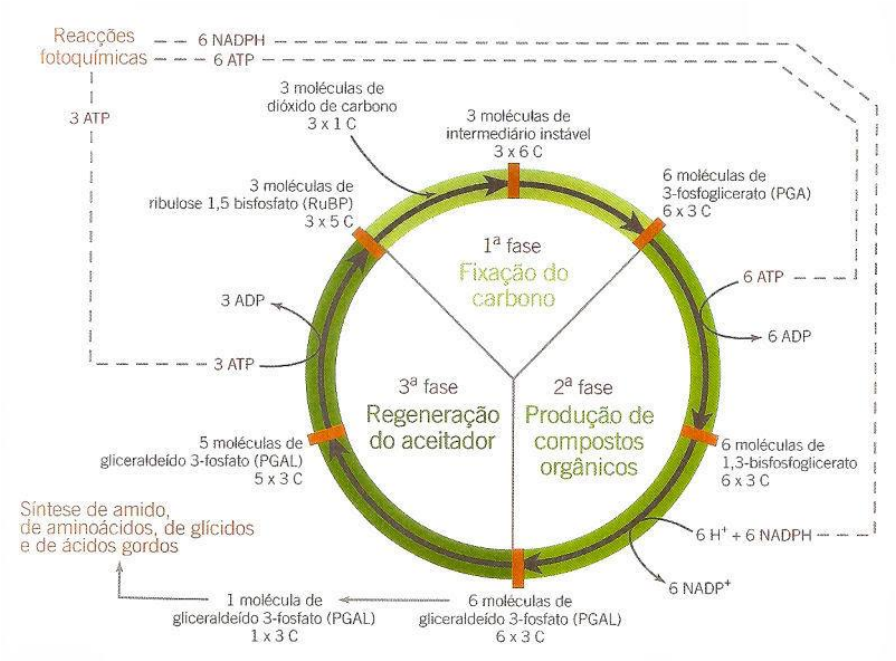

Figura 3.3 – Ciclo de Calvin (Carrajola; Castro; Hilário, 2007).

No ciclo de Calvin, 3 moléculas de ATP e 2 moléculas de NADPH são consumidas para cada molécula de CO_2 convertida em carboidrato, de acordo com a Equação 3.2:

$$3CO_2 + 9ATP + 6NADPH + \text{água} \rightarrow \text{gliceraldeído } 3 - \text{fosfato} + 8P_i + 6NADP^+ \qquad (3.2)$$

O gliceraldeído 3-fosfato produzido nos cloroplastos pelo ciclo de fixação do carbono é um açúcar de 3 carbonos que serve como intermediário central da glicólise. Grande parte dele é transportada pelo citosol, onde pode ser convertido em frutose-6-fosfato e glicose-1-fosfato (ALBERTS et al., 2004).

3.3 Composição das microalgas

Os carboidratos são os principais compostos derivados do processo de fotossíntese e fixação de carbono (Ciclo de Calvin) sendo acumulados nas células como produtos de reserva nos cloroplastos (amido) ou na composição estrutural de parede celular, por exemplo, na forma de celulose, pectina e polissacarídeos (CHEN et al., 2013). Algumas espécies de microalgas podem acumular carboidratos em torno de 50 % (peso seco) como cepas de *Chlorella, Scenedesmus, Dunalliella e Chlamydomonas* (JOHN et al., 2011; HO et al., 2013).

Os lipídeos fazem parte da membrana celular das microalgas, atuam como reserva energética e isolamento térmico. A produção de lipídeos depende principalmente das condições de crescimento de cultivo, tais como nutrientes, salinidade, intensidade de luz, temperatura e pH. Alguns fatores de estresse celular como a limitação de fonte de nitrogênio e fornecimento de CO_2 são estratégias para aumentar o acúmulo de ácidos graxos com elevado grau de saturação. No entanto, este método produz uma diminuição na produtividade de biomassa. Já foi demonstrado que a alta intensidade de luz e a alta temperatura, favorecem o acúmulo de triglicerídeos com um perfil de alta saturação. Enquanto isso, as baixas intensidades de luz e temperatura promovem a síntese de ácidos graxos poli-insaturados (PUFAS) (MATA; MARTINS; CAETANO, 2010; TANG et al., 2011).

A produção de carboidratos e lipídeos durante a fotossíntese estão associadas, uma vez que o glicerol-3-fosfato percursor para a síntese de triacilgliceróis (TAG) é produzido via glicólise). A produção desses compostos é variável entre as espécies de microalgas e favorecida em condições de estresse celular como limitação de nutrientes (CHEN et al., 2013).

As proteínas são componentes de fundamental importância para o ciclo de vida das microalgas, crescimento celular, atuam no reparo e manutenção das células, bem como na regulação catalítica enzimática e na defesa das células. A produção de proteínas é variável entre as espécies de microalgas e depende das condições de cultivo sendo favorecidas em culturas onde há o suprimento de nutrientes, principalmente fonte de nitrogênio. Algumas microalgas são capazes de apresentar quantidades significantes de proteínas e a qualidade dos aminoácidos presentes nas células são favoráveis e tem ações benéficas para a nutrição humana podendo ser comercializadas como suplemento alimentar (SAFI et al., 2014; KHANRA et al., 2018).

Os carotenoides são outros compostos produzidos pelas microalgas. Em condições adequadas de crescimento celular, as microalgas apresentam coloração verde, pois possuem clorofilas *a* e *b* que são necessários para a fotossíntese e atuam como pigmentos acessórios na captura de energia da luz. Sob condições de estresse celular, assim como para os lipídeos, os carotenoides são produzidos quando há limitação da fonte de nitrato, alta intensidade de luz e concentração salina (CHAGAS et al., 2015; TINOCO; TEIXEIRA; REZENDE, 2015).

Os carotenoides estão associados a foto proteção das moléculas de clorofila contra ação da luz e oxigênio. Os pigmentos produzidos por microalgas são utilizados na

indústria de alimentos e cosmética, uma vez que têm propriedades terapêuticas como ação antioxidante, prevenção de doenças crônicas e proteção do sistema imunológico (SAFI et al., 2014; KHANRA et al., 2018).

3.4 Cultivos de microalgas: classificação nutricional

As microalgas podem ser classificadas nutricionalmente em autotróficas e heterotróficas. A primeira forma exige para seu desenvolvimento apenas compostos inorgânicos, incluindo CO_2, e luz como fonte de energia. A segunda requer uma fonte externa de compostos orgânicos como fonte de energia e não realizam a fotossíntese. Algumas algas fotossintéticas são mixotróficas, tendo a capacidade de realizar fotossíntese e utilizar nutrientes orgânicos de fontes exógenas (BRENNAN; OWENDE, 2010).

O cultivo fotoautotrófico de microalgas representa um modelo ideal de fixação de CO_2 de fontes diversas, pois é um sistema que garante altas taxas de crescimento celular e conversão de CO_2 na produção renovável de compostos de valor agregado. No entanto, esse modo de cultura apresenta menor produtividade de biomassa que sistemas heterotróficos devido a dependência de intensidade luminosa e ao sombreamento das células quando atinge altas densidades nas culturas. Ainda assim, os cultivos fotoautotróficos apresentam menores custos de processo quando comparados aos sistemas heterotróficos melhorando a viabilidade de produção de compostos (ABREU et al., 2012; ADESANYA et al., 2014).

Os cultivos de microalgas são influenciados diretamente pela disponibilidade de macronutrientes (nitrogênio e fósforo) e micronutrientes (potássio, magnésio e enxofre) dissolvidos nos meios de cultura. As mudanças nos meios de culturas são estratégias extensivamente investigadas pelos pesquisadores para otimizar a produção de biomassa. As diferentes proporções e a limitação de determinados nutrientes nos meios de cultura são capazes de induzir as microalgas ao acúmulo de diferentes compostos de interesse. A limitação de nitrogênio, fósforo e incremento na salinidade dos meios de culturas são estratégias para modular a produção de biomassa e o conteúdo de pigmentos e lipídeos em espécies de clorofíceas (LOURENÇO, 2006; MATA; MARTINS; CAETANO, 2010; BENAVENTE-VALDÉS et al., 2016).

As microalgas são capazes de degradar os compostos nitrogenados presentes nas células para manutenção da atividade metabólica. Enquanto o suprimento de nitrogênio

no meio de cultivo é abundante verifica-se o aumento nas concentrações de proteínas e clorofila nas células. Quando há limitação de nitrogênio ocorre queda na taxa de divisão celular, bem como o teor de proteínas e clorofilas e partir dessa condição aumentam a concentração de produtos de reserva e carotenoides. Alterações na fonte e concentração de nitrogênio nos meios de cultura, pH, estresse salino, temperatura e intensidade luminosa podem aumentar o conteúdo de carboidratos e lipídeos. A limitação inicial de nitrogênio nos cultivos consequentemente gera baixa produtividade de biomassa, assim, o cultivo inicial na presença de nitrogênio fornece aporte nutricional para crescimento celular e, em seguida, na ausência de nitrogênio as células são capazes de acumular os compostos de reserva ao longo do tempo sem perdas significantes na concentração de biomassa (CHEN et al., 2011; PANCHA et al., 2015).

Associado ao conteúdo de nutrientes disponíveis nos meios de culturas, fatores externos como temperatura e intensidade luminosa exercem influência direta no crescimento e composição da biomassa de microalgas. A temperatura é um fator importante que afeta as reações metabólicas celulares e a condição ótima é amplamente variável, uma vez que depende da espécie e o ambiente de adaptação. A temperatura afeta a taxa de absorção de nutrientes, o crescimento celular, a integridade e fluidização das membranas celulares. A luz atua como força motriz no processo fotossintético e é o principal parâmetro externo de influência no metabolismo celular. Diversos estudos avaliaram o efeito da luz na obtenção de carboidratos, proteínas, pigmentos e ácidos graxos em diferentes espécies de microalgas e a otimização da intensidade luminosa pode proporcionar maior produção e viabilidade comercial de compostos da biomassa (KUMAR et al., 2014; BENAVENTE-VALDÉS et al., 2016; GONG; BASSI, 2016).

3.5 Sistemas de cultivos de microalgas

A condução dos cultivos de microalgas apresenta certa flexibilidade na operação e diversidade da configuração dos fotobiorreatores a fim de aumentar a produtividade do sistema. Os regimes de cultivos podem ser classificados em processo descontínuo (batelada), descontínuo alimentado e semi-contínuo (batelada repetida) e contínuo (LOURENÇO, 2006).

Os cultivos descontínuos ou em batelada são caracterizados por adição inicial de meio de cultura e inóculo de microalgas, no decorrer do processo não se adiciona nutrientes e é feito o controle de aeração, adição de antiespumantes e controle do pH. Ao

final do processo o biorreator é descarregado e o processo finalizado. O cultivo em batelada pode levar a baixos rendimentos e/ou produtividade devido a limitação de nutrientes ao longo dos cultivos e períodos de tempo morto entre as bateladas. Porém, este processo apresenta menores riscos de contaminação, flexibilidade de operação, estabilidade genética dos micro-organismos e é extensamente utilizado pelas indústrias (SCHMIDELL et al., 2001).

O processo semi-contínuo ou em batelada repetida consiste em iniciar o cultivo conforme o cultivo descontínuo e ao final do crescimento celular, parte do meio contendo biomassa é retirado mantendo outra parte no biorreator e adiciona-se um volume de meio de cultura igual ao volume retirado do cultivo. Esta etapa é denominada corte e é realizada quando atingir a concentração celular pré-determinada. O corte deve ser feito quando o microrganismo está na fase de crescimento exponencial, para não haver fase de adaptação, conseguindo-se assim, um processo quase contínuo de produção de biomassa. As vantagens deste processo estão em operar por longos períodos, aumento da produtividade e redução dos tempos mortos na operação dos biorreatores (SCHMIDELL et al., 2001; LOURENÇO, 2006).

O regime de cultivo contínuo caracteriza-se pela adição contínua de substrato, a uma vazão constante e retirada do produto na mesma vazão de alimentação. Esse regime de cultivo exige uma etapa de adaptação de vazão constante, até atingir um regime em estado permanente. O processo em batelada alimentada consiste da adição contínua de substrato ao longo do cultivo, eliminando o fenômeno de depleção pelos nutrientes, permitindo aumento no período produtivo do processo e os produtos permanecem no biorreator até o final do processo (SCHMIDELL et al., 2001; LOURENÇO, 2006).

3.6 Fotobiorreatores

Um sistema de cultivo fotoautotrófico ideal deve atender aos seguintes requisitos adequados para a produção de microalgas: ter baixo custo de instalação e operação, ótima transferência de massa (gás-líquido) e energia (luz), baixo nível de contaminação e mínimo espaço de terra cultivável. Os cultivos de microalgas, em escala comercial, podem ser realizados em diferentes sistemas de operação: abertos (*raceway* e *open-pounds*) e fotobiorreatores fechados (LAM; LEE, 2014).

Os sistemas abertos apresentam vantagens como baixo custo e operação, porém, o emprego desses sistemas limita-se às condições ambientais da região onde será

instalado, uma vez que os parâmetros externos como temperatura e iluminação não são controlados. Frente as limitações dos sistemas abertos, os fotobiorreatores fechados são projetados para suprir essas deficiências e garantir que os cultivos sejam realizados em condições ótimas (pH, temperatura, iluminação, nutrientes e mistura de ar/CO_2) específicas para cada espécie garantindo maior produtividade de biomassa (MATA; MARTINS; CAETANO, 2010).

Os sistemas fechados de fotobiorreatores apresentam alta transferência de massa e facilitam o sequestro de CO_2 por microalgas. A agitação dos sistemas pode ser feita de forma mecânica por meio de pás e bombas ou não-mecânicas pelo transporte de ar em fotobiorreatores conhecidos como coluna de bolhas, tubulares, placas planas e *airlift* (MOHAN et al., 2014).

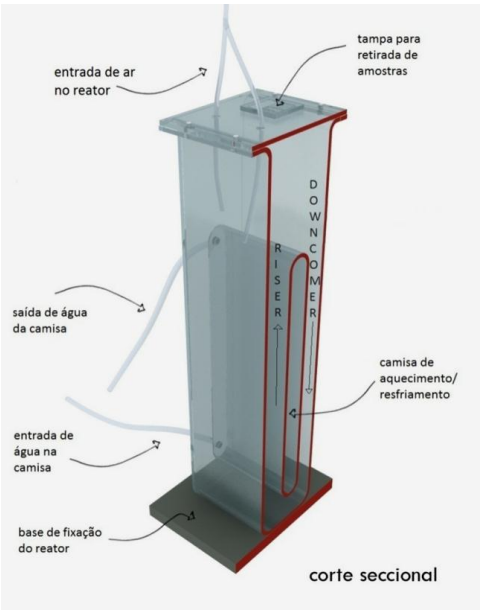

Figura 3.1 - Fotobiorreator de placa *airlift* (Kochem *et al.*, 2014).

Os cultivos de microalgas em fotobiorreatores *airlift* aumentam a fixação do CO_2 pela distribuição do gás ao longo do reator, bem como pelo uso de pulverizadores que liberam pequenas bolhas, aumentando a superfície de contato entre o gás e o líquido (LOURENÇO, 2006; COSTA; MORAIS, 2013). Os fotobiorreatores de placas planas (Figura 3.4) são extensivamente conhecidos para os cultivos de microalgas e podem atingir altas taxas de eficiência fotossintética (SIERRA et al., 2008; BUEHNER et al., 2009; MARSULLO et al., 2015). Este tipo de sistema pode apresentar algumas limitações no controle de temperatura, oxigênio e CO_2 dissolvidos quando comparados a fotobiorreatores tubulares. Kochem et al. (2014) desenvolveram um novo fotobiorreator

de placa plana *airlift* (2,2 L) com um trocador de calor interno presente entre as faces ascendente e descendente. Os autores obtiveram maior coeficiente volumétrico de transferência de massa e menor tempo de mistura a partir do aumento da velocidade do ar proporcionada pelos aeradores (parte inferior) resultando em alta velocidade específica de crescimento para as microalgas estudadas (*Dunaliella tertiolecta* e *Chlorella minutissima*).

3.7 Aquecimento global e mitigação de CO_2

Os impactos ambientais, as alterações nos ecossistemas e o aquecimento global são preocupações causadas pelas emissões de gases de efeito estufa. O rápido crescimento populacional e o desenvolvimento industrial demandaram maior consumo de energia e, consequentemente, maior geração e emissão desses gases para o ambiente. O dióxido de carbono (CO_2) representa 68 % da emissão de gases responsáveis pelo aquecimento global (ZENG et al., 2011; KASSIM; MENG, 2017; ZHOU et al., 2017). Países industrializados e a comunidade europeia assinaram um acordo conhecido como Protocolo de Kyoto que visa reduzir a emissão de gases de efeito estufa em 18 % abaixo do nível de 1990 em um período compreendido entre 2013-2020 (CHEAH et al., 2015). A redução na concentração de CO_2 atmosférico, através da minimização das emissões de CO_2 do desenvolvimento de processos que utilizam CO_2, é fundamental para garantir a sustentabilidade ambiental (ZENG et al., 2011).

Segundo Yang et al. (2008) há três opções para reduzir as emissões totais de CO_2 para a atmosfera: reduzir a quantidade de energia consumida, reduzir as emissões de carbono e aumentar a fixação do CO_2. A primeira opção requer o uso eficiente da energia. Em segundo, a mudança para uso de combustíveis não fósseis, como o hidrogênio e energia renovável. A terceira opção envolve o desenvolvimento de tecnologias para a captura e sequestro de CO_2.

As técnicas utilizadas para captura e fixação de CO_2 compreendem processos físicos (sequestro geológico, armazenamento oceânico, enterramento de biocarvão), químicos (depuração química, carbonização mineral) ou biológicos (reflorestamento, agricultura e microrganismos fotossintéticos) (GROVER et al., 2015; KASSIM; MENG, 2017). Os processos físicos e químicos apresentam desvantagens como custo de implantação, dificuldade de operação e não geração de produtos para comercialização.

Neste sentido, a fixação biológica de CO_2 por microrganismos fotossintetizantes como as microalgas surge como uma alternativa promissora e mundialmente difundida (YANG et al., 2008; BILANOVIC et al., 2009).

As microalgas são conhecidas pela maior capacidade de fixação de CO_2 (10-50 vezes) quando comparadas com as plantas terrestres (WANG et al., 2008). Estima-se que a produção de 1 kg de biomassa microalgal é equivalente a aproximadamente a fixação de 1,83 kg de CO_2. As microalgas têm a habilidade de utilizar o CO_2 em diversas concentrações e de diferentes fontes como o ar atmosférico, gases de usinas termoelétricas e de processos industriais, e ainda assim, carbonos inorgânicos ou orgânicos provenientes de águas residuais (CHEAH et al., 2015; ZHOU et al., 2017). Esses microrganismos fotossintéticos têm alta taxa de crescimento celular e habilidade de utilizar CO_2 como fonte de carbono para a produção de biomassa. O carbono é o principal componente celular representando cerca de 50 % do seu peso seco (KUMAR et al., 2010). A biomassa de microalgas pode ser matéria-prima para uma grande variedade de produtos que incluem carboidratos, lipídeos, proteínas, carotenoides e vitaminas, que podem ser utilizados para produção de biocombustíveis, alimentação humana, alimentação animal, produtos farmacêuticos e cosméticos (HARUN et al., 2010; CHEN et al., 2013).

3.8 Produção de CO_2 de cerveja

A produção nacional de cerveja, em 2016, foi 140 milhões de hectolitros, colocando o Brasil em terceiro lugar no ranking mundial. As regiões Sul e Sudeste do país somam 86 % da produção total de cervejas (CERVBRASIL, 2016). A cultura de produção e consumo e cervejas tem crescido a cada ano e uma grande variedade de tipos e sabores de cervejas tem sido desenvolvidos. O processo de produção de cerveja consiste basicamente em quatro etapas: brasagem/ malteação onde ocorre a germinação da cevada; produção do mosto compreendida na extração e hidrólise dos compostos insolúveis, seguido de filtração e adição do lúpulo; fermentação primária e maturação; e processamento final (estabilização e envase) (BRÁNYIK et al., 2005; DRAGONE; MUSSATTO; SILVA, 2007). A fermentação alcoólica é um processo anaeróbio em que as leveduras fazem a conversão dos açúcares em etanol e CO_2. Em termos de massa são produzidos aproximadamente 0,96 kg CO_2/kg etanol (MATSUDO et al., 2011; FERREIRA et al., 2012).

A alta produção de cerveja do setor e considerando a alta pureza do CO_2 gerado favorece algumas aplicações industriais como na carbonatação de refrigerantes, conservação de alimentos e atualmente têm-se investigado a utilização para processos biotecnológicos como a fixação por microalgas (XU; ISOM; HANNA, 2010; CHAGAS et al., 2015a).

As emissões de CO_2 provenientes da produção de cerveja chegam a 140 Mt/ano e a pureza do CO_2 pode atingir níveis de 99 % (CHAGAS et al., 2015). Os benefícios associados à utilização de CO_2 de produção de cerveja em processos biotecnológicos estão na redução de custos no sistema de sequestro e armazenamento do gás que representa 80-90 % do custo total. Além disso, os microrganismos fotossintetizantes, como as microalgas utilizam o CO_2 como fonte de carbono para produção de compostos de interesse industrial (RUBIN, 2008; CHAGAS et al., 2015).

3.9 Modelagem matemática e simulação dos cultivos de microalgas

A modelagem matemática em bioprocessos tem por finalidade descrever por meio de equações matemáticas os balanços de massa para os componentes do reator, as reações bioquímicas que ocorrem no processo e as velocidades com que as reações se processam. A simulação de processos permite prever o comportamento dinâmico e estacionário do processo, inclusive em condições não testadas experimentalmente, auxiliando na determinação de condições ótimas do sistema (SCHMIDELL et al., 2001).

No desenvolvimento de modelos matemáticos para processos biológicos existem algumas limitações como o grande número de parâmetros, as interações entre eles e não-linearidade dos sistemas (VATCHEVA et al., 2006). Na literatura alguns modelos são descritos para representar os sistemas de biorreatores e poucos demonstram a obtenção de modelos para os processos envolvendo microalgas.

Os modelos clássicos de Monod (1949) e Droop (1968) expressam a cinética de crescimento de microrganismos e têm sido utilizados para demonstrar o crescimento de microalgas. Esses modelos correlacionam o crescimento celular com a concentração de substrato no meio, como por exemplo, a fonte de nitrogênio. O modelo de Monod define que o consumo de substrato pelos microrganismos é instantaneamente convertido em biomassa. O modelo de Droop assume que a taxa de crescimento depende da concentração celular e da reserva de nutrientes intracelular separando da concentração de nutrientes externa conforme descrito abaixo (Equações 3.3-3.7). Alguns modelos têm

sido desenvolvidos com base no modelo de Droop para processos em batelada, porém estudos cinéticos de modelagem para cultivos de microalgas em batelada repetida e contínuo são escassos (VATCHEVA et al., 2006; DA FRÉ et al., 2016).

O modelo Droop possui uma cota celular interna de substrato (q) que desacopla a absorção do substrato e o crescimento celular estimado a partir do desvio da concentração inicial e ao longo do tempo (Equação 3.8). No entanto, ele não consegue prever o crescimento celular em culturas não limitadas por substrato.

$$\frac{dX}{dt} = \mu \cdot X \tag{3.3}$$

$$\frac{dN}{dt} = -\rho \cdot X \tag{3.4}$$

$$\frac{dq}{dt} = \rho - \mu \cdot q \tag{3.5}$$

$$\mu = \mu_m \cdot \left(1 - \frac{k_q}{q}\right) \tag{3.6}$$

$$\rho = \rho_{max} \cdot \left(\frac{N}{N + k_N}\right) \tag{3.7}$$

$$q = \frac{N_{in} - N}{X} \tag{3.8}$$

As modificações nos modelos de Monod foram propostas por Da Fré et al.(2016) considerando a reação catalisada por nitrogênio (ordem n) e o consumo de nitrogênio com um termo associado ao crescimento da taxa de consumo de nitrogênio (Y_{XN}) e um termo não associado ao crescimento (m_N). O modelo de ModN é baseado na hipótese de que o crescimento foi limitado pela falta de nitrogênio, de acordo com as Equações 3.2 e 3.3, seguidas pelas Equações 3.9 e 3.10.

$$\rho = \left(\frac{\mu}{Y_{XN}} + m_N\right) \cdot N \tag{3.9}$$

$$\mu = \mu_{max} \cdot \left(\frac{N}{N + k_N}\right) \tag{3.10}$$

Os modelos ModNkx e ModNXmax baseiam-se na hipótese de que o excesso de biomassa é responsável por limitar o crescimento de biomassa e a expressão para taxa de crescimento específica é substituída pelas Equações 3.11 e 3.12, respectivamente. O termo logístico $(1 - X/X_{max})$ é um modelo comum de crescimento populacional e representa a autoinibição das células como limitação de crescimento.

$$\mu = \mu_{max} \cdot \left(\frac{N}{N + k_N}\right) \cdot \left(\frac{k_X}{X + k_X}\right) \tag{3.11}$$

$$\mu = \mu_{max} \cdot \left(1 - \frac{X}{X_{max}}\right) \tag{3.12}$$

Além dos modelos cinéticos desenvolvidos e empregados para descrever os sistemas de crescimento celular diversos estudos de modelagem matemática acerca da formação de produtos vêm sendo investigados. Os produtos mais comumente estudados são a formação de carotenoides e lipídeos devido à importância e interesses biotecnológicos (ZHANG; SHI; CHEN, 1999; TEVATIA, 2012; DA FRÉ et al., 2016; HE et al., 2016; SACHDEVA et al., 2016). Assim, aplicando essa abordagem é possível conhecer o comportamento de produção de compostos intracelulares quando o micro-organismo é submetido a condições específicas de cultivo. Os produtos mais aplicados envolvem a produção de carotenoides e lipídeos.

Os modelos cinéticos existentes na literatura para descrever a formação de produtos (*P*) ao longo do cultivo são baseados no modelo de Luedeking-Piret (Equação 3.13). O modelo amplamente utilizado considera que a formação de produto apresenta um termo associado ao crescimento (α) e um termo não associado ao crescimento (β) (LUEDEKING; PIRET, 1959).

$$\frac{dP}{dt} = \alpha \cdot \frac{dX}{dt} + \beta \cdot X \tag{3.13}$$

4 MATERIAL E MÉTODOS

Nesta seção encontram-se detalhadas as metodologias que estão resumidamente descritas nos artigos desenvolvidos neste trabalho.

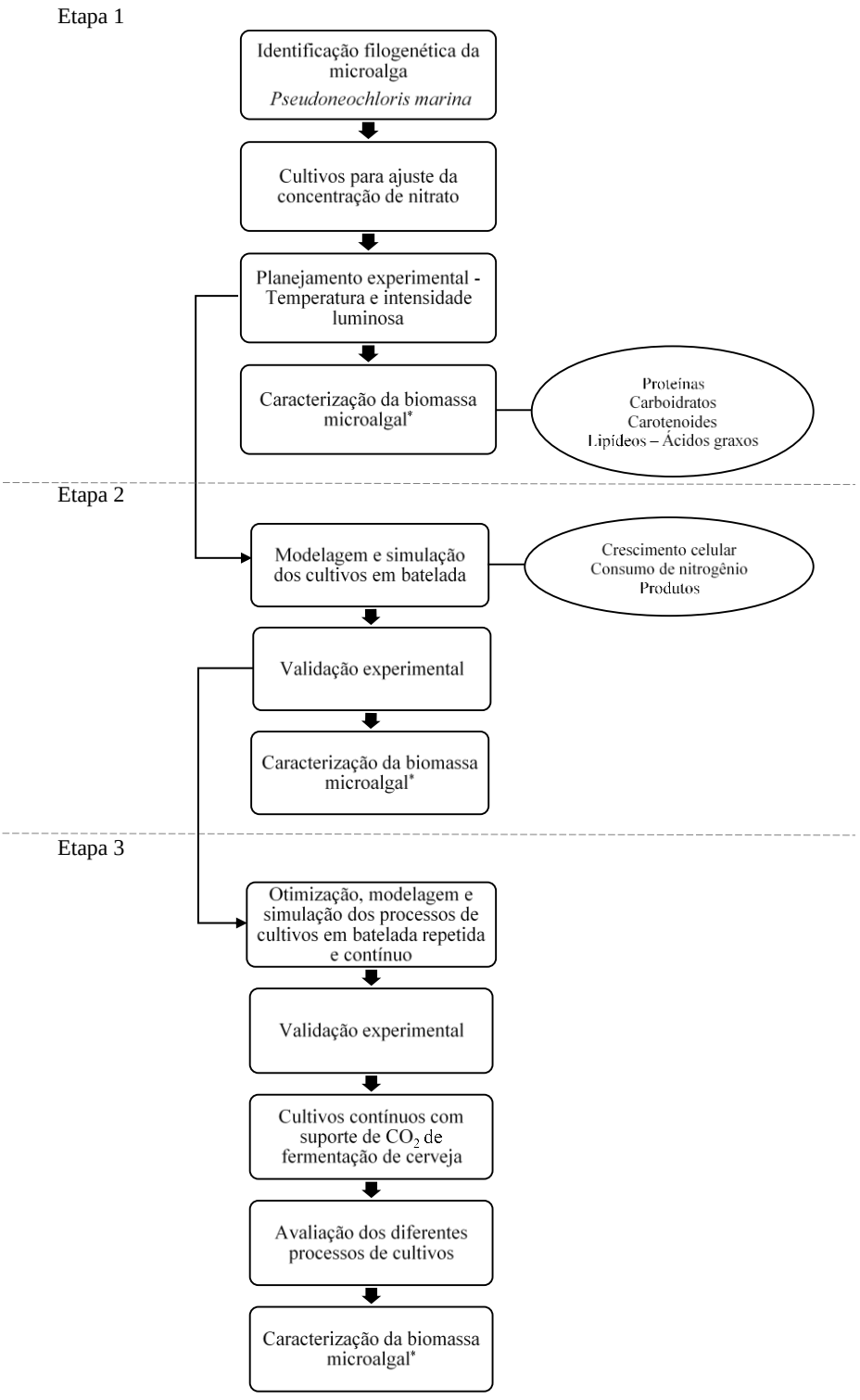

Figura 4.1 – Fluxograma geral das etapas de desenvolvimento do estudo.

4.1 Microalga e meio de cultivo

No presente estudo, foi investigada a cepa de microalgas eucarióticas BE-001 isolada originalmente pelo Departamento de Biologia Marinha da Universidade Federal Fluminense (Niterói, Rio de Janeiro, Brasil). A análise de DNA foi realizada pela Macrogen Inc. (Seoul, Korea). As amostras de DNA genômico foram extraídas usando um kit SV de extração de DNA genômico MG Plant (Doctor protein INC, Korea). A região rDNA 18S foi submetida a amplificação por PCR utilizando os iniciadores, MA1 (5 'GTAGTCATATGCTTGTCTC 3') e MA2 (5 'CTTCTGCAGGTTCACC 3'). A análise PCR foi realizada para ambos os marcadores com desnaturação inicial a 96 °C durante 5 min, 40 ciclos de desnaturação a 96 °C durante 1 min e 72 °C durante 1 min, com uma extensão final a 72 °C durante 5 min. (Hadi et al., 2016). Os produtos de PCR purificados foram então sequenciados em Sanger com o kit de sequenciamento BigDye Terminator v3.1 e um sequenciador automático 3730xl (Applied Biosystems, Foster City, CA). As sequências de nucleotídeos foram determinadas em ambas as cadeias de produtos de amplificação por PCR.

As sequências de rDNA 18S resultantes foram comparadas com sequências depositadas na base de dados da sequência de nucleotídeos do GenBank, utilizando a ferramenta Basic Local Alignment Search Tool (BLAST) (Kent, 2002). As sequências obtidas do GenBank foram adicionadas manualmente usando o software Molecular Evolutionary Genetics Analysis (MEGA7) (Kumar et al., 2016) e os alinhamentos foram realizados automaticamente usando múltiplos alinhamentos de sequência ClustalW (Thompson et al., 1994). A árvore filogenética foi construída usando o método de máxima verossimilhança baseado no modelo de Tamura-Nei (1993), conforme implementado pelo software MEGA7 (resultados apresentados no Capítulo 5).

A cepa identificada como *Pseudoneochloris marina* foi mantida em *Erlenmeyers* de 250 mL, contendo 100 mL de meio de cultivo f/2 (Guillard, 1975) em incubadora (BOD) sob 22 ºC com fotoperíodo de 12 h/12 h (claro/escuro).

A composição do meio f/2 para manutenção da cepa consiste em: 34 g L^{-1} de sal marinho (Red Sea Salt), 17 g L^{-1} de NaCl P.A., 300 mg L^{-1} de $NaNO_3$ P.A., 5 mg L^{-1} de $NaH_2PO_4.H_2O$ P.A., 30 mg L^{-1} de Na_2SiO_3. As soluções estoque foram preparadas segundo Lourenço (2006) e adicionados 1 mL L^{-1} ao meio de cultura f/2: solução de metais traço contendo 9,8 mg L^{-1} de $CuSO_4.5H_2O$ P.A., 22 mg L^{-1} de $ZnSO_4.7H_2O$ P.A., 1 mg L^{-1} de $CoCl_2.6H_2O$ P.A., 180 mg L^{-1} de $MnCl_2.4H_2O$ P.A. , 6,3 mg L^{-1} de

$Na_2MoO_4.H_2O$ P.A., 4,36 g L^{-1} de Na_2EDTA P.A. e 3,15 g de $FeCl_3.6H_2O$ P.A., solução de vitaminas contendo 100 mg L^{-1} de tiamina ($C_{12}H_{17}N_4OS$) P.A., 0,5 mg L^{-1} de cianocobolamina ($C_{63}H_{88}CoN_{14}O_{14}P$) P.A. e 0,5 mg L^{-1} de biotina ($C_{10}H_{16}N_2O_3S$) P.A.. A solução tampão foi composta por 50 g de tris ($C_4H_{11}NO_3$) P.A., aproximadamente 30 mL de HCl P.A. para ajuste de pH e água destilada para aferição de volume total de 200 mL. As soluções foram autoclavadas a 121 ºC por 15 min (Prismatec, Autoclave vertical CS), exceto a solução de vitaminas que foi esterilizada por microfiltração (*Sartorius Stedim Biotech*).

4.2 Inóculo de *Pseudoneochloris marina*

Os inóculos foram crescidos com meio de cultura estéril f/2 (Guillard, 1975) com adição de 17 g L^{-1} de NaCl P.A. e 300 mg L^{-1} de $NaNO_3$ P.A. induzindo estresse salino para maior produção de biomassa (DA FRÉ et al., 2016). Os inóculos foram preparados para 10 % do volume útil do fotobiorreator (2,4 L) em frascos do tipo *Erlenmeyers* (500 mL) estéreis adicionados de 216 mL de meio de cultura f/2 modificado e 24 mL de pré-inóculo. Os inóculos foram mantidos por 7 dias em incubadora (Oxylab, Oxy 304T) com agitação de 180 rpm, temperatura de 28 ºC e luminosidade de aproximadamente 42 µmol m^{-2} s^{-1} (Figura 4.2). O preparo do meio e as inoculações foram feitas em capela de fluxo laminar.

Figura 4.2 – Inóculos de *P. marina*.

4.3 Cultivo em fotobiorreatores de placa *air lift*

Os cultivos de microalga incialmente foram realizados em processo em batelada para realizar ajuste da fonte de $NaNO_3$ utilizando CO_2 sintético como fonte de carbono. As concentrações de $NaNO_3$ foram variadas entre 225 mg L^{-1} e 500 mg L^{-1} para avaliar a condição de maior produção de biomassa e esta foi fixada para a realização das demais etapas do trabalho.

A assepsia dos fotobiorreatores foi realizada pela adição de 5 mL de NaClO 2,5 % em cada reator e preenchidos totalmente com água mantendo aeração por 12 h. Após foi adicionado aos biorreatores 10 mL de solução de 250 g L^{-1} de $Na_2S_2O_3$ e mantido por 2 h com aeração. Após este período os fotobiorreatores foram esvaziados e lavados com água destilada estéril para recebimento do meio de cultivo e inóculo de microalgas.

Os cultivos foram realizados em fotobiorreatores de acrílico do tipo placa e *air lift* com volume útil de 2,4 L projetados de acordo com Kochem et al. (2014), providos de camisa interna para controle de temperatura conectada a banho térmico (Haake DC 30). A aeração do sistema foi realizada com vazão de 1 L min^{-1} de mistura de ar comprimido e CO_2 sintético e mantido em pH 7,0. A aeração foi distribuída por mangueiras com filtro de ar de 0,22 µm (Midisart®2000, Sartorius Stedim Biotech). A extremidade imersa no cultivo é composta por pedras porosas conectadas às mangueiras e as vazões de ar controladas por rotâmetros (Figura 4.3).

Figura 4.3 – Sistema de fotobiorreatores de placa *air lift* para cultivos de *P. marina*.

A iluminação foi realizada por painel com lâmpadas eletrônicas de 30 W e a luminosidade fornecida continuamente ao sistema. A iluminação foi variada em 140 µmol m^{-2} s^{-1}, 252 µmol m^{-2} s^{-1} e 364 µmol m^{-2} s^{-1} e medida por luxímetro digital (MS6610, Akso). As medidas serão realizadas na parede anterior (*riser*) dos fotobiorreator. A temperatura dos cultivos também foi avaliada a 20 ºC, 28 ºC e 36 ºC. A iluminação ótima e temperatura foram definidas em estudo apresentado no Capíluo 5.

4.4 Caracterização do cultivo e biomassa microalgal

Diariamente foram retiradas amostras dos cultivos para a realização de medidas de concentração celular, consumo de nitrogênio, carotenoides totais, proteínas e lipídeos. Ao final dos experimentos as biomassas obtidas foram separadas do meio de cultivo por centrifugação a 1000 × *g* por 10 min (4 ºC), liofilizadas e armazenadas para análises na biomassa final.

4.4.1. Crescimento celular

O crescimento foi avaliado por densidade ótica, tanto para o cultivo do inóculo, como para o teste nos biorreatores. Para realizar o ensaio, foram coletadas, diariamente, amostras em duplicata de cada cultivo teste, a densidade ótica foi medida utilizando espectrofotômetro a 750 nm. Os valores de absorbância foram convertidos para concentração de biomassa em peso seco (*X*), utilizando-se curva de calibração previamente definida.

4.4.2. Determinação de nitrato, lipídeos e carotenoides.

As análises de nitrato, lipídeos e carotenoides foram realizadas diariamente para acompanhamento da cinética de consumo de substrato e formação de produtos. O consumo de nitrato foi determinado por espectrofotometria pela metodologia de Cataldo et al. (1975), que consiste na nitração do ácido salicílico (ácido 2-hidrobenzóico) por íons NO_3^- que ocorre em pH alcalino formando o ácido 5-nitrossalicílico de coloração amarela (λ = 410 nm). Os resultados foram convertidos em teores de N-NO_3 por matéria seca da biomassa, utilizando curva de calibração.

Os teores de lipídeos foram determinados por método colorimétrico proposto por Mishra et al. (2014), que utiliza o reagente sulfo-fosfo-vanilina (SPV) para quantificação direta de cultura líquida de microalgas. Esse método foi utilizado para quantificar o conteúdo de lipídeos nas amostras de biomassa coletadas diariamente nos cultivos. O SPV reage com lipídeos e produz coloração rosa clara e pode ser quantificada utilizando espectrofotometria a 530 nm. Óleo de canola foi utilizado para definir a curva de calibração para determinação do conteúdo lipídico.

A quantificação de carotenoides totais foi determinada por método colorimétrico segundo Lichtentlhaler e Buschmann (2001), utilizando álcool etílico (95 %) como solvente. A densidade ótica (DO) foi medida em espectrofotômetro nas faixas de comprimentos de onda de 664 nm, 649 nm e 470 nm. A quantificação dos carotenoides totais foi realizada aplicando equação definida pelos autores.

4.4.3 Determinação de proteínas e carboidratos da biomassa microalgal

O teor de proteínas e carboidratos foi determinado pelos métodos de Lowry et al. (1951) e Dubois et al. (1956), respectivamente. As biomassas foram hidratadas *overnight* e mantidas a 4 ºC. As amostras foram centrifugadas (10000 × *g*, 5 min), o sobrenadante foi descartado, e 1 mL de NaOH (1N) foi adicionado ao pellet, misturado por agitador vortex e aquecido a 100 ºC por 30 min. As amostras foram arrefecidas até a temperatura ambiente e centrifugadas (10000 × *g*, 5 min). O conteúdo proteico foi determinado por método colorimétrico utilizando o reagente de Folin-Ciocalteu que sofre redução quando reage com proteínas, na presença do catalisador Cu^{+2} e produz um composto em absorção máxima de 750 nm.

A análise total de carboidratos foi medida após a hidrólise ácida da biomassa das microalgas. A biomassa foi acrescida de ácido sulfúrico (80 %, v v^{-1}) e mantidas *overnight* a 4 ºC. As amostras foram centrifugadas (10000 × *g*, 5 min) e o sobrenadante foi usado para a medição de carboidratos pelo método fenol-ácido sulfúrico que se baseia na reação dos açúcares incluindo metil ésteres com fenol em meio ácido produzindo compostos de coloração amarelo-alaranjado com absorção em 488 nm. Como padrão para as curvas de calibração foram utilizados albumina bovina e glicose para curvas de proteínas e carboidratos, respectivamente.

4.4.4 Identificação de carotenoides e ácidos graxos por cromatografia

As biomassas liofilizadas (0,020 g) foram utilizadas para extração de carotenoides utilizando o método descrito por Mandelli et al. (2012) e adaptado por Diprat et al. (2017). A extração exaustiva consiste na hidratação prévia das amostras, ruptura das paredes celulares por maceração utilizando acetato de etila seguido de metanol. As amostras foram dissolvidas usando metanol/metil-tert-butil-eter (MeOH:MTBE 1:1, v v^{-1}). Os carotenoides foram quantificados usando cromatógrafo Waters HPLC série 2695 (Wilmington, EUA) equipado com um detector de arranjo de diodos (Waters 2998 dual series) e usando coluna YMC-C30 (tamanho de partícula de 5 μm, 250 mm × 4.6 mm) (Waters, Wilmington, EUA). A vazão foi de 0,9 mL min^{-1} e a temperatura da coluna a 29 °C, eluída pela fase móvel de gradiente linear de MeOH: MTBE de 95:5 a 70:30 em 30 min, seguida de 50:50 em 20 min e mantendo essa proporção por 15 min (Rodrigues et al., 2014). A curva analítica de β-caroteno (0,13 a 15 mg L^{-1}) foi utilizada para quantificação de carotenoides (Menegol et al., 2017). A identificação dos carotenoides foi realizada de acordo com Menegol et al. (2017) usando um HPLC (Shimadzu, Kyoto, Japão) conectado em série com um detector de arranjo de diodos (DAD) e um espectrômetro de massa (MS) e fonte de ionização química de pressão atmosférica (APCI) (Bruker Daltonics, Esquire modelo 6000, Bremen, Alemanha).

O teor total de lipídeos foi determinado de acordo com Bligh e Dyer (1959) utilizando 0,30 g de biomassa liofilizada. Para a quantificação de ácidos graxos, a fração lipídica foi aquecida a 100 ºC durante 30 min com uma solução de metanol a 14 % de BF_3 sob atmosfera de N_2, de acordo com o modo descrito por Joseph e Ackman (1992). As amostras foram dissolvidas em solvente hexano e identificadas usando cromatografia gasosa (CG Modelo 2010, Shimadzu, Kyoto, Japão) equipado com amostrador e injetor automatizados, detector de ionização de chama e coluna capilar de sílica fundida (30 m × 0,25 mm, 0,25 μm espessura do filme, Rtx-Wax, Restek). Um mililitro de amostras foi injetado usando uma relação de divisão de 1:50. As temperaturas do detector de ionização de chama e injetor (FID) foram de 250 ºC. A temperatura do forno foi ajustada a 50 durante 1 min e aumentada para 200 ºC a um gradiente de 25 min^{-1}, 3 min^{-1} a 230 ºC/18 min. A quantificação dos ácidos graxos foi realizada de acordo com o método AOCS (1997). A identificação dos ácidos graxos presentes nas amostras foi realizada comparando o tempo de retenção com uma mistura padrão de ésteres metílicos de ácidos

graxos (FAME-MIX 37, Sigma) previamente analisados por cromatografia gasosa acoplada à espectrometria de massas (GC-MS).

4.5 Cultivos em batelada repetida e processo contínuo

Os cultivos foram realizados sob as condições de ambientais conforme descrito na seção 4.3. Inicialmente, os sistemas de cultivos em batelada repetida e contínuo foram mantidos em batelada por 7 dias até atingirem o início da fase estacionária de crescimento celular. Após esse período, para os cultivos em batelada repetida, foi iniciado o processo de retirada e adição de parte do volume dos cultivos (Figura 4.4). O volume do meio de renovação foi substituído a cada 48 h, com base na produtividade ótima de biomassa prevista pelo processo de simulação.

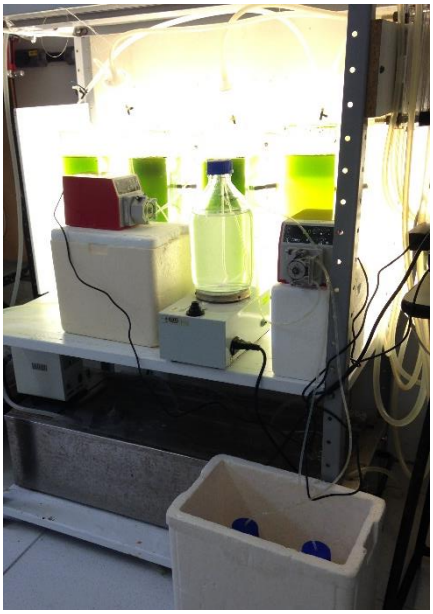

Figura 4.4 – Cultivos em batelada repetida e contínuo.

Os cultivos contínuos (Figura 4.4) quando iniciados foram mantidos em vazão constante de alimentação de entrada de meio e saída de cultura controladas por bombas peristálticas (400DM3, Watson-Marlow). Nesta condição, o meio f/2 foi suplementado com 1 mL L^{-1} de solução de fosfato (50 g L^{-1}) para suprir as necessidades de crescimento de microalgas em processo contínuo. Ambos os sistemas de cultivos foram mantidos por 456 h para avaliar a estabilidade de crescimento celular. A biomassa retirada dos

fotobiorreatores foi centrifugada (10000 × *g*, 5 min, 4 ºC), o sobrenadante foi descartado e a biomassa lavada com água destilada e novamente centrifugada. A biomassa resultante foi liofilizada e armazenada a −18 ºC para análises posteriores.

4.6 Cultivo contínuo de microalgas com sistema integrado de fotobiorreatores e fermentadores de cerveja

4.6.1 Produção de cerveja

A produção de cerveja foi realizada usando malte Pilsen, lúpulo *nuggets* 11 % AM T-90 e levedura liofilizada S-33 (*S. cerevisiae*). O malte foi triturado em moinho de disco para rompimento da casca para melhor extração do endosperma (Figura 4.5a) e misturado com água de infusão na relação 1:5 (peso/volume), utilizando o equipamento Grain Father (Figura 4.5b) sob a curva de aquecimento de 20 ºC a 66 ºC por 80 min e na sequência o aquecimento do mosto a 76 ºC por 20 min. O mosto foi clarificado usando uma peneira de aço inoxidável presente no interior do equipamento com recirculação de água. O material sólido foi retirado do Grain Father e a ebulição do mosto foi iniciada com adição de *nuggets* de lúpulo (1 g L^{-1}) e mantido por 60 min, após esse tempo, o mosto foi resfriado a 20 ºC a partir da recirculação do mosto e armazenado em frascos a -18 ºC.

Figura 4.5 – Moagem do malte (a) e produção do mosto no equipamento Grain Father (b).

4.6.2 Cinética de fermentação de cerveja e produção de CO_2

As fermentações (Figura 4.6) foram realizadas em triplicata utilizando frascos de Duran esterilizados (1 L), adicionados 0,5 g L^{-1} de levedura e mantidos a 20 ºC em banho termostático por 39 h. A produção cinética de CO_2 foi avaliada coletando amostras a cada 3 h para determinação da produção de etanol por metodologia de HPLC segundo Cortivo et al. (2018). A produção de CO_2 foi determinada por estequiometria considerando que 1 mol de CO_2 foi formado para cada 1 mol de etanol produzido. A taxa de acúmulo de CO_2 (g L^{-1} h^{-1}) durante a fermentação foi obtida pela derivada das curvas cinéticas.

Figura 4.6 – Cinética de fermentação de cerveja.

4.6.3 Cultivos contínuos utilizando CO_2 de fermentação de cerveja

Os cultivos contínuos foram realizados sob as condições igualmente como descritas na seção 4.5. As culturas experimentais foram mantidas em sistema de batelada por 7 dias com suprimento de CO_2 sintético. Após culturas contínuas foram adaptadas, conforme mostra a Figura 4.7, integrando os fermentadores com 20 % ($R_{5:1}$) e 40 % ($R_{2.5:1}$) do volume útil dos fotobiorreatores. Os fermentadores foram integrados aos cultivos a cada 24 h e adicionando-se 0,5 g L^{-1} de levedura e mantidos a 20 ºC em banho termostático. A operação de entrada e saída de meio de cultivo foi a mesma descrita

anteriormente para o sistema contínuo. Cada fermentador permaneceu conectado ao fotobiorreator por 48 h. Todas as culturas foram realizadas em duplicatas e os resultados expressam a média dos dados experimentais.

Figura 4.7 – Sistema integrado entre fotobiorreatores e fermentadores de cerveja.

4.7 Análise estatística

As análises estatísticas foram realizadas utilizando o *software* Statistica 10.1 (StatSoft, Inc.). Os experimentos e as análises da biomassa foram realizados em duplicata. Os resultados foram comparados pelo teste de Tukey a um nível de significância de 5 %.

INTRODUÇÃO AO DESENVOLVIMENTO DO TRABALHO

Os Capítulos 5, 6 e 7 apresentam os resultados do trabalho no formato de artigos científicos que constam de introdução, material e métodos, discussão e conclusão pertinentes a cada etapa desenvolvida. O Capítulo 6 apresenta as perspectivas do trabalho com base nos resultados obtidos até o presente momento.

O Capítulo 5 incialmente apresenta a identificação da microalga verde *P. marina* e nesta etapa foram avaliados os efeitos da concentração de nitrogênio, temperatura e intensidade luminosa na produtividade e composição da biomassa desta microalga cultivada em batelada com utilização de CO_2 como fonte de carbono. O artigo foi intitulado "Biochemical composition of green microalgae *Pseudoneochloris marina* grown under different temperature and light conditions*"* e publicado no periódico Biocatalysis and Agricultural Biotechnology, classificação Qualis A2 (Cite score 2.19) na área de Ciência de Alimentos.

O Capítulo 6 foi desenvolvido com base nas melhores condições nutricionais e ambientais avaliadas no Capítulo 5. Neste capítulo, intitulado "Kinetic modeling of cell growth, nitrogen consumption and intracelular bioproducts of *Pseudoneochloris marina* cultures in airlift photobioreactors", foi realizada a modelagem matemática de crescimento celular, consumo de nitrogênio e formação de produtos (carotenoides, proteínas e lipídeos) para de cultivos em batelada de *P. marina*. As modelagens matemáticas de crescimento celular e consumo de nitrogênio e simulação do processo foram baseados em cinco modelos cinéticos e formação de produtos a partir de quatro modelos desenvolvidos e descritos na literatura e será submetido em periódico da área.

No Capítulo 7, intitulado "Simulation and optimization of repeated-batch and continuous cultures of *Pseudoneochloris marina*: validation with experimental data and use of CO_2 from beer fermentation", está apresentado o estudo da simulação e otimização dos processos de cultivos de *P. marina* em batelada repetida e contínuo com base nos resultados obtidos no Capítulo 6. Adicionalmente foi testado o potencial uso de CO_2 de fermentação de cerveja para suprir o fornecimento de CO_2 aos cultivos de microalgas.

5 BIOCHEMICAL COMPOSITION OF GREEN MICROALGAE *Pseudoneochloris marina* GROWN UNDER DIFFERENT TEMPERATURE AND LIGHT CONDITIONS

Carolina Ferrer Gonçalves, Tania Menegol, Rosane Rech*

Food Science and Technology Institute, Federal University of Rio Grande do Sul, Av. Bento Gonçalves, 9500, PO Box 15090, ZC 91501-970 Porto Alegre, RS, Brazil. Phone 55 51 3308 1356
*E-mail: rrech@ufrgs.br

ABSTRACT

Environmental factors such as temperature, light intensity, and nutrient availability, are central in microalgae metabolism, affecting their growth and composition. This study evaluated the effects of nitrogen concentration (37.1 – 78.8 mg L^{-1} $N\text{-}NO_3$), temperature (20 – 36 ºC) and light intensity (140 – 364 µmol m^{-2} s^{-1}) on biomass productivity and biochemical composition of *Pseudoneochloris marina*. The highest biomass productivity (0.26 g L^{-1} d^{-1}) was achieved with 74.1 mg L^{-1} $N\text{-}NO_3$ at 28 ºC and 252 – 364 µmol m^{-2} s^{-1}. Protein content decreased with the increment of factors levels and the highest content was 236 ± 18 mg g^{-1} at 20 ºC and 140 µmol m^{-2} s^{-1}. The carotenoids and lipids were affected negatively by light intensity. The highest xanthophylls and carotenes contents were, respectively, 2.55 ± 0.39 mg g^{-1} and 1.25 ± 0.01 mg g^{-1} at 20 ºC/28 ºC and 140 µmol m^{-2} s^{-1}. The major carotenoids were all-*trans*-lutein (36.0 ± 2.9 %) and all-*trans*-β-carotene (13.2 ± 1.2 % of total carotenoids). The saturated, monounsaturated and polyunsaturated fatty acids represented 46.1 ± 1.5 %, 10.6 ± 1.7 % and 43.3 ± 1.0 % of total fatty acids. The main fatty acids were C16:0, C18:2n-6, C18:3n-3 and C18:1. The lowest ω6:ω3 ratio was 1.6 ± 0.1, at the lowest temperature.

Key-words: *Pseudoneochloris*; lutein; polyunsaturated fatty acids; light; temperature; nitrogen

5.1 Introduction

Microalgae are a source of a wide range of natural products including carbohydrates, proteins, lipids and high-value products, such as carotenoids and polyunsaturated fatty acids. Microalgal biomass is able to accumulate significant amounts of these compounds and can be used in pharmaceutical products, food additives, feed supplements or in the production of biofuels (i.e. biodiesel, bioethanol, biohydrogen or methane) (ANJOS et al., 2013; BENAVENTE-VALDÉS et al., 2016; D'ALESSANDRO; ANTONIOSI FILHO, 2016).

Interest in green algae has been growing. However, it is estimated that more than 5000 species have not yet been described (HADI et al., 2016). Due to the complexity of identifying single-celled green algae and ancient taxonomic identification conflicts, this group is often undergoing new taxonomic revisions (KRIENITZ et al., 2004; NEUSTUPA et al., 2009; DARIENKO et al., 2010; SOMOGYI et al., 2013; KRIENITZ; HUSS; BOCK, 2015; PEGG et al., 2015). Currently, DNA barcoding techniques that identify species based on DNA sequence similarity comparing with the database is the most used method to differentiate species with similar morphology (HADI et al., 2016).

Through the photosynthesis, CO_2 from the atmosphere is converted into biomass by autotrophic microorganisms when associated with nutrient supply and under adequate growth conditions. Microalgae are known to have a higher growth rate and a higher capacity for CO_2 biofixation when compared to terrestrial plants (ZENG et al., 2011).

The photosynthesis process is affected by nutrient availability and environmental parameters of cultivation. Nitrogen is an essential nutrient for the metabolic activities of microalgae cells. Nitrogen limitation decreases cell growth, protein synthesis, and increases reserve compounds, like carbohydrates and lipids (PANCHA et al., 2014). Temperature and light intensity are known as the most critical extrinsic factors in photoautotrophic cultures, affecting microalgae metabolism, cell growth rate and biomass composition (HO et al., 2014a; THAWECHAI et al., 2016). Also, the inorganic carbon acquisition depends directly on light intensity and indirectly on temperature, which modulates the enzymatic activity. The simultaneous impact of these two environmental factors are worth to be studied to better understand the daily pattern of carbon acquisition and storage (BONNEFOND et al., 2016; MINHAS et al., 2016).

Considering the interest of the biotechnological industry to explore alternative sources for extraction of high-value compounds, the investigation of untraditional

microalgae species and different culture conditions are essential steps in the development of strategies to large-scale microalgae production. The green microalgae *Pseudoneochloris marina* (*Chlorophyta)* was identified by Watanabe et al. (2000) and belongs to the class of *Ulvophyceae*. To the best of our knowledge, few studies report *P. marina*, none of them studying culture parameters on cell growth and biochemical composition of its biomass. Thereby, this study evaluated the effects of nitrogen, temperature and light intensity in *P. marina* cultures on biomass productivity and composition (carbohydrates, proteins, carotenoids, lipids). Additionally, the carotenoid and fatty acids profiles were determined for each culture condition.

5.2 Material and methods

5.2.1 Analysis of phylogenetic identification

In the present study, we investigated the eukaryotic microalgal strain BE-001 isolated originally by the Department of Marine Biology, Fluminense Federal University (Niteroi, RJ, Brazil). The cultures were maintained in a growth chamber at 22 ºC under a photoperiod of 12/12 h (light/dark) in 250 mL Erlenmeyer flasks containing 100 mL of culture medium f/2 (GUILLARD, 1975) with modified $NaNO_3$ concentration (300 mg L^{-1}) and an additional amount of NaCl (17 g L^{-1}) to induce saline stress.

The DNA analysis was performed by Macrogen Inc. (Seoul, Korea). Genomic DNA samples were extracted using an MG Plant Genomic DNA extraction SV kit (Doctor protein INC, Korea). The 18S rDNA region was subjected to PCR amplification using the primers MA1 (5' GTAGTCATATGCTTGTCTC 3') and MA2 (5' CTTCTGCAGGTTCACC 3'). The PCR reaction was performed for both markers with initial denaturation at 96 °C for 5 min, 40 cycles of denaturation (96 °C for 1 min) and annealing (72 °C for 1 min), with a final extension at 72 °C for 5 min (HADI et al., 2016). The purified PCR products were then Sanger-sequenced with the BigDye Terminator v3.1 sequencing kit and a 3730xl automated sequencer (Applied Biosystems, Foster City, CA). Nucleotide sequences were determined on both strands of PCR amplification products. The resulted 18S rDNA sequences were compared to sequences deposited in the GenBank nucleotide sequence database using the Basic Local Alignment Search Tool (BLAST) (KENT, 2002). Sequences obtained from GenBank were manually added using the

Molecular Evolutionary Genetics Analysis (MEGA7) software (KUMAR; STECHER; TAMURA, 2016) and the alignments were performed automatically using multiple sequence alignment ClustalW (THOMPSON; HIGGINS; GIBSON, 1994). The phylogenetic tree was constructed using the Maximum Likelihood method based on the Tamura-Nei model (TAMURA; NEI, 1993), as implemented by MEGA7 software.

5.2.2 Pre-cultures and cultivation

The pre-cultures were prepared in 500 mL Erlenmeyer flasks with 240 mL working volume using modified f/2 medium, as described above, and inoculated with 24 mL of stock culture. The flasks were incubated in a rotatory shaker (Oxylab, Oxy 304T) at 28 ºC and 180 rpm with continuous illumination of 42 µmol m^{-2} s^{-1} for 7 days.

All cultures were performed in flat-panel airlift photobioreactors (KOCHEM et al., 2014) filled with 2.16 L of modified f/2 medium, according to the specific experiment, and 240 mL of pre-cultures. The cultures were daily supplemented with 1 mL L^{-1} of phosphate solution and 1 mL L^{-1} of trace-metals solution to avoid nutrient limitation (CHAGAS et al., 2015). The airflow was kept at 1 L min^{-1} of CO_2-enriched filtered air (0.22 µm Midisart®2000, Sartorius Stedim Biotech) controlled by rotameters. The mixture of CO_2 and compressed air was adjusted by rotameter to maintain the culture at pH 7.0. The pH was measured using pH-indicator strips (MColorpHast™, Merck, Germany). The light intensity was measured using a digital luximeter.

The experiments to determine optimum nitrogen concentration in the culture medium (f/2 plus 17 g L^{-1} NaCl) used different $NaNO_3$ concentrations (225 to 475 mg L^{-1} $NaNO_3$ equivalent to 37.1 to 78.2 mg L^{-1} N-NO_3), 28 °C, 252 µmol m^{-2} s^{-1} for 7 days (DA FRÉ et al., 2016; MENEGOL et al., 2017). Experiments to determine the effect of temperature (20 °C, 28 °C and 36 °C) and light intensity (140 µmol m^{-2} s^{-1}, 252 µmol m^{-2} s^{-1}, and 364 µmol m^{-2} s^{-1}) on microalgae growth and composition were performed in modified f/2 medium (addition of 17 g L^{-1} NaCl and 450 mg L^{-1} $NaNO_3$) for 7 days, according to a face-centered design split into two blocks.

Biomass concentration was measured during cultivation by optical density at 750 nm and correlated with dry cell weight (X). At the end of cultures, the entire content of the bioreactors was centrifuged (10,000 × g, 5 min, 4 ºC), the supernatant was discarded, and the biomass was washed with distilled water and centrifuged again. The resulting biomass was lyophilized and stored at −18 ºC.

5.2.3 Carotenoids Analysis

The lyophilized biomasses (0.020 g) were used for carotenoids extraction using the method described by Mandelli et al. (2012) and adapted by Diprat et al. (2017). The exhaustive extraction consists of the previous hydration of the samples, rupture of cell walls by maceration using ethyl acetate followed by methanol. The samples were dissolved using methanol/methyl tert-butyl ether (MeOH:MTBE 1:1, v v^{-1}). Carotenoids were quantified by Waters HPLC 2695 series system (Wilmington, EUA) equipped with a diode array detector (Waters 2998 dual series) and using YMC-C30 column (5 μm particle size, 250 mm × 4.6 mm) (Waters, Wilmington, USA). The flow rate was 0.9 mL min^{-1} and column temperature 29 °C, eluted by linear gradient mobile phase of MeOH:MTBE from 95:5 to 70:30 in 30 min, followed by 50:50 in 20 min and maintaining this proportion for 15 min (RODRIGUES et al., 2014). Analytical β-carotene curve (0.13 to 15 mg L^{-1}) was used for carotenoid quantification (DIPRAT et al., 2017). The carotenoid identification was performed according to Menegol et al. (2017) using an HPLC (Shimadzu, Kyoto, Japan) connected in series with a diode array detector (DAD) and a mass spectrometer (MS) with an ion trap analyzer and atmospheric pressure chemical ionization (APCI) source (Bruker Daltonics, Esquire model 6000, Bremen, Germany). The carotenoid chromatogram is shown in Supplementary Material (Figure 5.S1).

5.2.4 Lipids content and fatty acid composition

The total lipid content was determined according to Bligh and Dyer (BLIGH; DYER, 1959) using 0.30 g of lyophilized biomass. For fatty-acids quantification, the lipid fraction was boiled for 30 min with a 14 % BF_3-methanol solution under N_2 atmosphere according to the method described by Joseph and Ackman (1992). The samples were dissolved in hexane solvent and identified using gas chromatography (GC Model 2010, Shimadzu, Kyoto, Japan) equipped with automated sampler and injector, flame ionization detector and a capillary column of fused silica (30 m × 0.25 mm, 0.25 μm film thickness, Rtx-Wax, Restek). One milliliters of samples were injected using split ratio of 1:50. The injector and flame ionization detector (FID) temperatures were 250 °C. The oven temperature was set at 50 °C for 1 min and increased to 200 °C at a gradient of 25 °C min^{-1}, followed by a gradient of 3 °C min^{-1} until 230 °C. The fatty acids quantification was performed according to the AOCS method (1997). The identification of the fatty acids

present in the samples was performed comparing the retention time with a standard mixture of fatty acid methyl esters (FAME-MIX 37 standard Sigma) previously analyzed by gas chromatography-mass spectrometry (GC–MS). The fatty acids chromatogram is shown in Supplementary Material (Figure 5.S2).

5.2.5 Measurement of carbohydrates and proteins content

The lyophilized biomass was hydrated overnight with 5 mL of distilled water and kept at 4 ºC. The samples were centrifuged (10,000 × g, 5 min), the supernatant was discarded, and 1 mL of NaOH (1 N) was added to the pellet, mixed by vortex stirrer and heated at ebullition temperature for 30 min. The samples were cooled to room temperature and centrifuged (10,000 × g, 5 min). The protein content was measured in the supernatant according to Lowry et al. (1951). The results were correlated by calibration curve using bovine serum albumin as protein standard. The total carbohydrate analysis was measured after acid hydrolysis of the microalgae biomass. Aqueous sulfuric acid (80 %, v v^{-1}) was added to the biomass and the mixture was kept overnight at 4 ºC. The samples were centrifuged (10,000 × g, 5 min) and the supernatant was used for carbohydrate measurement by the phenol-sulfuric acid method (DUBOIS et al., 1956). The results were correlated to a calibration curve of glucose.

5.2.6 Statistical analysis

The statistical analyses were performed using Statistica 10.1 software (StatSoft, Inc.). The results were compared by Tukey test at a significance level of 5 %. The experimental data of the face-centered design were analyzed by multiple regression analysis using a second-order polynomial equation:

$$Y = \beta_0 + \beta_1 X_1 + \beta_2 X_2 + \beta_{11} X_1^2 + \beta_{22} X_2^2 + \beta_{12} X_1 X_2$$

Where Y is the predicted response value; β_0, β_i, β_j, β_{ii}, β_{jj} and β_{ij} are the parameters estimated from the regression results. The responses described above were used to assess the interaction outcomes of temperature (X_1) and light intensity (X_2). The responses evaluated were biomass productivity, carotenoids, xanthophyll, lipids, fatty acid methyl esters (FAMES), carbohydrates and proteins.

5.3 Results and discussion

5.3.1 Microalgae identification

The 18s rDNA of the green algae culture BE 001 was successfully amplified by the MA1 primer and showed high similarity (96 %) to *Pseudoneochloris marina* U41102.1. However, the MA2 primer used in this study presented a low similarity (56 %) with *Pseudoneochloris marina* U41102.1 and high similarity to *Urospora* genus (83 %). Watanabe et al. (WATANABE et al., 2000) reported that *Pseudoneochloris marina*, formerly described as *Neochloris* sp., is grouped in a clade with members of Ulvophyceae together with members Ulotrichales and very close to the genus *Acrosiphonia*. This report may explain the results obtained in this study, the low similarity of the sequence obtained with the MA2 primer with the genus *Urospora* and *Pseudoneochloris*. Since BE 001-MA2 sequence was not conclusive, the microalga identification was based on BE 001-MA1 that clearly binds BE 001 to *Pseudoneochloris marina* U41102.1 (Figure 5.1).

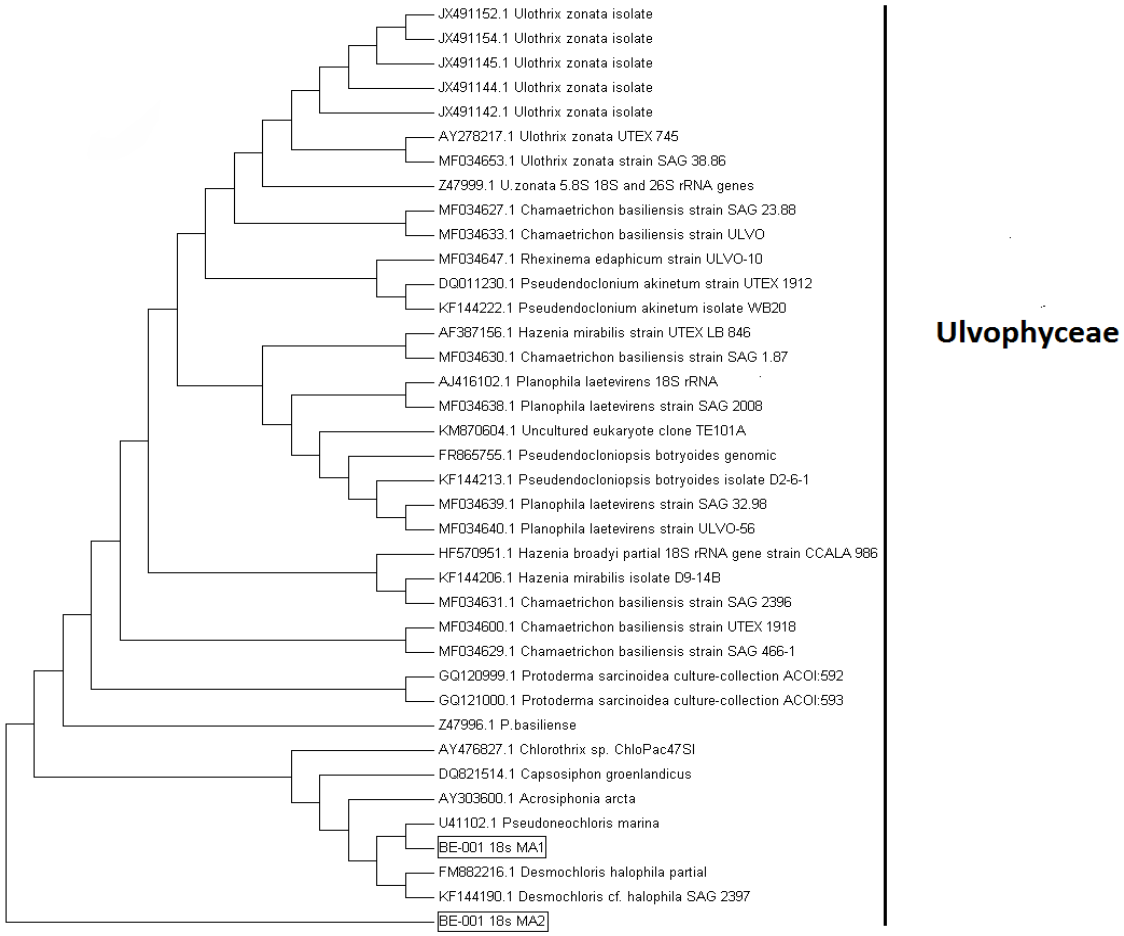

Figure 5.1 - Phylogenetic tree showing the relationships among sequences de 18S rDNA – BE 001 18sMA1, BE 001 18sMA2 and the most similar sequences retrieved from databases.

5.3.2 Microalga growth and composition

In closed systems of microalgae cultures, CO_2 and nutrients supply, in addition to external parameters such as temperature and light intensity, are crucial for photosynthetic efficiency, affecting cell growth rate and biomass composition. *P. marina* is a green microalgae species identified recently (WATANABE et al., 2000) and its biotechnological potential has not been explored yet.

Preliminary tests were performed using different nitrogen concentration in culture medium to determine the best condition for biomass production by *P. marina* (Table 5.1). The highest biomass concentration (2.02 ± 0.21 g L^{-1}) was achieved using 74.1 mg L^{-1} $N\text{-}NO_3$, but with no significant difference to the values obtained using 68.4 mg L^{-1} or 78.2 mg L^{-1} $N\text{-}NO_3$. Decreasing $NaNO_3$ concentration resulted in lower cell growth, probably due to nutrient limitation. This way, the 74.1 mg L^{-1} $N\text{-}NO_3$ (450 mg L^{-1} $N\text{-}NO_3$) concentration was chosen for further experiments to evaluate the effect of temperature and light intensity on biomass growth and composition (carbohydrates, lipids, proteins, carotenoids and FAMES).

Table 5.1 - Biomass concentration of *P. marina* grown under different nitrogen conditions.

$NaNO_3$ (mg L^{-1})	Biomass (g L^{-1})
225	1.33 ± 0.09^{b}
300	1.47 ± 0.21^{b}
375	1.46 ± 0.09^{b}
415	1.58 ± 0.04^{ab}
450	2.02 ± 0.21^{a}
475	1.76 ± 0.01^{ab}

Different letter in the same column indicates significant difference by Tukey test at 5 % significance level.

The cell growth kinetics for the different conditions of temperature and light intensity is shown in Figure 5.2. The highest biomass concentration (1.80 g L^{-1}) was achieved using light intensities of 252 µmol m^{-2} s^{-1} or 364 µmol m^{-2} s^{-1} at 28 ºC. Cell growth limitation was observed in the experiments where the lower levels of light were applied: biomass of 0.70 g L^{-1} and 0.87 g L^{-1} were obtained under the conditions of

140 µmol m^{-2} s^{-1} and temperature of 20 °C and 36 °C, respectively. The temperature is known to affect nitrate uptake, changing the biochemistry of nitrogen metabolism. The high temperature increases the activity of intracellular proteolytic enzymes, resulting in the degradation of nitrogen reductase. In association with light, extreme temperature levels contribute to the inhibition of cell growth (HO et al., 2014b; KIRAN et al., 2016). The optimization of light intensity and temperature parameters are essential to reach maximal biomass productivity.

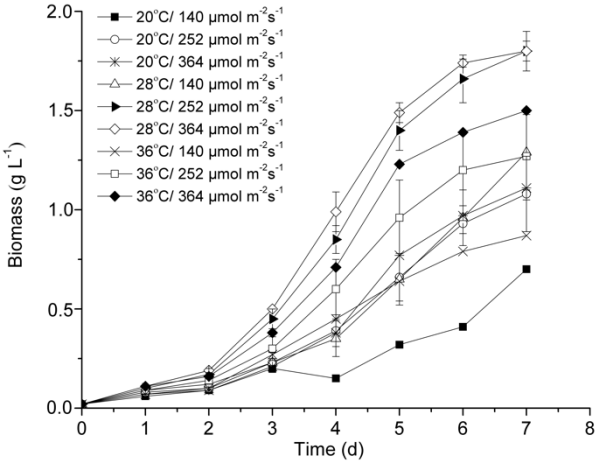

Figure 5.2 - Kinetics of *P. marina* growth under different conditions of temperature and light intensity.

The mathematical models for biomass productivity (P_X) of *P. marina* under different temperature and light, as well as its major biomass components (proteins, lipids and carbohydrates), are shown in Table 5.2. Biomass productivity was affected by both temperature and light intensity. The response surface generated from the mathematical model (Figure 5.3) shows that the increase of light availability favors the biomass productivity of *P. marina*, while for temperature, there is a maximum between 26 °C and 32 °C. The highest biomass productivity of *P. marina* (0.26 g L^{-1} d^{-1}) was reached at 28 ºC and light intensity between 252 and 364 µmol m^{-2} s^{-1}. Ho et al. (HO et al., 2014b) studied the biomass production of *Desmodesmus* sp. under different temperatures (30 – 40 ºC) and light intensities (300 – 1100 µmol m^{-2} s^{-1}). The authors verified that biomass productivity increased with the rising of temperature and light intensity and the optimum level of biomass productivity (0.76 g L^{-1} d^{-1}) was achieved when the cells were grown at 35 ºC and 700 µmol m^{-2} s^{-1}.

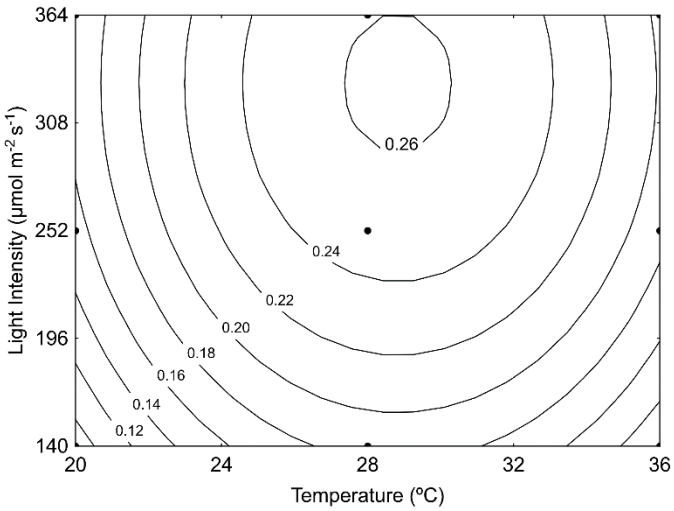

Figure 5.3 - Effects of temperature and light intensity on biomass productivity (g L^{-1} d^{-1}) of *P. marina* grown in batch culture.

The protein and carbohydrate contents were also affected by both variables. The highest protein content (236 ± 18 mg g^{-1}) was obtained at the lowest temperature (20 ºC) and light intensity (140 µmol m^{-2} s^{-1}) conditions, that also correspond the lowest biomass productivity of all experiments. At low light intensity, temperature showed a pronounced positive effect on protein content, while at high light intensity, protein content was little affected by temperature (Figure 5.4).

Table 5.2 - Regression coefficients of the coded variables for biomass productivity, protein, carbohydrate, total carotenoid and lipid content in *P. marina* biomass cultured under different temperatures (X_1, 20 to 36 °C) and light intensities (X_2, 140 to 364 μmol m^{-2} s^{-1}).

Regression coefficients	Biomass Productivity (g L^{-1} d^{-1})		Protein (mg g^{-1})		Carbohydrate (mg g^{-1})		Carotenoid (mg g^{-1})		Lipid (mg g^{-1})	
	Coeff.	*p*-value	Coeff.	*p*-value	Coeff.	*p*-value	Coeff.	*p*-value	Coeff.	*p*-value
β_0	0.249	<0.001	108.8	<0.001	439.3	<0.001	2.836	<0.001	108.038	<0.001
β_1	0.017	0.05	-22.56	0.010	-		-	-	-	-
β_2	0.370	<0.001	-28.17	<0.001	42.9	0.002	-0.492	<0.001	-17.513	<0.001
β_{11}	-0.080	<0.001	-	-	47.6	0.010	-	-	-	-
β_{22}	-0.027	0.028	28.89	0.013	-		0.245	0.048	6.075	0.048
β_{12}	-		23.93	0.010	-		-	-	-	
Blocks	-		-11.35	0.013	-		-0.428	<0.001	-	
R^2	0.893		0.924		0.651		0.896		0.865	
Regression *p*-value	2.8×10^{-5}		2.8×10^{-5}		0.001		3.5×10^{-6}		2.2×10^{-6}	
Lack of fit *p*-value	0.910		0.752		0.386		0.046		0.059	

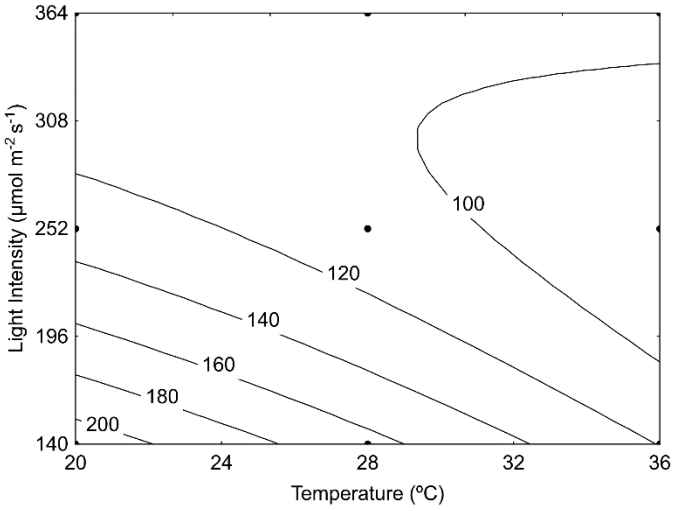

Figure 5.4 - Effects of temperature and light intensity on protein content (mg g^{-1}) of *P. marina* grown in batch culture.

Renaud et al. (2002) related that high temperatures decrease protein content significantly in some tropical microalgal species, this fact that can be explained by the breakdown of protein conformation and interference with enzyme regulators. The high light intensity promotes better photosynthesis efficiency. Also, the nitrogen starvation at the end of the cultures (data not shown) resulted in low protein content in consequence of intracellular nitrogen consumption for cell growth (PAES et al., 2016). Therefore, under high light, nitrogen starvation and CO_2 supply, the protein in biomass microalgae can be consumed as a nitrogen source and, carbohydrate accumulation may increase during cell growth (CHEN et al., 2013).

The carbohydrate content was positively affected by both light intensity and temperature (Table 5.2), however, as it showed a low determination coefficient (R^2 = 0.651), the contour lines have not been plotted. The carbohydrates content ranged between 379 ± 10 mg g^{-1} at 28 ºC and 140 µmol m^{-2} s^{-1} and 538 ± 13 mg g^{-1} at 36 ºC and 364 µmol m^{-2} s^{-1}. The synthesis of carbohydrates depends on temperature and light intensity, which influences cell growth rate when applied to cultures at optimal levels. Also, the accumulation of carbohydrates in microalgae biomass is due to CO_2 biofixation during the photosynthetic process (CHEN et al., 2013; MINHAS et al., 2016).

Carvalho et al. (2009), in *Pavlova lutheri* cultivation, demonstrated that an increase on the light intensity in the range of 30 – 400 µmol m^{-2} s^{-1} subtly increased the accumulation of carbohydrates. Additionally, cultures of *Chlorella vulgaris* in airlift

photobioreactors showed an increase in carbohydrates content from 8.5 % to 40 % (d.w.) when increasing light intensity from 215 to 330 μmol m^{-2} s^{-1} (FERNANDES et al., 2010).

Lipids and carotenoids contents were affected only by light intensity (Table 5.2, Figure 5.5). For carotenoids, the increase in light intensity on cultures resulted in a slight decrease from 3.6 ± 0.6 mg g^{-1} to 2.6 ± 0.4 mg g^{-1}. This result suggests that carotenoids damage is related with the photoprotective role of carotenoids in cells, which stabilizes light-harvesting by membranes of chloroplasts, reducing the singlet oxygen production and scavenging free radicals induced by high light stress (HUANG et al., 2017). The same behavior was observed for lipid content, whereby the rise in light intensity level from 140 to 364 μmol m^{-2} s^{-1} provided a reduction of 132 ± 7 mg g^{-1} to 97 ± 3 mg g^{-1}.

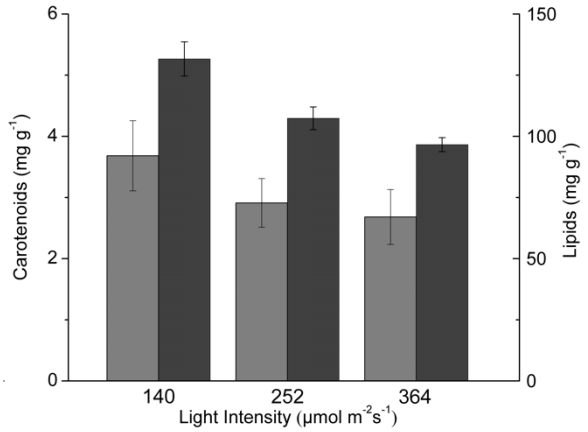

Figure 5.5 - Carotenoids (■) and lipids (■) content in *P. marina* biomass cultured under different light intensities. Error bars represent the standard deviation of each culture condition.

Light intensity in photoautotrophic microalgae systems strongly acts on cell growth, CO_2 fixation, and may change the biomass biochemical composition, such as carbohydrates and lipids (CHEN et al., 2013). Zhu et al. (2016) showed that, for many microalgae species, lipid accumulation is associated with cell growth, thereby an increase in the light intensity promotes high cell growth and lipid content. On the other hand, the authors exposed that the relationship between light intensity and intracellular lipid accumulation is microalgae-specific. Additionally, some stress conditions can cause photoinhibition, which damages microalgae photosystems and thus reduces lipids accumulation. This correlation agrees with our study, which was observed that an increase in light intensity was favorable to rise the carbohydrate content but not lipid accumulation.

5.3.3 Carotenoid identification

The carotenoid biosynthesis differs from one species to another. Carotenoids absorb light and quench the excess of energy in photosynthetic metabolism. Some primary carotenoids, such as lutein, are used as accessory pigments, which can transfer absorbed energy to chlorophylls (YE; JIANG; WU, 2008). Temperature and light intensity are both critical environmental factors that affect carotenoid accumulation in microalgae cells.

Carotenoids are divided into two groups: xanthophylls and carotenes. The increment in the temperature and light intensity affected xanthophylls negatively, while carotenes content was influenced positively by temperature and negatively by light intensity (Table 5.3). Xanthophylls and carotenes contents ranged between 1.61 ± 0.34 mg g^{-1} and 2.51 ± 0.02 mg g^{-1}, 0.66 ± 0.03 mg g^{-1} and 1.25 ± 0.01 mg g^{-1}, respectively (Table 5.4). The major carotenoids identified from *P. marina* were all-*trans*-lutein, all-*trans*-zeaxanthin, all-*trans*-β-carotene and all-*trans*-α-carotene.

Carotenoids have an essential function in membrane stabilization acting in light harvesting, thermal energy dissipation and scavenging reactive oxygen species (ROS) (GARCÍA-CAÑEDO et al., 2016). Thereby, under high light exposure, the reduction of carotenoids can be associated with photoprotection of membrane cells of some species of microalgae, including *P. marina* evaluated in this study. In batch cultures of *Neochloris oleabundans* with CO_2 input and nitrogen supply, the authors observed that an increment on light intensity from 240 to 400 μmol m^{-2} s^{-1} slightly reduced the total carotenoids (9.4 ± 0.1 to 8.9 ± 0.1 mg L^{-1} d^{-1}) and lutein productivities (3.3 ± 0.0 to 2.6 ± 0.1 mg L^{-1} d^{-1}) (URRETA et al., 2014). The highest β-carotene content (118 mg L^{-1}) of *D. salina* cultivated under different environmental conditions was achieved in the range of 22 ºC to 25 ºC and light intensity of 135 μmol m^{-2} s^{-1}. The authors observed that an increment in the light intensity showed no difference in β-carotene accumulation and that lower or higher light intensity level could restrain algae growth (WU et al., 2016).

Table 5.3 - Regression coefficients of the coded variables for xanthophylls, carotenes, saturated (ΣSFA), monounsaturated (ΣMUFA) and polyunsaturated (ΣPUFA) fatty acids contents in *P. marina* biomass cultured under different temperatures (X_1, 20 to 36 °C) and light intensities (X_2, 140 to 364 μmol m^{-2} s^{-1}).

Regression coefficients	Xanthophylls (mg g^{-1})		Carotenes (mg g^{-1})		ΣSFA (mg g^{-1})		ΣMUFA (mg g^{-1})		ΣPUFA (mg g^{-1})	
	Coeff.	*p*-value	Coeff.	*p*-value	Coeff.	*p*-value	Coeff.	*p*-value	Coeff.	*p*-value
β_0	1.945	<0.001	0.960	<0.001	13.332	<0.001	2.794	<0.001	12.524	<0.001
β_1	-0.210	0.010	0.118	<0.001	-0.651	0.006	0.459	<0.001	-	-
β_2	-0.301	<0.001	-0.192	<0.001	-0.884	<0.001	-0.264	0.017	-1.223	<0.001
β_{11}	-	-	-	-	-0.680	0.030	0.0358	0.021	-0.593	0.036
β_{22}	-	-	0.105	0.010	-	-	-	-	-	-
β_{12}	-	-	-	-	-	-	-	-	-	-
Blocks	-0.283	<0.001	-0.145	<0.001	-	-	-	-	-	-
R^2	0.838		0.939		0.759		0.756		0.800	
Regression *p*-value	5.0×10^{-5}		1.3×10^{-6}		0.001		0.001		2.9×10^{-5}	
Lack of fit *p*-value	0.044		0.012		0.380		0.383		0.354	

Table 5.4 - Carotenoids composition of *P. marina* biomass grown under different conditions of temperature and light intensity.

Peak[†]	Temperature (ºC)	20	20	20	28	28	28	36	36	36
	Light intensity (μmol m^{-2} s^{-1})	140	252	364	140	252	364	140	252	364
	Xanthophylls (mg g^{-1})									
1	all-*trans*-violaxanthin	0.29 ± 0.00	0.08 ± 0.00	0.04 ± 0.00	0.2 ± 0.16	0.18 ± 0.05	0.17 ± 0.03	0.22 ± 0.01	0.13 ± 0.02	0.26 ± 0.02
2	cis-violaxanthin	0.20 ± 0.01	0.12 ± 0.03	0.11 ± 0.00	0.16 ± 0.05	0.12 ± 0.01	0.09 ± 0.04	0.14 ± 0.02	0.10 ± 0.03	0.14 ± 0.01
3	all-*trans*-luteoxanthin	0.04 ± 0.00	0.02 ± 0.00	0.02 ± 0.01	0.03 ± 0.01	0.03 ± 0.00	0.02 ± 0.01	0.04 ± 0.00	0.06 ± 0.01	0.03 ± 0.00
4	13-cis-lutein	0.06 ± 0.00	0.06 ± 0.01	0.06 ± 0.00	0.08 ± 0.02	0.09 ± 0.01	0.05 ± 0.01	0.10 ± 0.01	0.08 ± 0.03	0.14 ± 0.01
5	13'-cis-lutein	0.03 ± 0.00	0.02 ± 0.00	0.02 ± 0.00	0.02 ± 0.00	0.03 ± 0.00	0.02 ± 0.00	0.00 ± 0.00	0.03 ± 0.00	0.02 ± 0.00
6	all-*trans*-lutein	1.38 ± 0.02	1.24 ± 0.20	0.99 ± 0.01	1.27 ± 0.28	1.02 ± 0.10	0.91± 0.14	0.97 ± 0.07	1.06 ± 0.11	1.09 ± 0.06
7	all-*trans*-zeaxanthin	0.52 ± 0.01	0.61 ± 0.14	0.49 ± 0.00	0.57 ± 0.08	0.41 ± 0.07	0.34 ± 0.11	0.17 ± 0.03	0.18 ± 0.02	0.22 ± 0.01
	Total	2.51 ± 0.02	2.13 ± 0.40	1.73 ± 0.00	2.34 ± 0.61	1.86 ± 0.20	1.61 ± 0.34	1.65 ± 0.11	1.64 ± 0.23	1.91 ± 0.09
	Carotenes (mg g^{-1})									
8	15-cis-β-carotene	0.05 ± 0.00	0.03 ± 0.00	0.03 ± 0.00	0.04 ± 0.01	0.03 ± 0.01	0.03 ± 0.00	0.06 ± 0.02	0.04 ± 0.00	0.03 ± 0.00
9	all-*trans*-α-carotene	0.52 ± 0.00	0.21 ± 0.02	0.15 ± 0.01	0.30 ± 0.15	0.26 ± 0.04	0.24 ± 0.05	0.47 ± 0.00	0.37 ± 0.04	0.40 ± 0.03
10	13-cis-β-carotene	0.05 ± 0.00	0.08 ± 0.01	0.06 ± 0.00	0.11 ± 0.05	0.12 ± 0.02	0.10 ± 0.03	0.13 ± 0.01	0.11 ± 0.01	0.12 ± 0.00
11	all-*trans*-β-carotene	0.34 ± 0.00	0.38 ± 0.03	0.29 ± 0.02	0.47 ± 0.17	0.36 ± 0.05	0.32 ± 0.05	0.44 ± 0.01	0.41 ± 0.04	0.42 ± 0.03
12	9-cis-β-carotene	0.11 ± 0.00	0.15 ± 0.02	0.13 ± 0.01	0.18 ± 0.05	0.18 ± 0.03	0.16 ± 0.03	0.15 ± 0.01	0.16 ± 0.01	0.17 ± 0.01
	Total	1.25 ± 0.01	0.85 ± 0.08	0.66 ± 0.03	1.10 ± 0.44	0.95 ± 0.15	0.84 ± 0.17	1.24 ± 0.03	1.09 ± 0.09	1.15 ± 0.03
	Total carotenoids	3.77 ± 0.03	2.99 ± 0.48	2.39 ± 0.03	3.44 ± 1.05	2.81 ± 0.35	2.45 ± 0.51	2.89 ± 0.08	2.73 ± 0.51	3.06 ± 0.12

[†] Numbered according to the chromatogram shown in Figure 5.S1.

5.3.4 Fatty acids methyl esters (FAMEs) identification

The fatty acid profile of *P. marina* was strongly affected by both light intensity and temperature (Table 5.3). The contour lines of saturated fatty acids (SFA - Figure 5.6a), monounsaturated fatty acids (MUFA - Figure 5.6b) and poly-unsaturated fatty acids (PUFA - Figure 5.6c) showed different behavior, as high temperature affected negatively the SFA content, positively the MUFA content, and showed low influence on PUFA content in *P. marina* biomass. The temperature in FAMEs content is vital to maintain the specific membrane functions, such as of light uptake complexes, photosystems, and membrane protein. At low temperature, more PUFA are synthesized for the correct regulation of membrane fluidity (SHARMA; SCHUHMANN; SCHENK, 2012; LOS; MIRONOV; ALLAKHVERDIEV, 2013; SCHÜLER et al., 2017).

The high light intensity slightly decreased both the content of SFA, MUFA and PUFA as well as the lipid content discussed above. *P. marina* presented fatty acids profile similar to other marine microalgae species (Table 5.5) (BREUER et al., 2012; SAHU et al., 2013; JAESCHKE et al., 2016). The FA are part of the structure of cell membranes and are produced in association with cellular growth during carbon assimilation as reserve product. The amount and profile depend on the conditions of saline stress, nitrogen depletion and factors such as temperature and light (SCHÜLER et al., 2017). The major SFA identified in all conditions were palmitic acid (C16:0, 40.3 ± 0.8 % of total FA), followed by C14:0 (2.5 % to 4.7 % of total FA), and small amounts of C18:0 and C23:0. The MUFA content ranged between 8.8 % and 13.8 % of total FA. The major MUFA identified was C18:1, whose synthesis was favored at the highest temperature, followed by C14:1 and C16:1.

The essential ω6 and ω3 FA linoleic acid (C18:2n-6, LA) and α-linolenic acid (C18:3n-3, ALA) were the main PUFAS identified in all experimental conditions, followed by C20:3n-3 C18:3n-6 and C20:5n-3 (eicosapentaenoic acid, EPA). The ω3 series protect microalgal cells from oxidative damage by ROS acting as an antioxidant (OKUYAMA; ORIKASA; NISHIDA, 2008). The LA content increased with temperature, ranging from 23.4 % to 33.4 % of total FA, while the ALA content decreased with temperature, ranging from 5.6 % to 14.1 % of total FA. *Nannochloropsis salina* grown under different temperature and light intensity presented similar responses for FA composition compared with this study (VAN WAGENEN et al., 2012). Overall, the FA

content is inversely proportional to cell growth, which indicates that the faster growth needs more material to assembly components and do not accumulate lipids quickly.

The ω6:ω3 ratio from human dietary is vital to maintain human health (SIMOPOULOS, 2008). Modern lifestyle leads to the consumption of food with unhealthful high ω6:ω3 ratios (around 20:1). An ω6-rich diet shifts the physiological body state to a predisposition to develop inflammatory and thrombotic diseases and increases blood viscosity (SIMOPOULOS, 2016). In this study, *P. marina* showed the lowest ω6:ω3 ratio, around of 1.6:1, when cultured at the lowest temperature (Table 5.5). This result is similar to the one reported for *H. luteoviridis* cultured under different temperature and nitrogen concentration, where the lowest ω6:ω3 ratio, around of 1.4:1, was observed at the lowest temperature (MENEGOL et al., 2017). Thereby, microalgae biomass can be used as an important source of PUFA to improve ω6:ω3 ratio in human alimentation, especially if cultured under low temperature.

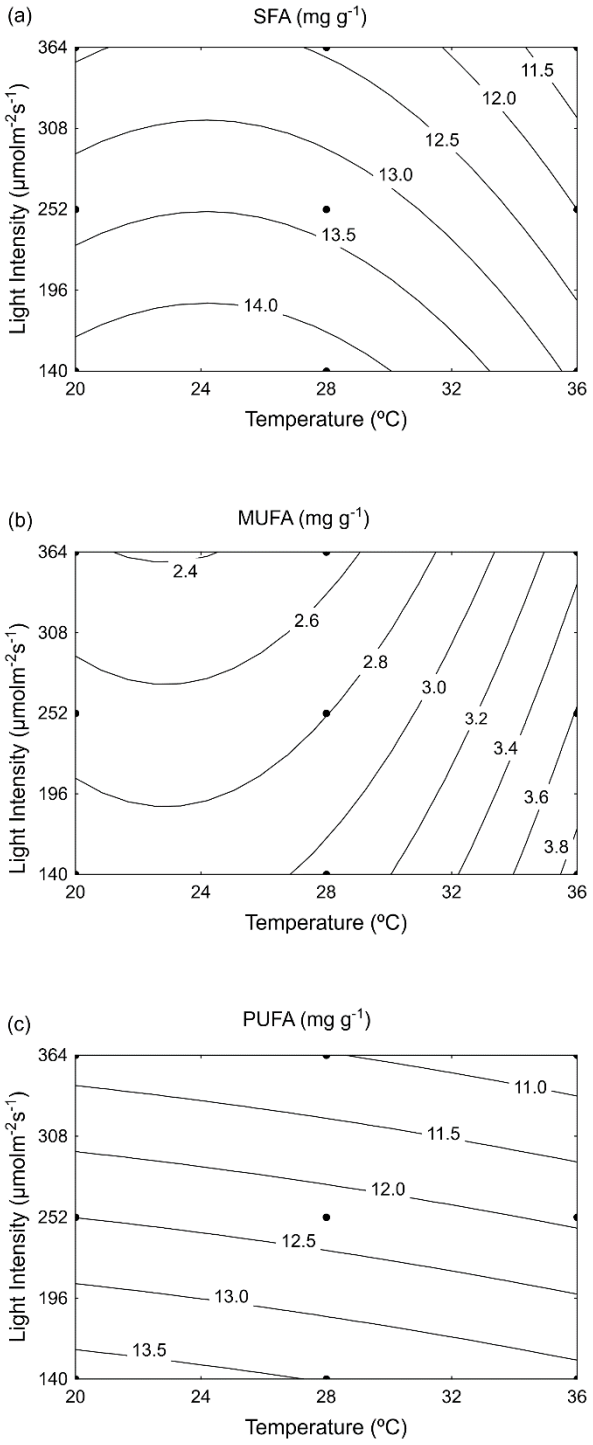

Figure 5.6 - Effects of temperature and light intensity on saturated fatty acid (a), monounsaturated fatty acid (b), polyunsaturated fatty acid (c) contents in *P. marina* biomass grown in batch culture.

Table 5.5 - Fatty acids composition of *P. marina* biomass grown under different conditions of temperature and light intensity.

Peak†	Temperature (ºC)	20	20	20	28	28	28	36	36	36
	Light intensity (µmol $m^{-2} s^{-1}$)	140	252	364	140	252	364	140	252	364
•	• Saturated fatty acids (% of total fatty acids)									
1	C14:0	4.6 ± 0.2 ^{a}	4.7 ± 0.4^{a}	4.6 ± 0.2^{a}	4.4 ± 0.1^{a}	3.9 ± 0.1^{ab}	4.2 ± 0.1^{a}	2.5 ± 0.1^{c}	2.5 ± 0.3^{bc}	2.6 ± 0.0^{c}
3	C16:0	40.0 ± 0.8^{a}	40.9 ± 0.1^{a}	40.4 ± 0.2^{a}	39.5 ± 0.0^{a}	41.4 ± 0.9^{a}	40.9 ± 0.1^{a}	38.6 ± 0.4^{a}	40.3 ± 0.8^{a}	40.5 ± 0.8^{a}
5	C18:0	0.5 ± 0.0^{a}	0.4 ± 0.0^{a}	0.5 ± 0.0^{a}	0.5 ± 0.0^{a}	0.6 ± 0.0^{a}	0.7 ± 0.0^{a}	0.8 ± 0.1^{a}	0.7 ± 0.2^{a}	0.7 ± 0.0^{a}
14	C22:0	0.4 ± 0.1^{ab}	0.3 ± 0.1^{ab}	0.4 ± 0.0 ^{a}	0.2 ± 0.0^{b}	0.2 ± 0.0^{b}	0.2 ± 0.0^{ab}	0.2 ± 0.1^{ab}	0.2 ± 0.0^{ab}	0.2 ± 0.0^{ab}
15	C23:0	0.5 ± 0.0^{a}	0.6 ± 0.1^{a}	0.5 ± 0.1^{a}	0.7 ± 0.1^{a}	0.7 ± 0.1^{a}	0.9 ± 0.1^{a}	0.5 ± 0.0^{a}	0.7 ± 0.2^{a}	0.5 ± 0.0^{a}
16	C24:0	0.4 ± 0.1^{ab}	0.7 ± 0.1^{a}	0.8 ± 0.1^{a}	0.2 ± 0.0^{bc}	0.3 ± 0.1^{bc}	0.2 ± 0.0^{bc}	-	-	-
	Total	46.5 ± 0.8^{abc}	47.6 ± 0.6^{a}	47.2 ± 0.2^{ab}	45.5 ± 0.2^{abc}	47.1 ± 0.8^{a}	47.1 ± 0.1^{ab}	42.6 ± 0.2^{c}	44.4 ± 0.2^{bc}	44.6 ± 0.7^{abc}
•	• Monounsaturated fatty acids (% of total fatty acids)									
2	C14:1	1.7 ± 0.0^{a}	0.9 ± 0.0^{bc}	0.8 ± 0.1^{bc}	1.1 ± 0.0^{b}	0.6 ± 0.1^{c}	0.5 ± 0.1^{c}	1.0 ± 0.1^{bc}	0.8 ± 0.2^{bc}	0.7 ± 0.0^{bc}
4	C16:1	0.7 ± 0.1^{a}	0.7 ± 0.1^{a}	1.2 ± 0.3^{a}	1.2 ± 0.7^{a}	0.9 ± 0.1^{a}	0.6 ± 0.0^{a}	0.7 ± 0.1^{a}	0.8 ± 0.3^{a}	0.5 ± 0.1^{a}
6	C18:1	8.2 ± 0.0^{bc}	7.3 ± 0.3^{c}	8.0 ± 0.1^{c}	7.0 ± 0.2^{c}	8.5 ± 0.3^{c}	8.5 ± 0.3^{c}	11.2 ± 0.5^{ab}	12.2 ± 0.7^{a}	11.3 ± 0.6^{a}
	Total	10.7 ± 0.4^{abcd}	8.8 ± 0.4^{d}	10.0 ± 0.0^{bcd}	9.4 ± 0.5^{cd}	10.0 ± 0.6^{bcd}	9.6 ± 0.2^{cd}	12.9 ± 0.5^{ab}	13.8 ± 0.5^{a}	12.4 ± 0.8^{abc}
•	• Polyunsaturated fatty acids (% of total fatty acids)									
7	C18:2n-6	23.6 ± 0.0^{c}	24.9 ± 0.2^{c}	23.4 ± 0.4^{c}	28.6 ± 0.5^{b}	29.1 ± 0.3^{b}	29.6 ± 0.3^{b}	33.1 ± 0.1^{a}	32.4 ± 1.0^{a}	33.4 ± 0.0^{a}
8	C18:3n-6	1.9 ± 0.0^{a}	1.6 ± 0.1^{b}	1.4 ± 0.1^{bc}	1.1 ± 0.1^{cd}	0.6 ± 0.0^{e}	0.6 ± 0.0^{e}	1.0 ± 0.1^{d}	0.7 ± 0.0^{e}	0.6 ± 0.0^{e}
9	C18:3n-3	14.1 ± 0.2^{a}	13.1 ± 0.1^{a}	13.0 ± 0.1^{a}	12.5 ± 0.0^{a}	9.7 ± 0.5^{b}	9.7 ± 0.4^{b}	6.4 ± 0.2^{c}	5.6 ± 0.6^{c}	6.0 ± 0.2^{dc}
10	C20:3n-6	0.5 ± 0.1^{a}	0.6 ± 0.0^{a}	0.7 ± 0.0^{a}	0.5 ± 0.0^{a}	0.6 ± 0.1^{a}	0.5 ± 0.0^{a}	0.2 ± 0.0^{a}	0.3 ± 0.0^{a}	0.2 ± 0.0^{a}
11	C20:3n-3	1.8 ± 0.0^{b}	2.1 ± 0.1^{ab}	2.5 ± 0.1^{ab}	2.1 ± 0.0^{ab}	2.2 ± 0.1^{ab}	2.1 ± 0.1^{ab}	2.8 ± 0.1^{a}	2.6 ± 0.1^{b}	2.6 ± 0.0^{ab}
12	C20:4n-6	0.2 ± 0.1^{abcd}	0.4 ± 0.0^{ab}	0.5 ± 0.0^{a}	0.1 ± 0.1^{bcd}	0.2 ± 0.1^{abc}	0.2 ± 0.0^{abcd}	-*	-*	-*
13	C20:5n-3	0.8 ± 0.0^{abcd}	1.0 ± 0.0^{ab}	1.3 ± 0.1^{a}	0.4 ± 0.0^{cd}	0.5 ± 0.1^{bcd}	0.7 ± 0.1^{bcd}	1.0 ± 0.6^{abc}	0.2 ± 0.0^{d}	0.2 ± 0.1^{d}
	Total	42.9 ± 0.5^{ab}	43.6 ± 0.1^{ab}	42.9 ± 0.3^{ab}	45.2 ± 0.3^{a}	43.0 ± 0.6^{b}	43.3 ± 0.4^{ab}	44.6 ± 0.7^{ab}	41.8 ± 0.3^{b}	43.0 ± 0.1^{ab}
	Total fatty acids (mg g^{-1})	30.0 ± 0.3^{ab}	28.6 ± 0.0^{ab}	25.6 ± 0.1^{ab}	31.5 ± 0.7^{a}	28.6 ± 1.4^{ab}	25.8 ± 0.3^{b}	28.2 ± 1.0^{ab}	27.9 ± 0.4^{ab}	25.1 ± 1.1^{b}
	ω6:ω3 ratio	1.6 ± 0.1^{c}	1.7 ± 0.0^{c}	1.5 ± 0.0^{c}	2.0 ± 0.1^{bc}	2.4 ± 0.1^{bc}	2.5± 0.0^{bc}	3.3± 0.1^{ab}	4.0± 0.5^{a}	3.9± 0.0^{a}

Different letter in the same column indicates significant difference by Tukey test at 5 % significance level.

† Numbered according to the chromatogram shown in Figure 5.S2.

5.4 Conclusion

Pseudoneochloris marina showed high potential to be used in microalgae large-scale cultures. It reached 1.80 g L^{-1} of dry biomass, with biomass productivity of 0.26 g L^{-1} d^{-1}, under photoautotrophic growth conditions. *P. marina* biomass can be an alternative source of high-value products such as carotenoids (all-*trans*-lutein, all-*trans*-zeaxanthin, all-*trans*-β-carotene and all-*trans*-α-carotene) and essential polyunsaturated fatty acids (linoleic acid and α-linolenic acid). Moreover, depending on light and temperature conditions, it was possible to reach high carbohydrate (53.77 %) and saturated fatty acid (44.11% of total FA) content, showing that this microalga can also be explored for biofuels production.

Acknowledgments

This work was supported by CNPq (National Council of Scientific and Technological Development, grant number 476741), FAPERGS (Foundation for Research Support of Rio Grande do Sul, grant number 2079-2551/13-8) and CAPES (Coordination for the Improvement of Higher Education, scholarships).

Declarations of interest: none

SUPPLEMENTARY MATERIAL

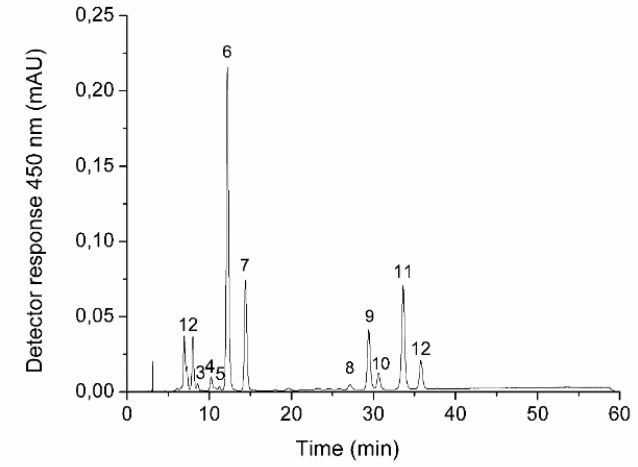

Figure 5.S1. Chromatogram of carotenoids identified in *P. marina* by HPLC-DAD. Peaks identified are described in Table 5.4.

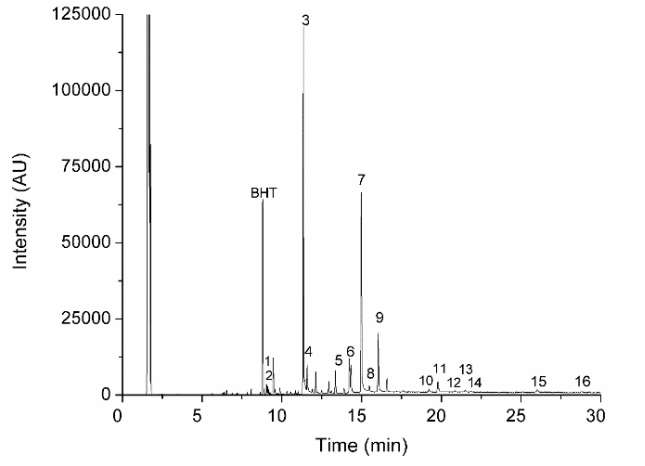

Figure 5.S2. Chromatogram of fatty acids profile from *P. marina* by CG-MS. The retention time: internal standard BHT=8.8 min. Peaks identified in Table 5.5.

6 KINETIC MODELING OF CELL GROWTH, NITROGEN CONSUMPTION AND INTRACELLULAR BIOPRODUCTS OF *Pseudoneochloris marina* CULTURES IN AIRLIFT PHOTOBIOREACTORS

Carolina F. Gonçalves, Rosane Rech*

Food Science and Technology Institute, Federal University of Rio Grande do Sul, Av. Bento Gonçalves, 9500, PO Box 15090, ZC 91501-970 Porto Alegre, RS, Brazil. Phone +55 51 3308 1356

*E-mail: rrech@ufrgs.br

ABSTRACT

The mathematical modeling of microalga biomass growth and nutrient consumption is an effective tool to understand culture behavior and predict culture performance under different conditions. This study tested five different models to describe biomass and nitrogen kinetics of *Pseudoneochloris marina* grown in batch cultures. The DroopLog model showed the best fitting for both biomass ($R^2 = 0.995$) and nitrogen ($R^2 = 0.977$) data. The kinetics of the intracellular lipid content was modeled using Luedeking-Piret equation ($R^2 = 0.986$). Three models were proposed to fit the intracellular content of carotenoids and proteins. They were successfully modelled by an expression that considers that their synthesis is associated to cell growth, as in Luedeking-Piret model, but the growth-associated term is multiplied by a Monod-type expression.

KEY-WORDS: carotenoid, protein, kinetics, modeling, microalga.

6.1 Introduction

Microalgae are being extensively investigated as potential sources of compounds of interest in several industrial sectors such as human nutrition, nutraceutics, animal feed and biofuels production, as well as bioactive compounds like pigments and polyunsaturated fatty acids (PANCHA et al., 2015; SOLIMENO et al., 2015). In addition, microalgae have high photosynthetic efficiency, do not compete with crops for arable land, and many species have the ability to uptake dissolved inorganic carbon from environmental, or industrial CO_2, helping in greenhouse gases mitigation (PANCHA et al., 2015; MA et al., 2016).

Mathematical modeling of microalgae growth kinetics and products formation are important to understand the growth behavior of microalgae in laboratory-scale studies and can aid scale-up and process optimization of cultivation systems for commercial algal-based technologies. The development of mathematical models for biological processes has some limitations such as the large number of parameters, the interactions between them, and the non-linearity of the systems (VATCHEVA et al., 2006).

Droop (1968) and Monod (1949) models have been widely used to express biomass growth and nutrient consumption kinetics for autotrophic and heterotrophic microorganisms, respectively. These models correlate cell growth to substrate concentration in the culture medium, such as the nitrogen source. The Droop model assumes that growth rate depends on the cell concentration and on the intracellular nutrient reserve, dissociating growth from nutrient consumption. However, it fails in predicting cell growth in cultures not limited by substrate (DA FRÉ et al., 2016). The Monod model defines that the substrate consumed by microorganisms is instantly converted into biomass. Da Fré et al. (2016) proposed three models to describe *Dunaliella tertiolecta* growth and nitrogen consumption once Droop model was not capable to describe the culture behavior under conditions of high nitrogen concentration. The ModN model is based on the hypothesis that growth is limited by lack of nitrogen, $ModNk_x$ and $ModNX_{max}$ models presume that cell growth is limited by the excess of biomass in cultures. Several models have been proposed to model microalgae growth; however kinetic modeling studies for products formation in microalgae cultures are scarce (VATCHEVA et al., 2006; DA FRÉ et al., 2016). In addition, usually products are expressed in terms of bioreactor volume (mg L^{-1}), underestimating the variation of their intracellular content in the beginning of the culture, when the biomass concentration is very low.

In the present study, mathematical models were evaluated to describe the kinetics of cell growth, nitrogen consumption and products formation (lipids, carotenoids and proteins) by *Pseudoneochloris marina* in autotrophic cultures. As will be shown, there are large variations in protein and carotenoids intracellular content in the beginning of the culture that would be masked if multiplied by the low biomass concentration. So, this study presents a new approach for product formation modeling as the products concentrations were expressed in terms of their content in the biomass (mg g^{-1}).

Five kinetic models were used to model biomass and nitrogen curves in batch cultures. The lipids intracellular content was described using Luedeking-Piret equation. In addition, three models were proposed to describe the kinetics of carotenoids and protein intracellular contents in batch cultures of *P. marina*.

6.2 Material and methods

6.2.1 Microorganism and pre-cultures

The marine strain *Pseudoneochloris marina* BE 001 was maintained by BioEng Laboratory (Food Science and Technology Institute/ UFRGS) in germination chambers at 22 ºC under photoperiod of 12/12 h (light/dark) in 250 mL Erlenmeyer flasks containing 100 mL of culture medium f/2 (GUILLARD, 1975) and an additional amount of NaCl (17 g L^{-1}) to induce saline stress. The pre-cultures were prepared in 500 mL Erlenmeyer flasks with 240 mL working volume using modified f/2 medium, as described above, with modified $NaNO_3$ concentration (300 mg L^{-1}) (CHAGAS et al., 2015a) and inoculated with 24 mL of stock culture. The flasks were incubated in rotatory shaker (Oxylab, Oxy 304T) at 28 ºC and 180 rpm under continuous illumination (42 µmol m^{-2} s^{-1}) for 7 days.

6.2.2 Experimental database acquisition

Batch cultures were carried out to obtain an experimental database of cell growth and nitrogen consumption to apply in the parameters estimation from the kinetic models. The cultures were performed in 2.4 L flat-panel airlift photobioreactors (KOCHEM et al., 2014) using modified f/2 medium (17 g L^{-1} NaCl and 450 mg L^{-1} $NaNO_3$) (GONÇALVES; MENEGOL; RECH, 2019). The photobioreactors were inoculated with 240 mL of pre-cultures and maintained for 16 days. The photobioreactors were continuously illuminated at the riser side (252 µmol m^{-2} s^{-1}) and the temperature was maintained at 28 ºC (GONÇALVES; MENEGOL; RECH, 2019). To avoid nutrient limitation, 1 mL L^{-1} of phosphate solution and 1 mL L^{-1} of trace-metals solution were added daily to the cultures (CHAGAS et al., 2015). The airflow was kept at 1 L min^{-1} of CO_2-enriched filtered air (0.22 µm Midisart®2000, Sartorius Stedim Biotech). The mixture of CO_2 and compressed air was controlled by rotameter to maintain the culture at pH 7.0. The pH was measured using pH-indicator strips (MColorpHast™, Merck, Germany). The experimental cultures were performed in duplicate.

Daily samples were collected to measure the cell growth, biomass composition and nitrate content. Biomass was measured by optical density at 750 nm (OD_{750}) and correlated with dry cell weight (X, g L^{-1}) by the Equation (6.1). The nitrate content in the supernatant was determined according the method described by Cataldo et al. (1975).

$$X = 0.634 \times OD_{750} \qquad (R^2 = 0.98) \qquad (6.1)$$

6.2.3 Analytical methods

The total carotenoids were quantified by colorimetric method according to Lichtenthaler and Buchmann (2001) using ethanol 95 % as solvent. The absorbances were measured by spectrophotometer at the wavelengths of 664 nm, 649 nm and 470 nm. The protein content was determined according Lowry et al. (1951) method after previous reaction of 1 mL of 1 M NaOH (100 ºC/ 30 min) added to the cell pellets. Bovine serum albumin was used to obtain the calibration curve. The lipid content was determined by the colorimetric method proposed by Mishra et al. (2014), which uses the sulfo-phospho-vanillin (SPV) reagent for direct quantification of liquid microalgae cultures and measured by spectrophotometer at 530 nm. Calibration curve was determined using canola oil.

6.2.4 Kinetic models

6.2.4.1 Microalgae growth and nitrogen consumption models

Droop model (1968) has been widely used to model algal growth and nitrogen consumption in nitrogen-limited cultures and is described below (Equations 6.2 - 6.6). This model presents an internal substrate cell quota (q), uncoupling substrate consumption and cell growth.

$$\frac{dX}{dt} = \mu \cdot X \qquad (6.2)$$

$$\frac{dN}{dt} = -\rho \cdot X \qquad (6.3)$$

$$\frac{dq}{dt} = \rho - \mu \cdot q \qquad (6.4)$$

$$\mu = \mu_{\max} \cdot \left(1 - \frac{k_q}{q}\right) \qquad (6.5)$$

$$\rho = \rho_{\max} \cdot \left(\frac{N}{N + k_N}\right) \qquad (6.6)$$

The DroopLog model differs from the Droop model by replacing equation (6.5) by the Logistic equation (6.7). The Logistic equation is widely used to model of population growth and represents the auto-inhibition of the cells as growth limitation (VOGELS et al., 1975; HE et al., 2016). DroopLog model is described by equations (6.2 - 6.4, 6.6 and 6.7).

$$\mu = \mu_{\max} \cdot \left(1 - \frac{X}{X_{\max}}\right) \quad (6.7)$$

Monod-based models and other expressions based on different biomass-limited and external nutrient concentration have been successfully used to explain growth and nitrogen consumption kinetics of microalgae species (ADESANYA et al., 2014; DA FRÉ et al., 2016; HE et al., 2016). ModN model, proposed by Da Fré et al. (2016) is a model that combines the biomass and nitrogen balances (Equations 6.2 and 6.3) with a nitrogen-catalyzed expression for nitrogen consumption that uses a growth associated term (Y_{XN}, g g^{-1}) and a non-growth associated term (m_N, g g^{-1} h^{-1}) (Equation 6.8). It also considers the hypothesis that biomass growth is limited by nitrogen starvation using a Monod expression (Equation 6.9):

$$\rho = \left(\frac{\mu}{Y_{XN}} + m_N\right) \cdot N \quad (6.8)$$

$$\mu = \mu_{\max} \cdot \left(\frac{N}{N + k_N}\right) \quad (6.9)$$

On the other hand, $ModNk_x$ and $ModNX_{max}$ models (DA FRÉ et al., 2016) are based on the hypothesis that the excess of biomass is responsible for limiting biomass growth and the expression for specific growth rate, Equation (6.9), was replaced by Equations (6.10) and (6.7), respectively. Equation 6.10, used in $ModNk_X$ model, considers a combined effect of nitrogen starvation and cell growth auto-inhibition using a Monod based expression. $ModNk_X$ is composed by equations (6.2, 6.3, 6.8 and 6.10). $ModNX_{max}$ is a combination between ModN model and the Logistic equation and is composed by equations (6.2, 6.3, 6.7 and 6.8).

$$\mu = \mu_{\max} \cdot \left(\frac{N}{N + k_N}\right) \cdot \left(\frac{k_X}{X + k_X}\right) \quad (6.10)$$

6.2.5 Models for carotenoid, protein and lipid intracellular contents

The most used model to describe the kinetics of products formation by cell was proposed by Luedeking-Piret (1959). Luedeking-Piret model describes product formation by a cell considering that production has a growth-associated term (α, mg g^{-1}) and a non-growth-

associated term (β, mg g^{-1} h^{-1}), as shown in Equation (6.11), where P is the product concentration in culture medium (mg L^{-1}).

$$\frac{dP}{dt} = \alpha \cdot \frac{dX}{dt} + \beta \cdot X \quad (6.11)$$

In this study, the Luedeking-Piret equation was used to describe the kinetics of lipids accumulation by cells. However, the kinetics of carotenoids and proteins production showed a very different behavior, strongly related to the nitrogen uptake by cells, as it will be shown in the Results section. Three models were proposed to describe the kinetics of carotenoids and protein synthesis by *P. marina*. Model CP1 (Equation 6.12) considers that carotenoids and proteins synthesis are associated to the nitrogen uptake by cells (γ, mg g^{-1}). Models CP2 (Equation 6.13) and CP3 (Equation 6.14) consider that carotenoids and proteins synthesis are associated to cell growth, as in Luedeking-Piret model, but the growth-associated term (α) is multiplied by a Monod-type expression; protein and carotenoid synthesis will decrease as nitrogen concentration decreases in culture medium. Model CP3 also considers product degradation (k_d, h^{-1}).

$$\frac{dP}{dt} = \gamma \cdot \rho \cdot X \quad (6.12)$$

$$\frac{dP}{dt} = \alpha \cdot \frac{N}{N + k_{NP}} \cdot \mu \cdot X \quad (6.13)$$

$$\frac{dP}{dt} = \alpha \cdot \frac{N}{N + k_{NP}} \cdot \mu \cdot X - k_d \cdot P \quad (6.14)$$

As lipids, protein and carotenoids where analyzed in the biomass, Equations (6.11 - 6.14) where transformed to use the intracellular content of the targeted products (C, mg g^{-1}), expressed in milligrams of lipids, proteins or carotenoids per gram of dry biomass and became Equations (6.15 - 6.18), respectively:

$$\frac{dC}{dt} = \mu \cdot (\alpha - C) + \beta \quad (6.15)$$

$$\frac{dC}{dt} = \alpha \cdot \rho - \mu \cdot C \quad (6.16)$$

$$\frac{dC}{dt} = \alpha \cdot \mu \cdot \left(\frac{N}{N + k_{NP}}\right) - \mu \cdot C \quad (6.17)$$

$$\frac{dC}{dt} = \alpha \cdot \mu \cdot \left(\frac{N}{N + k_{NP}}\right) - \mu \cdot C - k_d \cdot C \quad (6.18)$$

6.2.5.1 Parameters estimation

The models were implemented for parameters estimation and processes simulation in the software EMSO - Environment for Modeling, Simulation and Optimization, version 10.9 (SOARES; SECCHI, 2003). The parameters were estimated based on experimental data to minimize the objective function (F_{obj}) of the ordinary least squares. The fitness of kinetic models was evaluated by determination coefficient (R^2) and the root mean squared error (*RMSE*). Firstly, only biomass growth and nitrogen consumption data were modeled. The parameters of the product models (lipids, carotenoids and proteins) were estimated for each product individually with biomass and nitrogen curves being described by the model chosen previously.

6.3 Results and discussion

6.3.1 Experimental results

The kinetic characteristics of microalgal cell growth and nitrogen consumption, as well as the contents of carotenoids, proteins and lipids in the biomass, were experimentally investigated in batch culture (Figure 6.1). The cultures were maintained for 314 h; the stationary growth phase started at 144 h and the final biomass concentration was 2.22 g L^{-1} with observed maximum specific growth rate (μ_{max}) of 0.0323 h^{-1} (Figure 6.1a). Nitrogen was consumed during the first 96 h of culture; after this time, the cell growth can be explained by the consumption of the intracellular nitrogen content. This internal nutrient usage is a well-established phenomenon in phytoplankton (ADESANYA et al., 2014).

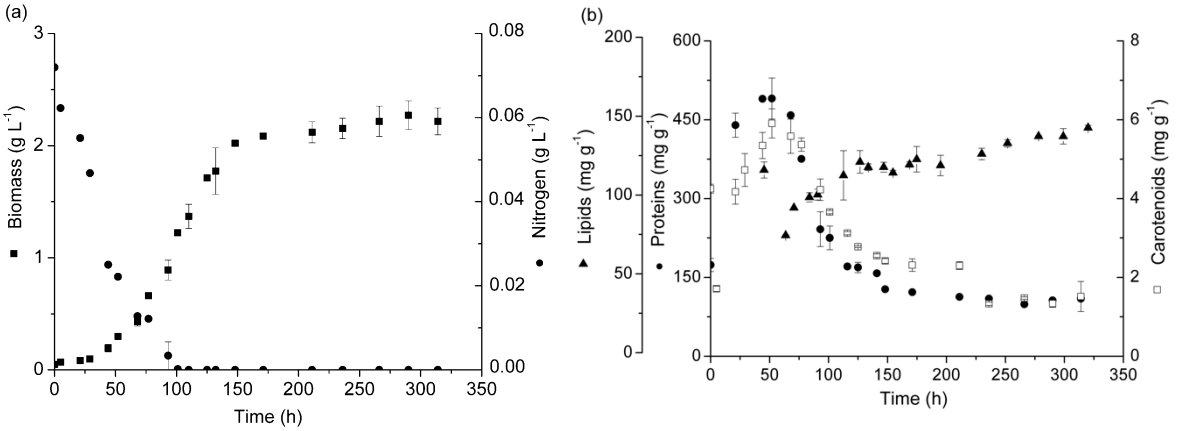

Figure 6.1- Experimental data for (a) biomass and nitrogen consumption and (b) carotenoids, protein and lipids content in the biomass during *P. marina* batch cultures in 2.4 L photobioreactors.

The kinetic data for carotenoids, proteins and lipids content in the biomass are shown in Figure 6.1b. The carotenoids and protein kinetics exhibit a similar behavior. The carotenoid and protein contents increased during the beginning of the culture, reaching their highest concentrations, 5.91 mg g^{-1} and 491 mg g^{-1}, respectively, at 52 h of cultivation, when nitrogen concentration in culture medium was very low. After this time the carotenoid and protein intracellular contents decreased, as cells continue to grow, and stabilized around 150 h of culture, when the biomass reached the stationary growth phase. The final carotenoid and protein contents were 1.52 mg g^{-1} and 110 mg g^{-1}. These results can be explained by the ability of microalgae to use intracellular nitrogenous compounds to maintain metabolic activity. The supply of nitrogen in the culture medium provides the nitrogen input for cell growth, chlorophyll *a* and *b* and protein synthesis (CHEN et al., 2011; PANCHA et al., 2014). The lipid intracellular content slightly increased after nitrogen starvation, reaching 143 mg g^{-1} in the final culture. Nutrient starvation, as nitrogen, can result in accumulation of nutritional reserve compounds, as carbohydrates and lipids (MATA; MARTINS; CAETANO, 2010; BENAVENTE-VALDÉS et al., 2016).

6.3.2 Biomass growth and nitrogen consumption modeling

The experimental data of biomass growth and nitrogen uptake were used to estimate the parameters of five different growth models, as shown in Table 1. All models were capable to represent biomass behavior (Figure 6.2a). The DroopLog, $ModNk_x$ and $ModNX_{max}$ models provided the highest fit for biomass growth; Droop and ModN models showed slightly lower fit results, but still had a good representation of the experimental biomass data.

Table 6.1- Parameters estimated for different kinetic models for *P. marina* biomass growth and nitrogen consumption.

Parameters	**Unit**	**Droop**	**Drooplog**	**ModN**	**ModNk$_X$**	**ModNX$_{max}$**
$\mu_{\max}$	h^{-1}	0.04160	0.03846	0.03423	0.03429	0.03847
$\rho_{\max}$	h^{-1}	0.85546	1.4005	-	-	-
k_N	g L^{-1}	3.12902	8.42161	0.00165	0.00023	-
q	g g^{-1}	0.02074	0.36656	-	-	-
k_q	g g^{-1}	0.03277	-	-	-	-
k_X	g L^{-1}	-	-	-	5.56734	-
Y_{XN}	g g^{-1}	-	-	0.39004	0.27353	0.22192
m_N	g g^{-1} h^{-1}	-	-	0.00874	0.00578	0.00092
$X_{\max}$	g L^{-1}	-	2.21772	-	-	2.21762
R^2 *X*		0.99516	0.99476	0.99527	0.99474	0.99509
RMSE X		0.04698	0.05463	0.04404	0.04138	0.05446
R^2 *N*		0.94430	0.97668	0.95316	0.97729	0.98293
RMSE N		0.00526	0.00307	0.00747	0.00459	0.00339
F_{obj}		423	338	390	885	293

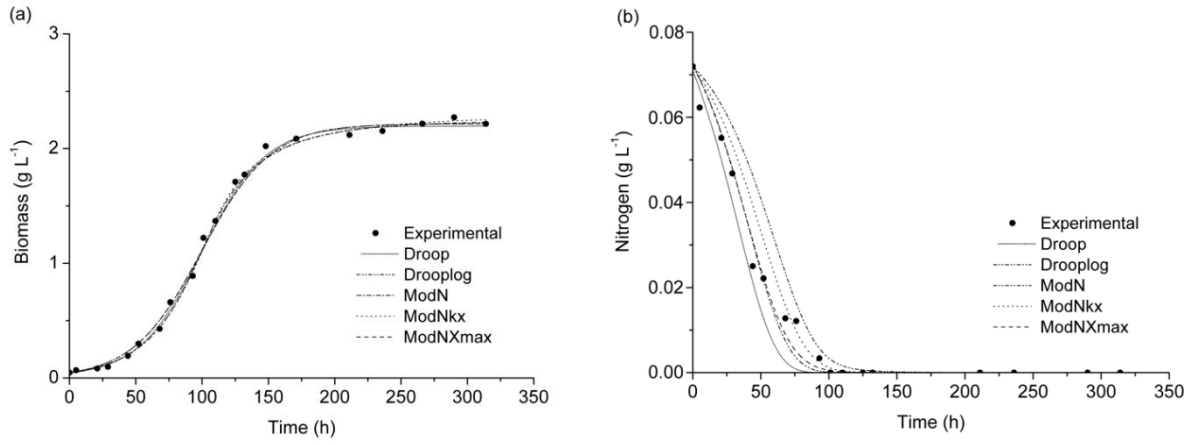

Figure 6.2 - Experimental data and simulated curves of biomass (a) and nitrogen (b) during *P. marina* batch cultures in 2.4 L photobioreactors.

Regarding nitrogen consumption, the models that consider that cell growth is limited by cell concentration, as DroopLog, ModNkx and ModNX$_{max}$, showed a good fitting to nitrogen

data, while the ones that consider that nitrogen concentration was the limiting factor for cell growth tended to underestimate (Droop) or overestimate (ModN) nitrogen values (Figure 6.2b). Droop model presented the worst fitting among the tested models, confirming its limitation in predicting the kinetics of microalgae growth under non-limited nitrogen conditions (DA FRÉ et al., 2016). $ModNX_{max}$ showed the best fitting, with the highest R^2 value. In addition, $ModNX_{max}$ has only 4 parameters, while DroopLog and $ModNk_x$ models have 5 parameters each. Also, the values of the parameters μ_{max} and X_{max} were very close the observed (experimental) ones, 0.038 h^{-1} and 2.22 g L^{-1}, respectively.

Photosynthesis is a complex process allowing different mathematical approach strategies. Microalgae kinetic models have been developed in different culture systems, under both autotrophic or heterotrophic conditions, to describe algal biomass growth and metabolites production (PACKER et al., 2011; LEE; JALALIZADEH; ZHANG, 2015; RIBEIRO et al., 2017). Nitrogen is an essential nutrient for cell growth. The Droop model assumes that algal biomass growth does not depend on external nitrogen uptake from culture medium but on the intracellular nitrogen stock. The $ModNX_{max}$ model predicts that the end of cell growth is associated with self-inhibition by the cell concentration, due shadowing effect, expressed by logistic equation. The experimental cultures demonstrated that nitrogen in culture medium was depleted at 101 h and the stationary cell growth was reached at 168 h. The same behavior was observed in autotrophic and mixotrophic cultures of *Chlorella vulgaris* under nitrogen limitation, where extracellular nitrogen was depleted quickly but cell continued to grow, and high starch accumulation occurred, followed by triacyl glycerides. Droop model was proposed and presented good fit to experimental data for all the investigated growth conditions (ADESANYA et al., 2014). Da Fré et al. (2016) reported a good fitting of $ModNX_{max}$ model to predict *Dunaliella tertiolecta* biomass growth and nitrogen consumption in batch cultures under high initial nitrogen concentrations. The authors demonstrated that other kinetic models, Droop, ModN and $ModNk_x$, were able to describe microalgal cell growth but failed to predict nitrogen consumption under those conditions.

6.3.3 Models for the intracellular content of lipids, proteins and carotenoids

The experimental data of carotenoids, protein and lipids were used to estimate the parameters of Luedeking-Piret model (LP, for lipids), and models CP1, CP2 and CP3 for carotenoids and proteins (Table 6.2). Biomass growth and nitrogen consumption were described by $ModNX_{max}$ model using the parameters of Table 1.

The CP1 model showed the worst fit for both carotenoid (R^2 = 0.75) and protein (R^2 = 0.96) intracellular contents (Table 6.2). CP1 model associate product synthesis to nitrogen uptake by cells and do not consider cell growth and product degradation as is proposed by CP2 and CP3 models, respectively. Both CP2 and CP3 models were capable to describe the kinetics of protein intracellular content (Figure 6.3a and 6.3b). These models explained satisfactorily carotenoid and protein synthesis by cells when there is plenty of nitrogen in the cultures and the decrease of their intracellular content under nutrient limitation. The very small difference between the fitting of models CP2 and CP3 for both carotenoids and protein intracellular contents shows that, in the culture conditions used in this study, carotenoid and protein degradation are almost inexistent and can be neglected in the kinetic model. The decrease of the intracellular contents of carotenoids and proteins observed between the nitrogen starvation in the culture medium and the end of the cell growth phase can be entirely explained by the decrease in the rate of the synthesis of these components, eventually reaching zero when nitrogen is completely depleted, and their consequent dilution through an increasing biomass concentration.

Table 6.2 - Parameters estimated for different kinetic models of total carotenoids, protein and lipids formation for *P. marina*.

Parameters	**Unit**	**Carotenoids**			**Protein**			**Lipids**
		CP1	CP2	CP3	CP1	CP2	CP3	LP
γ	mg g^{-1}	36.7437	-	-	3128.2	-	-	-
α	mg g^{-1}	-	7.8554	7.528	-	1049.9	913.3	115.78
β	mg g^{-1} h^{-1}	-	-	-	-	-	-	0.1308
k_{NP}	g L^{-1}	-	0.00679	0.00398	-	0.03581	0.02509	-
k_d	h^{-1}	-	-	0.00155	-	-	0.00083	-
R^2		0.7516	0.9692	0.9823	0.9643	0.9898	0.9911	0.9865
RMSE		1.3735	0.8696	0.8311	51.669	16.670	13.418	24.345
F_{obj}		172	137	158	138	151	179	126

LP: Luedeking-Piret equation (15); CP1: equation (16); CP2: equation (17); CP3: equation (18).

The widely used Luedeking-Piret model fitted well (R^2 = 0.99) the experimental data of intracellular lipid content of *P. marina* during autotrophic batch growth (Figure 6.3c). The neutral lipid accumulation, expressed in grams per liter (g L^{-1}), in batch cultures of

Chlamydomonas reinhardtii showed good fit (R^2 = 0.98) to Luedeking-Piret model (TEVATIA, 2012). The authors stated that lipid production is dependent on both the growth and non-growth related coefficients (α and β, respectively) and classified lipid as a class II ($\alpha \neq 0$ and $\beta \neq 0$), in which product formation is indirectly related to the primary metabolism pathway and involves more complex process in many pathways (GADEN; GADEN JR., 2000).

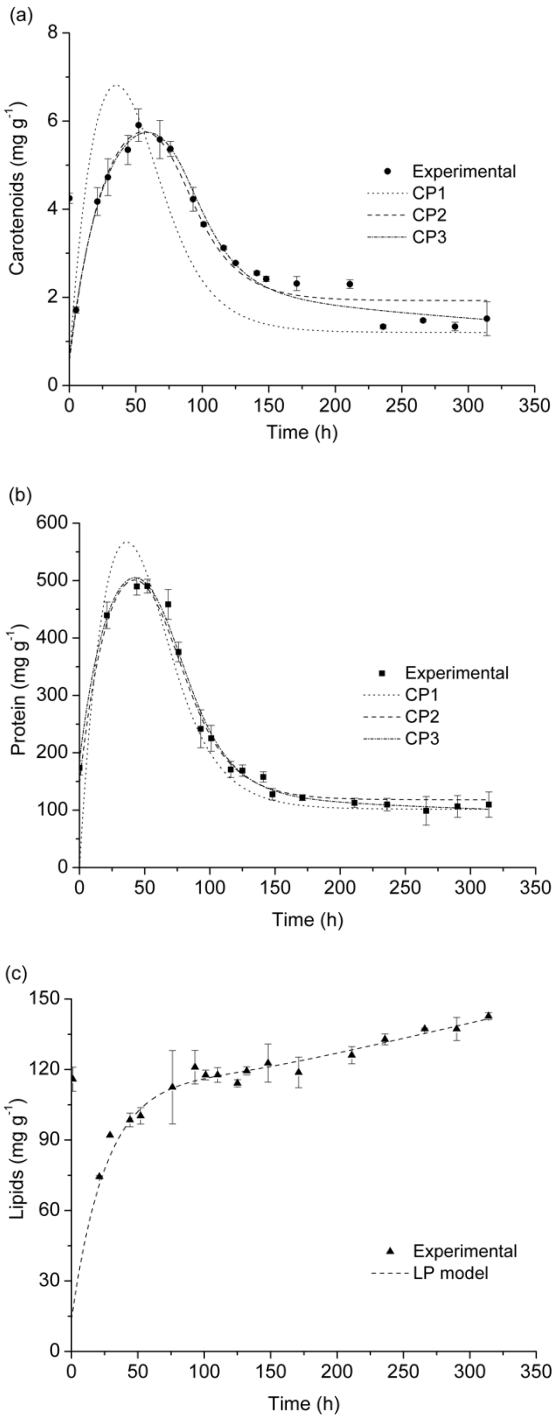

Figure 6.3 - Experimental data and simulated curves of carotenoids (a), protein (b) and lipid (c) content during *P. marina* batch cultures in 2.4 L photobioreactors.

6.4 Conclusion

All kinetic models were able to predict the cell growth, however Droop and ModN models failed to described nitrogen consumption; $ModNX_{max}$ showed the best fitting. The lipid formation was described satisfactorily by Luedeking-Piret equation. Carotenoids and protein were successfully modelled by an expression that considers that their synthesis is associated to cell growth and decreased with nitrogen concentration.

The models proposed help to understand the kinetics of proteins and carotenoids synthesis by *P. marina* cells under conditions of nitrogen availability followed by nitrogen starvation. Their capacity to describe proteins and carotenoids synthesis should be tested for other microalgae.

Funding: This work was supported by CNPq (National Council of Scientific and Technological Development, grant number 476741), FAPERGS (Foundation for Research Support of Rio Grande do Sul, grant number 2079-2551/13-8) and CAPES (Coordination for the Improvement of Higher Education, scholarships).

Nomenclature

Symbol		Unit
μ	h^{-1}	specific growth rate
$\mu_{\max}$	h^{-1}	maximum specific growth rate
$X_{\max}$	$g\ L^{-1}$	maximum biomass concentration
X	$g\ L^{-1}$	cell growth
N	$g\ L^{-1}$	nitrogen concentration
q	$g\ g^{-1}$	internal nitrogen cell quota
P	$g\ g^{-1}\ h^{-1}$	nitrogen uptake rate
$\rho_{\max}$	$g\ g^{-1}h^{-1}$	maximum nitrogen uptake rate
k_N	$g\ L^{-1}$	half saturation constant for nitrogen
k_X	$g\ L^{-1}$	Half-saturation constant for biomass
k_q	$g\ g^{-1}$	minimum cell quota
m_N	$g\ g^{-1}\ h^{-1}$	nitrogen non-growth-associated term
Y_{XN}	$g\ g^{-1}$	nitrogen growth-associated term
α	$mg\ g^{-1}$	Product growth-associated term
β	$mg\ g^{-1}\ h^{-1}$	Product non-growth-associated term
C	$mg\ g^{-1}$	Product concentration
k_d	h^{-1}	saturation constant for product
k_{NP}	$g\ L^{-1}$	half saturation constant for nitrogen/product
F_{Obj}	-	objective function
R^2	-	coefficient of determination
$RMSE$	-	Root mean squared error

7 SIMULATION AND OPTIMIZATION OF REPEATED-BATCH AND CONTINUOUS CULTURES OF *Pseudoneochloris marina*: VALIDATION WITH EXPERIMENTAL DATA AND USE OF CO_2 FROM BEER FERMENTATION

Carolina Ferrer Gonçalves, Rosane Rech*

Food Science and Technology Institute, Federal University of Rio Grande do Sul, Av. Bento Gonçalves, 9500, PO Box 15090, ZC 91501-970 Porto Alegre, RS, Brazil. Phone 55 51 3308 1356

*E-mail: rrech@ufrgs.br

ABSTRACT

This study used a mathematical model developed for a batch culture of the microalga *Pseudoneochloris marina* to simulate and maximize biomass productivity in repeated-batch and continuous cultures. The results predicted by the model were validated trough experimental data and achieved biomass productivities of 0.54 ± 0.02 g L^{-1} d^{-1} and 0.66 ± 0.04 g L^{-1} d^{-1} for repeated-batch and continuous cultures respectively. The biomass composition was also affected by culture system, mainly in its protein and carotenoids content, as was well as fatty acid profile. Finally, the continuous culture was performed fed with CO_2 released form beer fermentation. The results show that beer fermentation is a potential source of CO_2 for microalgae growth, being clean and advantageous for producing microalgae biomass to be used as food supplement or nutraceuticals.

Key-words: carotenoids, fatty acids, logistic equation.

7.1 Introduction

Microalgae biomass is an important and potential industrial source of supplement of foods, biofuels production (e.g. biodiesel, bioethanol) and high value compounds such as carotenoids (lutein and β-carotene) and long chain fatty acids (MATA; MARTINS; CAETANO, 2010; DIPRAT et al., 2017). Photosynthetic organisms, especially, microalgae are capable to fix CO_2 at a faster rate compared to terrestrial plants and have been grown using inorganic carbon from industrial process. The CO_2 supply from microalgae cultivation is attractive to reduce of greenhouse gas emissions, biogas purification and improve the photosynthetic efficiency enhancing biomass productivity (KUMARI et al., 2014; KUMAR; GURIA; PATHAK, 2017). Fermentation processes emit almost pure CO_2 gas, and integrated systems between fermenters and photobioreactors have been explored to evaluate the potential CO_2 mitigation by microalgae biomass production (CHAGAS et al., 2015; YEN; HSU; CHEN, 2016; MENEGOL; RODRIGUES; RECH,). In addition, the optimization of light intensity and dissolved CO_2 in microalgae cultures are both essential factors to improve the biomass productivity in autotrophic cultures systems (YEN; HSU; CHEN, 2016).

Several kinetic models have been proposed based on Monod (1949) and Droop (1968) models capable of simultaneously predicting biomass production and nitrogen consumption in batch processes (GONÇALVES; RECH, ; MENEGOL et al., ; DA FRÉ et al., 2016). In previous work the kinetics of the autotrophic growth of *Pseudoneochloris marina* was modelled successfully by ModNX_{max} model (GONÇALVES; RECH,).

Thus, the aim of this work is the simulation and optimization of repeated-batch and continuous cultures of *Pseudoneochloris marina* based on kinetic model that showed the best fitting to the experimental data to maximizing biomass productivity. The predictions were validated trough bench-scale experiments. In addition, continuous cultures were performed in order to evaluate the potential use of CO_2 from beer fermentation. Moreover, biomass composition for *P. marina* was analyzed under all culture conditions.

7.2 Material and methods

7.2.1 Simulation and optimization of repeated-batch and continuous cultures

The kinetics of biomass growth and nitrogen consumption of *P. marina* in repeated-batch and continuous cultures was simulated to maximize biomass productivity using the $ModNX_{max}$ model proposed by Da Fré et al. (2016). $ModNX_{max}$ model combines the biomass and nitrogen balances (Equations 7.1 and 7.2) with a nitrogen-catalyzed expression for nitrogen uptake (ρ, g g^{-1} h^{-1}) uses a growth associated term (Y_{XN}, g g^{-1}) and a non-growth associated term (m_N, g g^{-1} h^{-1}) (Equation 7.3). It is based on the hypothesis that the excess of biomass is responsible for limiting biomass growth and uses the Logistic equation for specific growth rate (μ, h^{-1}) (Equation 7.4).

$$\frac{dX}{dt} = \mu \cdot X \tag{7.1}$$

$$\frac{dN}{dt} = -\rho \cdot X \tag{7.2}$$

$$\rho = \left(\frac{\mu}{Y_{XN}} + m_N\right) \cdot N \tag{7.3}$$

$$\mu = \mu_{\max} \cdot \left(1 - \frac{X}{X_{\max}}\right) \tag{7.4}$$

The ModNXmax model was implemented in EMSO software (SOARES; SECCHI, 2003) using the parameters values estimated for *P. marina* growth in batch culture of (Table 7.1) in a previous work (GONÇALVES; RECH,)

Table 7.1 - Parameters estimated of growth and nitrogen consumption for ModNXmax model. (GONÇALVES; RECH,).

Parameters	**Unit**	**Value**
$\mu_{\max}$	h^{-1}	0.03847
Y_{XN}	g g^{-1}	0.22192
m_N	g g^{-1} h^{-1}	0.00092
$X_{\max}$	g L^{-1}	2.21762

The repeated-batch cultures were simulated using several renewal volumes (V_R), between 1.0 L and 1.6 L, every 48 h. Firstly, an initial batch culture was simulated until the beginning of the stationary growth phase and then the repeated-batches started until constant biomass concentration at the end of each cycle. The nitrogen concentration in the initial and the feeding media was set to 0.450 g L^{-1}. The biomass productivity of each simulation was determined by Equation 7.5:

$$P_X = \frac{X \cdot V_R}{t \cdot V} \tag{7.5}$$

Where P_X is biomass productivity (g L^{-1} d^{-1}); V_R is renewal volume (L), t is the time interval between two batches (2 days), and V is the photobioreactor working volume (2.4 L).

The feed rate that maximize the biomass productivity of the continuous cultures calculated by the optimization entity of EMSO software, using the equations of the chosen model applied for a steady-state continuous process (Equations 7.6 – 7.9).

$$\mu = D \tag{7.6}$$

$$D(N_F - N) = \left(\frac{\mu}{Y_{XN}} + m_N\right) \cdot N \cdot X \tag{7.7}$$

$$P_X = D \cdot X \tag{7.8}$$

$$D = \frac{F}{V} \tag{7.9}$$

Where D is dilution rate (d^{-1}); N_F is the nitrogen concentration (0.450 g L^{-1}) in the feeding stream F (L d^{-1}).

7.2.2 Experimental validation of optimized repeated-batch and continuous cultures

The pre-cultures of *Pseudoneochloris marina* were prepared in 500 mL Erlenmeyer flasks with 240 mL working volume using f/2 medium with modified $NaNO_3$ concentration (300 mg L^{-1}) and NaCl (17 g L^{-1}) and inoculated with 24 mL of stock culture. The flasks were incubated in rotatory shaker (Oxylab, Oxy 304T) at 28 ºC and 180 rpm under continuous illumination (42 µmol m^{-2} s^{-1}) for 7 days.

The experimental cultures were performed in 2.4 L flat-panel airlift photobioreactors and modified f/2 medium (0.450 g L^{-1} $NaNO_3$ and 17 g L NaCl) to verify the results predicted by the optimizations described in the previous section. The photobioreactors containing 2.16 L of culture medium were inoculated with 240 mL of pre-cultures. The photobioreactors were continuously illuminated at the riser side (252 µmol m^{-2} s^{-1}) and the temperature was

maintained at 28 ºC. To avoid nutrient limitation, 1 mL L^{-1} of phosphate solution and 1 mL L^{-1} of trace-metals solution were added daily to the cultures (GONÇALVES; MENEGOL; RECH, 2019). The airflow was kept at 1 L min^{-1} of CO_2-enriched filtered air (0.22 µm Midisart®2000, Sartorius Stedim Biotech). The mixture of CO_2 and compressed air was controlled by rotameter to maintain the culture at pH 7.0. The pH was measured using pH-indicator strips (MColorpHast™, Merck, Germany). The experimental cultures were performed in duplicate.

Both repeated-batch and continuous cultures started as initial batch cultures for 7 days. The cell growth and nitrogen concentration were measured as described earlier. After this time, for repeated-batch cultures, the renewal medium volume was replaced each 48 h, based in the optimal biomass productivity predicted by simulation process. For continuous cultures the input and output feed streams where controlled by peristaltic pumps (400DM3, Watson-Marlow). The culture medium was supplemented with 1 mL L^{-1} of phosphate solution (50 g L^{-1}) to avoid nutrient limitation in continuous process. The medium containing biomass was withdrawn of photobioreactors when it reached the working volume level. The cultures were kept for 456 h. The biomass removed from photobioreactors was centrifuged (10000 × *g*, 5 min, 4 ºC), the supernatant was discarded, and the biomass was washed with distilled water and centrifuged again. The resulting biomass was lyophilized and stored at −18 ºC.

7.2.3 Integrated system of photobioreactors and fermenters - continuous cultures using CO_2 from beer fermentation

The cultures were performed under the best optimized conditions previously (Section 7.2.2), for evaluated the potential supply of CO_2 from beer fermentation in continuous cultures of *P. marina*.

Firstly, beer production was performed using Pilsen malt, hops nuggets 11 % AM T-90, and S-33 lyophilized yeast (*S. cerevisiae*). The malt was grounded and mixed with infusion water 1:5 ratio (weight/volume) using the Grain Father machine under the heating curve ranging from 20 to 66 ºC for 80 min and heat the wort at 76ºC for 20 min. The wort was clarified using a stainless-steel sieve into the machine with recirculation of water. Boiling of the wort was started with added of hops nuggets (1 g L^{-1}) and kept for 60 min, after this time, the wort was cooled to 20 ºC with the plumbing flow chiller and stored in flasks at -18 ºC further fermentation.

The fermentations were performed in triplicate using sterilized Duran flasks (1 L) and added 0.5 g L^{-1} of yeast and kept at 20 ºC in thermostatic bath for 39 h. The CO_2 kinetic

production was evaluated collecting samples every 3 h to determination of ethanol production by HPLC methodology according Cortivo et al.(2018). The CO_2 production was determined stoichiometrically considering that 1 mol of CO_2 was formed for every 1 mol of ethanol produced and derived in order to obtain the CO_2 production rate during the fermentation (CHAGAS et al., 2015).

The experimental cultures were kept under batch system for 7 days with cylinder-CO_2 supply, after continuous cultures started integrating the beer fermenters with 20% ($R_{5:1}$) and 40% ($R_{2.5:1}$) workload of photobioreactors volume and added 0.5 g L^{-1} of yeast and kept at 20 ºC in thermostatic bath. The operation of continuous phase was the same for system continuous previously described. Each fermenter remained connected to photobioreactor for 48 h. All cultures were carried out in duplicates and the results express the mean of experimental data.

7.2.4 Analytical methods

Samples were collected obtain the kinetic biomass composition of the analyzes described below. The protein content was determined according Lowry method after previous reaction of 1 mL of 1 M NaOH (100 ºC/ 30 min) add in the samples. The identification and quantification of carotenoids and fatty acids were performed in the lyophilized biomass.

The carotenoid profile was determined by method described by Mandelli et al.(2012) and adapted by Diprat et al.(2017). The exhaustive extraction of the samples (0.020 g) consists in the rupture of cell walls by maceration using ethyl acetate followed by methanol. The samples were dissolved using methanol/methyl tert-butyl ether (MeOH/MTBE, 1:1, volume fraction) and analyzed by high performance liquid chromatography-DAD method. Carotenoid content in the extracts was determined by Waters HPLC 2695 series system (Wilmington, EUA) equipped with a diode array detector (Waters 2998 dual series) and using YMC-C30 column (5 μm particle size, 250 mm × 4.6 mm) (Waters, Wilmington, USA). Flow rate was 0.9 mL min^{-1} and column temperature at 29 °C and eluted by linear gradient mobile phase applied according to Rodrigues et al. (2014). Analytical β-carotene curve was used to quantify the carotenoids (2017). The carotenoids identification was performed according Menegol et al. (2017) using an HPLC (Shimadzu, Kyoto, Japan) connected in series with a diode array detector (DAD) and a mass spectrometer (MS) with an iron trap analyzer and atmospheric pressure chemical ionization (APCI) source (Bruker Daltonics, Esquire model 6000, Bremen, Germany).

The total lipid content was determined according to Bligh and Dyer (1959) using 0.5 g of lyophilized biomass. For fatty acids quantification, the lipid fraction was boiled for 30 min with a 14 % BF_3-methanol solution under a N_2 atmosphere according to the method described

by Joseph and Ackman (1992). The samples were dissolved in hexane solvent and identified using gas chromatography (GC Model 2010, Shimadzu, Kyoto, Japan) equipped with automated sampler and injector, flame ionization detector and a capillary column of fused silica (30 m × 0.25 mm, 0.25 μm film thickness, DB-Wax, J&W 122-7032). The flame ionization detector (FID) was set at 280 °C with a H_2 and air flow at 40 mL min^{-1} and 450 mL min^{-1}, respectively. The oven temperature was set at 50 °C for 1 min and increased to 200 °C at a gradient of 25 °C min^{-1}, 3 °C min^{-1} to 230 °C. The quantification of the fatty acids was performed according to the method of American Oil Chemists' Society (1997). The identification of the fatty acids present in the samples was performed comparing the retention time with a standard mixture of fatty acid methyl esters (FAME-MIX 37 standard Sigma) previously analyzed by gas chromatography–mass spectrometry (GC–MS). The results were analyzed by analysis of variance (ANOVA) and Tukey test at a 95 % confidence level using Statistica software 12.

7.3 Results and discussion

The $ModNX_{max}$ model was used to simulate the repeated-batch cultures using different renewal volumes. Figure 7.1 shows the relationship between biomass productivity and renewal volume at 2-days interval in repeated-batch cultures. The optimum renewal volume was 1.4 L and resulted in 0.477 g L^{-1} d^{-1} of predicted biomass productivity. For continuous culture, the dilution rate (D) that maximizes biomass productivity, evaluated using EMSO optimization entity, was 0.461 d^{-1} with predicted biomass productivity of 0.514 g L^{-1} d^{-1}.

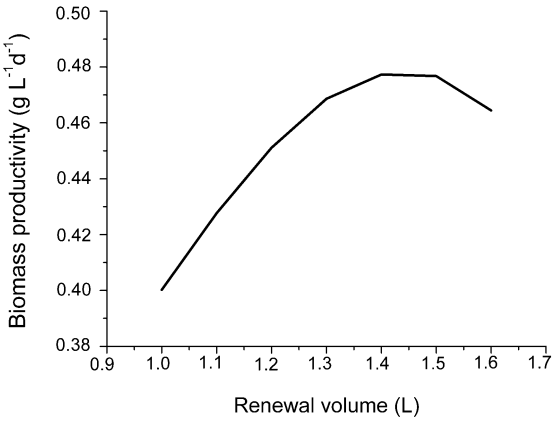

Figure 7.1 - Relationship between predicted biomass productivity and renewal volume at 2-days interval of *P. marina* repeated-batch cultures in 2.4 L photobioreactors.

An experimental repeated-batch culture was performed to validate the model prediction. Initially, a batch culture was performed until 168 h; after 1.4 L of culture were replaced by the same volume of fresh culture medium each 48 h (2 days). The experimental data agreed well with the simulated curves (Figure 7.2). The experimental average biomass concentration at the end of each cycle (1.86 ± 0.08 g L^{-1}) exceeded the predicted one (1.64 g L^{-1}). Nitrogen was consumed during the first 24 h of each cycle, as predicted by the model. The average experimental biomass productivity was 0.54 ± 0.02 g L^{-1} d^{-1}, 13 % higher than the predicted one. Semi-continuous cultures of *C. vulgaris* in bubble column photobioreactors with CO_2-enriched air showed similar behavior of cell growth compared with results showed in present study. The authors indicated a consistency in microalgae biomass production (0.84 ± 0.01 g L^{-1}) with a harvest each 5 days semi-continuous cycle (KHOO; LAM; LEE, 2016).

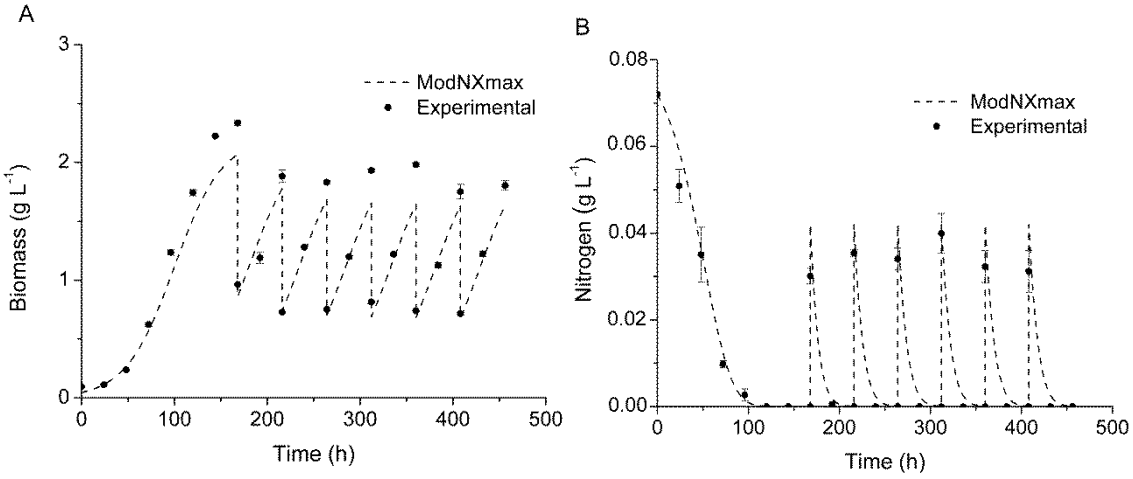

Figure 7.2-Experimental data and simulated $ModNX_{max}$ curves of biomass (A) and nitrogen (B) during *P. marina* repeated-batch (1.4 L/2 days) cultures in 2.4 L photobioreactors.

The experimental continuous cultures were run using standard CO_2-enriched air (CO_2 from cylinders) to validate the model predictions. Two other continuous cultures were run with air enriched with CO_2 prevenient of beer fermentation using two photobioreactor to beer fermenter volume ratios: 5:1 ($R_{5:1}$) and 2.5:1 ($R_{2.5:1}$). Firstly, the kinetics of CO_2 production during beer fermentation was determined (Figure 7.3). The CO_2 release started 3 h after the addition of the yeast into the fermenters and reached 1.39 ± 0.06 g L^{-1} h^{-1} at 24 h of beer fermentation, after that the rate of CO_2 release decreased until 39 h. The accumulated CO_2

produced was 32.1 ± 0.1 g L^{-1} in the end of the fermentation. To maintain an uninterrupted CO_2 supply for the experimental continuous cultures, a new beer fermenter to was coupled to the photobioreactor every 24 h and kept for 48 h. The estimated CO_2 supplied for the photobioreactors from beer fermentation during the integrated experiments $R_{5:1}$ and $R_{2.5:1}$ are shown in Figure 7.S1 (Supplementary material section).

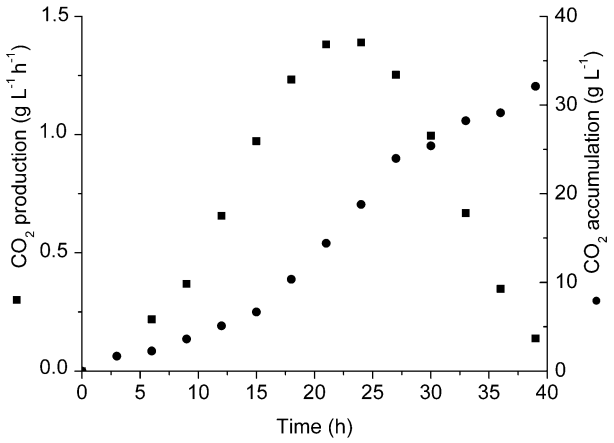

Figure 7.3 Kinetics of CO_2 production and CO_2 accumulation from beer fermentation.

As in repeated-batch culture, the experimental culture started with a 168-h batch culture followed by a continuous process with a feed rate of 1.107 L d^{-1}, as calculated by Equation 9. The experimental biomass presented good agreement with the simulated data for all continuous cultures (Figure 7.4A). The biomass decayed in the first 48 h of continuous feeding, as predicted by the simulation, and then the cultures of synthetic CO_2 supply reached a concentration until the end of the culture (1.41 ± 0.04 g L^{-1}), slightly above the predicted one (1.17 ± g L^{-1}). Already, the cultures with supply of CO_2 of beer fermentation presented slightly decline in biomass steady-state resulting in 1.27 ± 0.12 g L^{-1} and 1.29 ± 0.14 g L^{-1} to experimental cultures $R_{5:1}$ and $R_{2.5:1}$, respectively. Unlike the prediction, the experimental nitrogen concentration remained undetectable after the beginning of the feeding process (Figure 7.4B), fact that may be explained by the higher biomass concentration, resulting in a higher nutrient demand. The experimental biomass productivity was 0.66 ± 0.04 g L^{-1} d^{-1}, 29 % higher than the predicted one. Similarly to this result, continuous cultures of *Scenedesmus vacuolatus* performed in bubble column photobioreactors using CO_2-enriched air presented biomass productivity of 0.64 ± 0.2 g L^{-1} d^{-1} at the steady state condition (GARCÍA-CUBERO; MORENO-FERNÁNDEZ; GARCÍA-GONZÁLEZ, 2017).

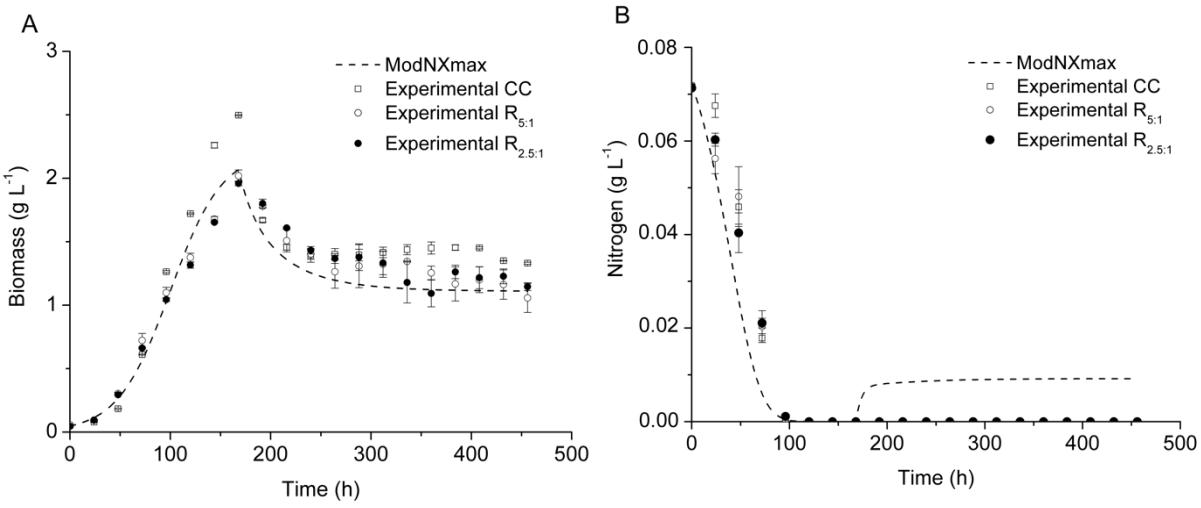

Figure 7.4 -Experimental data and simulated ModNXmax curves of biomass (A) and nitrogen (B) during *P. marina* continuous cultures (D = 0.461 d^{-1}) in 2.4 L photobioreactors.

Final biomass composition was deeply affected by culture system, i.e., batch, repeated-batch or continuous cultures (Figure 7.5). The highest protein content (309 ± 0 mg g^{-1}) was achieved in continuous culture, which can be associated to the constant nitrogen supply from the feeding medium. In batch cultures, on the other hand, the nitrogen content in culture medium was quickly depleted and the biomass continue to grow by using the intracellular nitrogen, resulting in a biomass with lower protein content (110 ± 5 mg g^{-1}). The biomass carbohydrate content was, in all cultures systems, around 517 ± 16 mg g^{-1}.

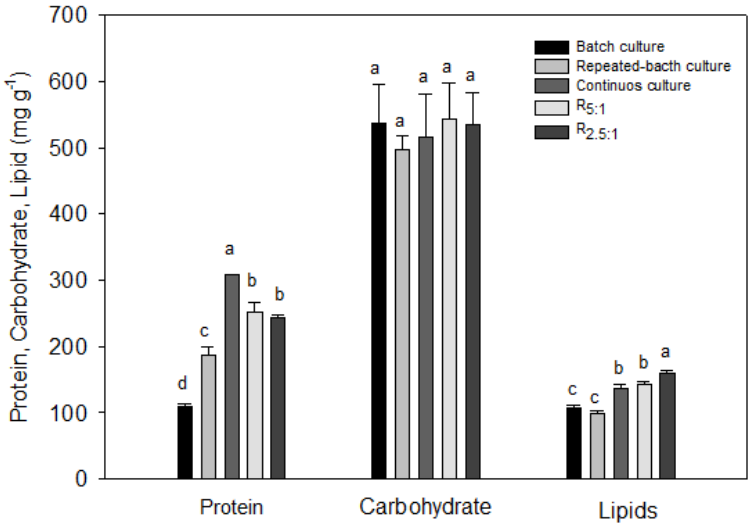

Figure 7.5 -Biomass composition of *P. marina* batch, repeated-batch and continuous cultures. Different letter in the same bar group indicate significant difference by Tukey test at 5 % significance level.

Lipid content was higher in continuous cultures (136 ± 7 mg g^{-1}), batch and repeated-batch cultures did not show significant difference ($p > 0.05$) resulting in 107 ± 4 mg g^{-1} and 98 ± 6 mg g^{-1}, respectively. Similarly to the present study, semi-continuous cultures of *Desmodesmus* sp. growth under specific conditions maintained the lipid production throughout the repeated cycles of fresh medium (HO et al., 2014b). The microalgae are able to degrade the nitrogenous compounds present in the cell to maintain metabolic activity (PANCHA et al., 2014). In many microalgae, the nitrogen excess promotes the cell growth, protein biosynthesis and under nitrogen limitation the metabolism is directed to positive regulation of lipid synthesis which stores in the energy form at the cost of ATP consumption trough photosynthesis (LI et al., 2011; JIA et al., 2015).

Continuous cultures showed the highest average carotenoid content (4.14 ± 0.14 mg g^{-1}), 47 % higher than the batch culture (2.81 ± 0.35 mg g^{-1}) and 34 % higher than the repeated-batch culture (3.08 ± 0.04 mg g^{-1}), as shown in Table 2. Under nitrogen limitation, the intracellular carotenoid content is reduced because the cells use intracellular nitrogen compounds to keep the metabolism, and in the same time lipids and carbohydrates start to accumulate in the cells.

Carotenoid profile of *P. marina* biomasses from repeated-batch and continuous cultures were identified and quantified (Table 2). The major xanthophylls and carotenes present were all-*trans*-lutein and all-*trans*-violaxanthin, and all-*trans*–α-carotene and β-carotene, respectively. The most important difference between the three culture systems was the higher xanthophylls and carotenes content in continuous culture when compared to repeated-batch culture. This relation may be explained due to the longer time that the continuous cultures were submitted to nitrogen starvation as shown in Figure 4B.

The carotenoids identified in *P. marina* were similar to the ones found in other microalgae as *D. tertiolecta* and *H. luteoviridis* (DIPRAT et al., 2017; MENEGOL et al., 2017). Jaeschke et al. (2016) performed repeated-batch cultures of *H. luteoviridis* for 38 days renewing 50 % the bioreactor volume every 2 days. The major carotenoids found were all-*trans*-lutein (0.86 ± 0.06 mg g^{-1}), all-*trans*-zeaxanthin (0.24 ± 0.02 mg g^{-1}) and β-carotene (0.18 ± 0.00 mg g^{-1}) followed by all-*trans*-α-carotene, 9-13-15-cis-β-carotene, cis-violaxanthin, all-*trans*-violaxanthin and 13–13'-cis-lutein presented in low concentrations.

Table 7.2 -Carotenoids profile in the final biomass of *P. marina* in repeated-batch and continuous cultures.

	Peak[a]	**Batch culture**	**Repeated-batch culture**	**Continuous culture**		
				Cylinder CO_2	**$R_{5:1}$**	**$R_{2.5:1}$**
	Xanthophylls (mg g^{-1})					
1	all-*trans*-violaxanthin	0.18 ± 0.05^{c}	0.57 ± 0.01^{b}	0.81 ± 0.07^{b}	1.18 ± 0.06^{a}	1.29 ± 0.08^{a}
2	cis-violaxanthin	0.12 ± 0.01^{b}	0.28 ± 0.00^{a}	0.31 ± 0.06^{a}	0.32 ± 0.02^{a}	0.32 ± 0.06^{a}
3	9-cis-violaxanthin	0.03 ± 0.00^{b}	0.08 ± 0.00^{a}	0.03 ± 0.00^{bc}	0.02 ± 0.00^{c}	0.02 ± 0.00^{c}
4	13-cis-lutein	0.09 ± 0.01^{a}	0.08 ± 0.01^{a}	0.07 ± 0.02^{a}	0.10 ± 0.04^{a}	0.13 ± 0.02^{a}
5	13'-cis-lutein	0.03 ± 0.00^{b}	0.00 ± 0.00^{c}	0.07 ± 0.00^{a}	0.02 ± 0.00^{b}	0.02 ± 0.00^{b}
6	all-*trans*-lutein	1.02 ± 0.10^{a}	0.83 ± 0.02^{a}	0.95 ± 0.05^{a}	1.10 ± 0.07^{a}	1.09 ± 0.10^{a}
7	all-*trans*-zeaxanthin	0.41 ± 0.07^{a}	0.23 ± 0.01^{ab}	0.36 ± 0.05^{ab}	0.19 ± 0.05^{b}	0.13 ± 0.04^{b}
	Total	1.86 ± 0.20^{c}	2.03 ± 0.06^{bc}	2.56 ± 0.16^{abc}	2.92 ± 0.13^{ab}	2.98 ± 0.30^{a}
	Carotenes (mg g^{-1})					
8	15-cis-β-carotene	0.03 ± 0.01^{a}	0.03 ± 0.00^{a}	0.03 ± 0.00^{a}	0.03 ± 0.00^{a}	0.03 ± 0.00^{a}
9	all-*trans*-α-carotene	0.26 ± 0.04^{c}	0.42 ± 0.01^{b}	0.71 ± 0.01^{a}	0.58 ± 0.03^{ab}	0.60 ± 0.06^{ab}
10	13-cis-β-carotene	0.12 ± 0.02^{a}	0.10 ± 0.00^{a}	0.15 ± 0.00^{a}	0.11 ± 0.01^{a}	0.11 ± 0.01^{a}
11	β-carotene	0.36 ± 0.05^{b}	0.39 ± 0.01^{b}	0.57 ± 0.02^{a}	0.59 ± 0.00^{a}	0.57 ± 0.05^{a}
12	9-cis-β-carotene	0.18 ± 0.03^{a}	0.10 ± 0.00^{a}	0.13 ± 0.01^{a}	0.12 ± 0.00^{a}	0.11 ± 0.01^{a}
	Total	0.95 ± 0.15^{c}	1.05 ± 0.02^{bc}	1.58 ± 0.02^{a}	1.42 ± 0.04^{ab}	1.41 ± 0.14^{ab}
	Total carotenoid (mg g^{-1})	2.81 ± 0.35^{b}	3.08 ± 0.04^{b}	4.14 ± 0.14^{a}	4.34± 0.17^{a}	4.40 ± 0.44^{a}

[a] Numbered according to the chromatogram shown in Figure 7.S2.

*Different letter in the same column indicate significant difference by Tukey test at 5 % significance level.

The fatty acids content in final biomass of *P. marina* were 29.6 ± 2.6 mg g^{-1} and 33.4 ± 2.3 mg g^{-1} for repeated-batch and continuous cultures, respectively. The fatty acids composition for all cultures systems is shown in Figure 7.6. The major saturated and monounsaturated fatty acids were C16:0 and C18:1. The major polyunsaturated fatty acids identified were C18:3n-6 (linoleic acid) and C18:3n-3 (α-linolenic acid). The linoleic acid amounts showed no difference among the different culture systems.

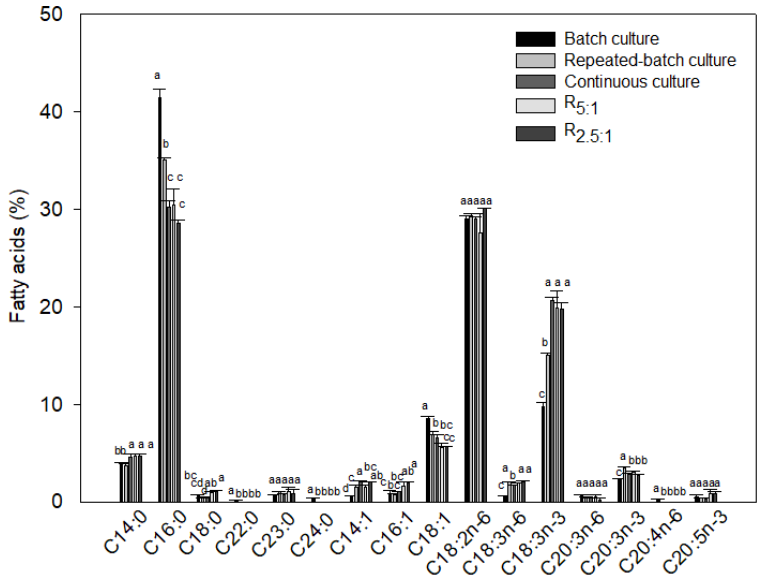

Figure 7.6 -Fatty acids composition in the final biomass of *P. marina* in batch, repeated-batch and continuous cultures. Different letter in the same bar group indicate significant difference by Tukey test at 5 % significance level.

The continuous culture showed high accumulation of α-linolenic acid (20.64 % of total fatty acids) compared with repeated-batch culture (15.01 % of total fatty acids). The both cultures produced low quantity of eicosapentanoic acid (C20:5n-3). Tang et al. (TANG et al., 2012) in continuous cultures of *C. minutissima* and *D. tertiolecta* under steady-state condition with CO_2 supply and continuous light intensity obtained total fatty acids content of 4.4 ± 0.2 % (d.w.) and 10.8 ± 0.04 % (d.w.) at dilution rate of 0.42 d^{-1}. The authors pointed that the dilution rate determines the average cell age, and consequently, affects the fatty acid profile of algal cells. This observation is consistent with the results showed in the present study where the total polyunsaturated fatty acid was increased cultures and some fatty acids as C22:0, C24:0 and C20:4 did not present significant amounts in continuous cultures when compared with batch culture of *P. marina* (data not shown). The ω6:ω3 ratio recommended by WHO (World Health

Organization) should be lower than 10 and the both cultures systems presented a ratio value less than 2. The health improving properties of polyunsaturated fatty acids of marine microalgae are recognized. These advantages of PUFAS consumption are associated a eicosapentaenoic (C20:5n-3) and docosahexaenoic acids (C22:6n-3) due to the regulation of mechanisms associated in several biological functions (SIMOPOULOS, 2016; ULMANN et al., 2017).

7.4 Conclusion

This study showed that a phenomenological mathematical model developed for a batch culture can be used successfully to predict the behaviors of repeated-batch and continuous cultures. The cultivation mode, batch, repeated-batch or continuous, not only affected biomass productivity, but also biomass composition. The constant nitrogen supply in continuous culture favored the synthesis of carotenoids, proteins and PUFAs, mainly omega-3.

The integrated system between beer fermenters and photobioreactors provided a satisfactorily CO_2 supply to maintain microalga growth, showing that beer fermentation is clean and advantageous for producing microalgae biomass to be used as food supplement or nutraceuticals.

SUPPLEMENTARY MATERIAL

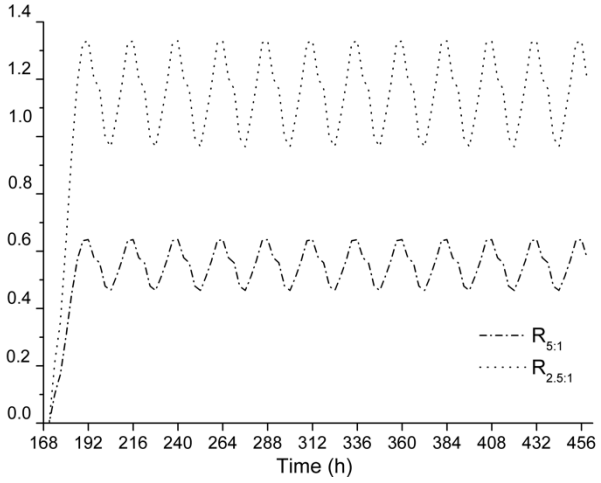

Figure 7.S1: Estimated CO_2 production from beer fermentation during the integrated experiments with fermenters and photobioreactors $R_{5:1}$ and $R_{2.5:1}$. CO_2 data is presented in grams of CO_2 supplied per liter of microalgal culture (photobioreactor) per hour (g L^{-1} h^{-1}).

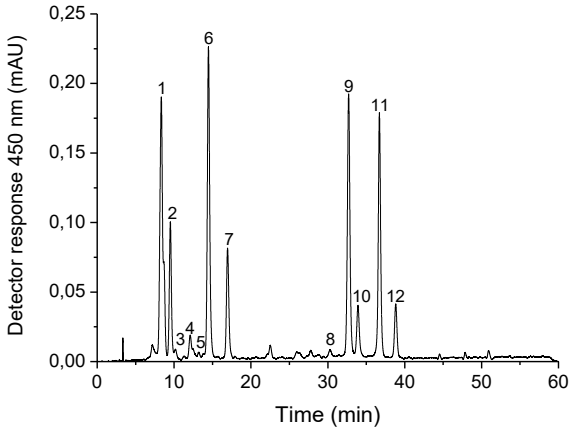

Figure 7.S2-Chromatogram of carotenoids identified in P. marina by HPLC-DAD. Peaks identified are described in Table 7.2.

Nomenclature

Symbol	Unit	
X	g L^{-1}	cell growth
X_{max}	g L^{-1}	maximum biomass concentration
μ	h^{-1}	specific growth rate
μ_{max}	h^{-1}	maximum specific growth rate
N	g L^{-1}	nitrogen concentration
ρ	g g^{-1} h^{-1}	nitrogen uptake rate
m_N	g g^{-1} h^{-1}	nitrogen non-growth-associated term
Y_{XN}	g g^{-1}	nitrogen growth-associated term
P_X	g $L^{-1}d^{-1}$	biomass productivity
Q_x	g $L^{-1}d^{-1}$	biomass productivity for continuous culture
D	d^{-1}	dilution rate
N_F	g L^{-1}	feed nitrogen concentration
F	L d^{-1}	feed rate
F_{Obj}	-	objective function
R^2	-	coefficient of determination
RMSE	-	root mean squared error

8 CONCLUSÃO GERAL

Considerando o interesse da indústria biotecnológica em explorar fontes alternativas de extração de compostos de alto valor, a investigação de diferentes condições de cultivo constitui um passo importante no desenvolvimento de estratégias para otimizar a produção de microalgas. Neste trabalho, foi possível avaliar os efeitos de concentração de nitrogênio bem como os parâmetros externos (temperatura e da intensidade luminosa) no crescimento celular e na composição da biomassa de *P. marina*. Em culturas fotoautotróficas e sob diferentes condições ambientais foi possível alcançar elevado teor de carboidratos (53,8 %) e ácidos graxos saturados (44,1 % do FA total), que podem ser explorados para a produção de biocombustíveis. Além disso, a biomassa pode ser uma fonte alternativa de produtos de alto valor, tais como carotenoides (all-*trans*-luteína, all-*trans*-zeaxantina, all-*trans*-β-caroteno e all-*trans*-α-caroteno) e ácidos graxos poli-insaturados (ácido linoleico e ácido α-linolênico). Nossos resultados permitiram o conhecimento da produtividade da biomassa sob diferentes condições de temperatura e intensidade luminosa e mostraram que *P. marina* apresentou potenciais aplicações biotecnológicas como extração de produtos de alto valor agregado e produção de biocombustíveis.

A modelagem matemática foi satisfatória para descrever o crescimento celular e consumo de nitrogênio dos cultivos de *P. marina* nos processos em batelada, batelada repetida e contínuos. Os resultados demonstraram que os cultivos em batelada repetida e contínuos aumentam a produtividade de biomassa quando comparados ao processo em batelada. Além disso, apresentam efeitos na composição da biomassa produzida como aumento no conteúdo de proteínas, carotenoides totais e de ácidos graxos poli-insaturados (ω3). O desenvolvimento do sistema integrado de cultivo para utilização de CO_2 biológico produzido por fermentação de cerveja utilizando a microalga *P. marina* resultou em um processo alternativo satisfatório, sob as condições avaliadas, para mitigação de CO_2 industrial e que apresenta vantagens como a produção renovável de compostos de interesse industrial. Com os resultados obtidos nesse trabalho, em que o uso de CO_2 de fermentação de cerveja integrado aos cultivos de *P. marina* foi suficientemente adequado para a produção de biomassa de microalgas, pode servir como modelo para desenvolver e avaliar novos processos de cultivos de microalgas com o uso de CO_2 gerado a partir de outros processos biotecnológicos.

9 SUGESTÕES PARA TRABALHOS FUTUROS

Mediante aos resultados obtidos nesse trabalho, segue abaixo algumas sugestões de trabalhos futuros:

- Avaliar outras fontes e concentrações de nitrogênio no cultivo de *Pseudoneochloris marina* quanto aos efeitos na produtividade e composição da biomassa.
- Aplicar os modelos matemáticos desenvolvidos de formação de produtos para simular a cinética de formação de produtos em cultivos contínuos de *P. marina*.
- Aplicar a modelagem matemática e simulação de crescimento celular, consumo de nitrogênio e formação de produtos para outras espécies de microalgas.
- Utilizar o CO_2 gerado a partir de produção de bioetanol e outros processos biotecnológicos para integração em cultivos *P. marina*.

10 REFERÊNCIAS BIBLIOGRÁFICAS

ABREU, A. P.; FERNANDES, B.; VICENTE, A. A.; TEIXEIRA, J.; DRAGONE, G. Mixotrophic cultivation of Chlorella vulgaris using industrial dairy waste as organic carbon source. **Bioresource Technology**, v. 118, p. 61–66, 2012.

ADESANYA, V. O.; DAVEY, M. P.; SCOTT, S. A.; SMITH, A. G. Kinetic modelling of growth and storage molecule production in microalgae under mixotrophic and autotrophic conditions. **Bioresource Technology**, v. 157, p. 293–304, 2014.

ALBERTS, B.; JOHNSON, A.; LEWIS, J.; RAFF, M.; ROBERTS, K.; WALTER, P. **Biologia Molecular da Célula**. 4. ed. Brasil: Artmed, 2004.

ANJOS, M.; FERNANDES, B. D.; VICENTE, A. A.; TEIXEIRA, J. A.; DRAGONE, G. Optimization of CO_2 bio-mitigation by *Chlorella vulgaris*. **Bioresource Technology**, v. 139, p. 149–154, 2013.

AOCS; SOCIETY, A. O. C.; AMERICAN OIL CHEMISTS' SOCIETY - AOCS; SOCIETY., A. O. C.; AOCS. **Sampling and analysis of commercial fats and oils. AOCS Official Method Cc 6-25**. 1997. n.i., Illinois, 1997.

BAUDELET, P. H.; RICOCHON, G.; LINDER, M.; MUNIGLIA, L. A new insight into cell walls of Chlorophyta. **Algal Research**, v. 25, p. 333–371, 2017.

BENAVENTE-VALDÉS, J. R.; AGUILAR, C.; CONTRERAS-ESQUIVEL, J. C.; MÉNDEZ-ZAVALA, A.; MONTAÑEZ, J. Strategies to enhance the production of photosynthetic pigments and lipids in chlorophycae species. **Biotechnology Reports**, v. 10, p. 117–125, 2016.

BILANOVIC, D.; ANDARGATCHEW, A.; KROEGER, T.; SHELEF, G. Freshwater and marine microalgae sequestering of CO2at different C and N concentrations - Response surface methodology analysis. **Energy Conversion and Management**, v. 50, n. 2, p. 262–267, 2009.

BLIGH, E. G.; DYER, W. J. A Rapid Method of Total Lipid Extraction and Purification. **Canadian journal of biochemistry and physiology**, v. 37, n. 8, p. 911–917, ago. 1959.

BONNEFOND, H.; MOELANTS, N.; TALEC, A.; BERNARD, O.; SCIANDRA, A. Concomitant effects of light and temperature diel variations on the growth rate and lipid production of *Dunaliella salina*. **Algal Research**, v. 14, p. 72–78, 2016.

BRÁNYIK, T.; VICENTE, A. A.; DOSTÁLEK, P.; TEIXEIRA, J. A. Continuous beer fermentation using immobilized yeast cell bioreactor systems. **Biotechnology Progress**, v. 21, n. 3, p. 653–663, 2005.

BRENNAN, L.; OWENDE, P. Biofuels from microalgae-A review of technologies for production, processing, and extractions of biofuels and co-products. **Renewable and Sustainable Energy Reviews**, v. 14, n. 2, p. 557–577, 2010.

BREUER, G.; LAMERS, P. P.; MARTENS, D. E.; DRAAISMA, R. B.; WIJFFELS, R. H. The impact of nitrogen starvation on the dynamics of triacylglycerol accumulation in nine microalgae strains. **Bioresource Technology**, v. 124, p. 217–226, 2012.

BUEHNER, M. R.; YOUNG, P. M.; WILLSON, B.; RAUSEN, D.; SCHOONOVER, R.; BABBITT, G.; BUNCH, S. Microalgae Growth Modeling and Control for a Vertical Flat Panel Photobioreactor. **2009 American Control Conference**, p. 2301–2306, 2009.

CARVALHO, A. P.; MONTEIRO, C. M.; MALCATA, F. X. Simultaneous effect of irradiance and temperature on biochemical composition of the microalga *Pavlova lutheri*. **Journal of Applied Phycology**, v. 21, n. 5, p. 543–552, 2009.

CATALDO, D. A.; HAROON, M.; SCHRADER, L. E.; YOUNGS, V. L. Rapid colorimetric determination of nitrate in plant-tissue by nitration of salicylic-acid. **Communications in Soil**

Science and Plant Analysis, v. 6, n. 1, p. 71–80, 1975.
CERVBRASIL. Anuário 2016. **Associação brasileira da indústria da cerveja**, p. 1–62, 2016. Disponível em: <http://cervbrasil.org.br/arquivos/informes/Informe_CervBrasil_12abr.pdf>.
CHAGAS, A. L. L.; RIOS, A. O. O.; JARENKOW, A.; MARCÍLIO, N. R. R.; AYUB, M. a. Z. A. Z.; RECH, R. Production of carotenoids and lipids by *Dunaliella tertiolecta* using CO2 from beer fermentation. **Process Biochemistry**, v. 50, n. 6, p. 981–988, 2015a.
CHAGAS, A. L.; RIOS, A. O.; JARENKOW, A.; MARCÍLIO, N. R.; AYUB, M. A. Z.; RECH, R. Production of carotenoids and lipids by *Dunaliella tertiolecta* using CO_2 from beer fermentation. **Process Biochemistry**, 2015b.
CHEAH, W. Y.; SHOW, P. L.; CHANG, J.-S.; LING, T. C.; CHING JUAN, J. Biosequestration of atmospheric CO2 and flue gas-containing CO 2 by microalgae. v. 184, p. 190–201, 2015.
CHEN, C. Y.; ZHAO, X. Q.; YEN, H. W.; HO, S. H.; CHENG, C. L.; LEE, D. J.; BAI, F. W.; CHANG, J. S. Microalgae-based carbohydrates for biofuel production. **Biochemical Engineering Journal**, v. 78, p. 1–10, 2013.
CHEN, M.; TANG, H.; MA, H.; HOLLAND, T. C.; NG, K. Y. S.; SALLEY, S. O. Effect of nutrients on growth and lipid accumulation in the green algae Dunaliella tertiolecta. **Bioresource Technology**, v. 102, n. 2, p. 1649–1655, 2011. Disponível em: <http://dx.doi.org/10.1016/j.biortech.2010.09.062>.
CORTIVO, P. R. D.; HICKERT, L. R.; HECTOR, R.; AYUB, M. A. Z. Fermentation of oat and soybean hull hydrolysates into ethanol and xylitol by recombinant industrial strains of Saccharomyces cerevisiae under diverse oxygen environments. **Industrial Crops and Products**, v. 113, n. January, p. 10–18, 2018. Disponível em: <https://doi.org/10.1016/j.indcrop.2018.01.010>.
COSTA, J. A. V.; MORAIS, M. G. An Open Pond System for Microalgal Cultivation. In: **Biofuels from Algae**. San Diego: Elsevier Ltd, 2014. p. 1–22.
D'ALESSANDRO, E. B.; ANTONIOSI FILHO, N. R. Concepts and studies on lipid and pigments of microalgae: A review. **Renewable and Sustainable Energy Reviews**, v. 58, p. 832–841, 2016.
DA FRÉ, N. C.; CHAGAS, A. L. das; RECH, R.; MARCÍLIO, N. R. Kinetic Modeling of Dunaliella tertiolecta Growth under Different Nitrogen Concentrations. **Chemical Engineering & Technology**, v. 39, n. 9, p. 1716–1722, 2016.
DARIENKO, T.; GUSTAVS, L.; MUDIMU, O.; MENENDEZ, C. R.; SCHUMANN, R.; KARSTEN, U.; FRIEDL, T.; PRÖSCHOLD, T. *Chloroidium*, a common terrestrial coccoid green alga previously assigned to Chlorella (*Trebouxiophyceae, Chlorophyta*). **European Journal of Phycology**, v. 45, n. 1, p. 79–95, 2010.
DIPRAT, A. B.; MENEGOL, T.; BOELTER, J. F.; ZMOZINSKI, A.; RODRIGUES VALE, M. G.; RODRIGUES, E.; RECH, R. Chemical composition of microalgae *Heterochlorella luteoviridis* and *Dunaliella tertiolecta* with emphasis on carotenoids. **Journal of the Science of Food and Agriculture**, v. 97, n. 10, p. 3463–3468, 2017.
DRAGONE, G.; MUSSATTO, S. I.; SILVA, J. B. D. a. Use of concentrated worts for high gravity brewing by continuous process: New tendencies for the productivity increase. **Ciencia e Tecnologia de Alimentos**, v. 27, p. 37–40, 2007.
DROOP, M. R. R. Vitamin B12 and Marine Ecology. IV. The Kinetics of Uptake, Growth and Inhibition in Monochrysis Lutheri. **Journal of the Marine Biological Association of the United Kingdom**, v. 48, n. 3, p. 689–733, 1968.
DUBOIS, M.; GILLES, K.; HAMILTON, J.; REBERS, P.; SMITH, F. Colorimetric method for determination of sugars and related substances. **Analytical Chemistry**, v. 28, n. 3, p. 350–356, 1956.

FERNANDES, B. D.; DRAGONE, G. M.; TEIXEIRA, J. A.; VICENTE, A. A. Light regime characterization in an airlift photobioreactor for production of microalgae with high starch content. **Applied Biochemistry and Biotechnology**, v. 161, n. 1–8, p. 218–226, 2010.
FERREIRA, L. S.; RODRIGUES, M. S.; CONVERTI, A.; SATO, S.; CARVALHO, J. C. M. Arthrospira (Spirulina) platensis cultivation in tubular photobioreactor: Use of no-cost CO2 from ethanol fermentation. **Applied Energy**, v. 92, p. 379–385, 2012.
GADEN, E. L.; GADEN JR., E. L. Fermentation Process Kinetics. **Biotechnology and Bioengineering**, v. 1, n. 4, p. 629–635, mar. 2000.
GARCÍA-CAÑEDO, J. C.; CRISTIANI-URBINA, E.; FLORES-ORTIZ, C. M.; PONCE-NOYOLA, T.; ESPARZA-GARCÍA, F.; CAÑIZARES-VILLANUEVA, R. O. Batch and fed-batch culture of Scenedesmus incrassatulus: Effect over biomass, carotenoid profile and concentration, photosynthetic efficiency and non-photochemical quenching. **Algal Research**, v. 13, p. 41–52, 2016.
GARCÍA-CUBERO, R.; MORENO-FERNÁNDEZ, J.; GARCÍA-GONZÁLEZ, M. Modelling growth and CO2 fixation by Scenedesmus vacuolatus in continuous culture. **Algal Research**, v. 24, n. March, p. 333–339, 2017.
GONÇALVES, C. F.; MENEGOL, T.; RECH, R. Biochemical composition of green microalgae Pseudoneochloris marina grown under different temperature and light conditions. **Biocatalysis and Agricultural Biotechnology**, v. 18, n. July 2018, p. 101032, 2019. Disponível em: <https://doi.org/10.1016/j.bcab.2019.101032>.
GONÇALVES, C. F.; RECH, R. Kinetic modeling of cell growth, nitrogen consumption and intracellular bioproducts of Pseudoneochloris marina cultures in airlift photobioreactors. **not submited-under review**, [s.d.]
GONG, M.; BASSI, A. Carotenoids from microalgae: A review of recent developments. **Biotechnology Advances**, v. 34, n. 8, p. 1396–1412, 2016.
GROVER, M.; MAHESWARI, M.; DESAI, S.; GOPINATH, K. A.; VENKATESWARLU, B. Elevated CO2: Plant associated microorganisms and carbon sequestration. **Applied Soil Ecology**, v. 95, p. 73–85, 2015.
GUILLARD, R. R. L. R. L. Culture of Phytoplankton for Feeding Marine Invertebrates. In: SMITH, W. L.; CHANLEY, M. H. (Ed.). **Culture of Marine Invertebrate Animals: Proceedings --- 1st Conference on Culture of Marine Invertebrate Animals Greenport**. Boston, MA, MA: Springer US, 1975. p. 29–60.
HADI, S. I. I. A.; SANTANA, H.; BRUNALE, P. P. M.; GOMES, T. G.; OLIVEIRA, M. E. C. M. D.; MATTHIENSEN, A.; OLIVEIRA, M. E. C. M. D.; SILVA, F. C. P.; BRASIL, B. S. A. F. DNA barcoding green microalgae isolated from neotropical inland waters. **PLoS ONE**, v. 11, n. 2, p. 1–18, 2016.
HARUN, R.; SINGH, M.; FORDE, G. M.; DANQUAH, M. K. Bioprocess engineering of microalgae to produce a variety of consumer products. **Renewable and Sustainable Energy Reviews**, v. 14, n. 3, p. 1037–1047, 2010.
HE, Y.; CHEN, L.; ZHOU, Y.; CHEN, H.; ZHOU, X.; CAI, F.; HUANG, J.; WANG, M.; CHEN, B.; GUO, Z. Analysis and model delineation of marine microalgae growth and lipid accumulation in flat-plate photobioreactor. **Biochemical Engineering Journal**, v. 111, p. 108–116, 2016.
HO, S. H.; CHANG, J. S.; LAI, Y. Y.; CHEN, C. N. N. Achieving high lipid productivity of a thermotolerant microalga *Desmodesmus* sp. F2 by optimizing environmental factors and nutrient conditions. **Bioresource Technology**, v. 156, p. 108–116, 2014a.
HO, S. H.; CHEN, C. N. N.; LAI, Y. Y.; LU, W. Bin; CHANG, J. S. Exploring the high lipid production potential of a thermotolerant microalga using statistical optimization and semi-continuous cultivation. **Bioresource Technology**, v. 163, p. 128–135, 2014b.

HO, S. H.; HUANG, S. W.; CHEN, C. Y.; HASUNUMA, T.; KONDO, A.; CHANG, J. S. Bioethanol production using carbohydrate-rich microalgae biomass as feedstock. **Bioresource Technology**, v. 135, p. 191–198, 2013.
HUANG, J. J.; LIN, S.; XU, W.; CHI, P.; CHEUNG, K. Occurrence and biosynthesis of carotenoids in phytoplankton. **Biotechnology Advances**, v. 35, n. 5, p. 597–618, 2017.
JAESCHKE, D. P.; MENEGOL, T.; RECH, R.; MERCALI, G. D.; DAMASCENO, L.; MARCZAK, F.; MARCZAK, L. D. F. Carotenoid and lipid extraction from *Heterochlorella luteoviridis* using moderate electric field and ethanol. **Process Biochemistry**, v. 51, n. 10, 2016. Disponível em: <http://dx.doi.org/10.1016/j.procbio.2016.07.016>.
JAJESNIAK, P.; ELDIN, H.; OMAR, M.; WONG, T. S.; JAJESNIAK, P.; ELDIN, H.; ALI, M. O. Carbon Dioxide Capture and Utilization using Biological Systems : Opportunities and Challenges. **Bioprocessing & Biotechniques**, v. 4, n. 3, p. 15, 2014.
JIA, J.; HAN, D.; GERKEN, H. G.; LI, Y.; SOMMERFELD, M.; HU, Q.; XU, J. Molecular mechanisms for photosynthetic carbon partitioning into storage neutral lipids in Nannochloropsis oceanica under nitrogen-depletion conditions. **Algal Research**, v. 7, p. 66–77, 2015.
JOHN, R. P.; ANISHA, G. S.; NAMPOOTHIRI, K. M.; PANDEY, A. Micro and macroalgal biomass: A renewable source for bioethanol. **Bioresource Technology**, v. 102, n. 1, p. 186–193, 2011.
JOSEPH, J. D. .; ACKMAN, R. G. Capillary column gas chromatographic method for analysis of encapsulated fish oils and fish oil ethyl esters: collaborative study. **Journal of AOAC International**, v. 75, n. 3, p. 488–506, 1992.
KASSIM, M. A.; MENG, T. K. Carbon dioxide (CO2) biofixation by microalgae and its potential for biorefinery and biofuel production. **Science of the Total Environment**, v. 584–585, p. 1121–1129, 2017.
KENT, W. J. BLAT—The BLAST-Like Alignment Tool. **Genome Research**, v. 12, n. 4, p. 656–664, abr. 2002.
KHANRA, S.; MONDAL, M.; HALDER, G.; TIWARI, O. N.; GAYEN, K.; BHOWMICK, T. K. Downstream processing of microalgae for pigments, protein and carbohydrate in industrial application: A review. **Food and Bioproducts Processing**, p. Accepted manuscript, 2018. Disponível em: <http://linkinghub.elsevier.com/retrieve/pii/S0960308518300105>.
KHOO, C. G.; LAM, M. K.; LEE, K. T. Pilot-scale semi-continuous cultivation ofmicroalgae Chlorella vulgaris in bubble column photobioreactor (BC-PBR): Hydrodynamics and gas-liquid mass transfer study. **Algal Research**, v. 15, p. 65–76, 2016.
KIRAN, B.; PATHAK, K.; KUMAR, R.; DESHMUKH, D. Statistical optimization using Central Composite Design for biomass and lipid productivity of microalga: A step towards enhanced biodiesel production. **Ecological Engineering**, v. 92, p. 73–81, 2016.
KOCHEM, L. H.; DA FRÉ, N. C.; REDAELLI, C.; RECH, R.; MARCÍLIO, N. R. Characterization of a novel flat-panel airlift photobioreactor with an internal heat exchanger. **Chemical Engineering and Technology**, v. 37, n. 1, p. 59–64, 2014.
KRIENITZ, L.; HEGEWALD, E. H.; HEPPERLE, D.; HUSS, V. A. R.; ROHR, T.; WOLF, M. Phylogenetic relationship of *Chlorella* and *Parachlorella* gen. nov. (*Chlorophyta, Trebouxiophyceae*). **Phycologia**, v. 43, n. 5, p. 529–542, 2004.
KRIENITZ, L.; HUSS, V. A. R.; BOCK, C. *Chlorella*: 125 years of the green survivalist. **Trends in plant science**, v. 20, n. 2, p. 67–9, fev. 2015.
KUMAR, A.; ERGAS, S.; YUAN, X.; SAHU, A.; ZHANG, Q.; DEWULF, J.; MALCATA, F. X.; VAN LANGENHOVE, H. Enhanced CO2fixation and biofuel production via microalgae: Recent developments and future directions. **Trends in Biotechnology**, v. 28, n. 7, p. 371–380, 2010.
KUMAR, A.; GURIA, C.; CHITRES, G.; CHAKRABORTY, A.; PATHAK, A. K. Modelling

of microalgal growth and lipid production in Dunaliella tertiolecta using nitrogen-phosphorus-potassium fertilizer medium in sintered disk chromatographic glass bubble column. **Bioresource Technology**, v. 218, p. 1021–1036, 2016.
KUMAR, A.; GURIA, C.; PATHAK, A. K. Potential CO_2 fixation and optimal *Dunaliella tertiolecta* cultivation : In fl uence of fertilizer , wavelength of light-emitting diodes , salinity and carbon supply strategy. **Journal of CO_2 Utilization**, v. 22, n. August, p. 164–177, 2017. Disponível em: <https://doi.org/10.1016/j.jcou.2017.09.013>.
KUMAR, M. S.; HWANG, J. H.; ABOU-SHANAB, R. A. I.; KABRA, A. N.; JI, M. K.; JEON, B. H. Influence of CO2 and light spectra on the enhancement of microalgal growth and lipid content. **Journal of Renewable and Sustainable Energy**, v. 6, n. 6, 2014.
KUMAR, S.; STECHER, G.; TAMURA, K. MEGA7: Molecular Evolutionary Genetics Analysis Version 7.0 for Bigger Datasets. **Molecular biology and evolution**, v. 33, n. 7, p. 1870–1874, jul. 2016.
KUMARI, A.; KUMAR, A.; PATHAK, A. K.; GURIA, C. Carbon dioxide assisted *Spirulina platensis* cultivation using NPK-10 : 26 : 26 complex fertilizer in sintered disk chromatographic glass bubble column. **Biochemical Pharmacology**, v. 8, p. 49–59, 2014. Disponível em: <http://dx.doi.org/10.1016/j.jcou.2014.07.001>.
LAM, M. K.; LEE, K. T. Scale-Up and Commercialization of Algal Cultivation and Biofuel Production. In: **Biofuels from Algae**. San Diego: Elsevier Ltd, 2014. p. 261–286.
LEE, E.; JALALIZADEH, M.; ZHANG, Q. Growth kinetic models for microalgae cultivation: A review. **Algal Research**, v. 12, p. 497–512, 2015.
LI, Y. S.; YU, Y. Z.; CHENG, X. L.; CHEN, G. Interface Movement and Microstructure Evolution of Interdiffusion in the Binary Alloy Diffusion Couples. **Materials Science Forum**, v. 689, p. 123–129, 2011.
LICHTENTHALER, H. K.; BUSCHMANN, C. Chlorophylls and Carotenoids: Measurement And Characterization by UV-VIS Spectroscopy. **Current Protocols in Food Analytical Chemistry**, v. 2–2, p. 171–178, 2001.
LOS, D. A.; MIRONOV, K. S.; ALLAKHVERDIEV, S. I. Regulatory role of membrane fluidity in gene expression and physiological functions. **Photosynthesis Research**, v. 116, p. 489–509, 2013.
LOURENÇO, S. O. **Cultivo de microalgas marinhas: princípios e aplicações**. 1. ed. São Carlos: RiMa, 2006.
LOWRY, O. H.; ROSEBROUGH, N. J.; FARR, A. L.; RANDALL, R. J. Protein measurement with the Folin phenol reagent. **The Journal of biological chemistry**, v. 193, n. 1, p. 265–75, 1 nov. 1951.
LUEDEKING, R.; PIRET, E. L. A kinetic study of the lactic acid fermentation. Batch process at controllet pH. **Journal of biochemical and microbiological technology and engineering**, v. 1, n. 4, p. 393–412, dez. 1959.
MA, X. N.; CHEN, T. P.; YANG, B.; LIU, J.; CHEN, F. Lipid production from *Nannochloropsis*. **Marine Drugs**, v. 14, n. 4, 2016.
MANDELLI, F.; MIRANDA, V. S.; RODRIGUES, E.; MERCADANTE, A. Z. Identification of Carotenoids with High Antioxidant Capacity Produced by Extremophile Microorganisms. **World Journal of Microbiology and Biotechnology**, v. 28, n. 4, p. 1781–1790, 2012.
MARSULLO, M.; MIAN, A.; ENSINAS, A. V.; MANENTE, G.; LAZZARETTO, A.; MARECHAL, F. Dynamic modeling of the microalgae cultivation phase for energy production in open raceway ponds and flat panel photobioreactors. v. 3, n. article 41, p. 18-, 2015.
MASOJÍDEK, J.; TORZILLO, G.; KOBLÍŽEK, M.; MASOJIDEK, J.; KOBLIZEK, M.; TORZILLO, G.; MASOJÍDEK, J.; TORZILLO, G.; KOBLÍŽEK, M. Photosynthesis in

Microalgae. In: HU, A. R. AND Q. (Ed.). **Handbook of Microalgal Culture: Applied Phycology and Biotechnology**. Chichester,UK: Willey Blackwell, 2013. p. 21–36.
MATA, T. M.; MARTINS, A. A.; CAETANO, N. S. Microalgae for biodiesel production and other applications: A review. **Renewable and Sustainable Energy Reviews**, v. 14, p. 217–232, 2010.
MATSUDO, M. C.; BEZERRA, R. P.; CONVERTI, A.; SATO, S.; CARVALHO, J. C. M. CO2 from alcoholic fermentation for continuous cultivation of Arthrospira (Spirulina) platensis in tubular photobioreactor using urea as nitrogen source. **Biotechnology Progress**, v. 27, n. 3, p. 650–656, 2011.
MENEGOL, T.; DIPRAT, A. B. A. B.; RODRIGUES, E.; RECH, R. Effect of temperature and nitrogen concentration on biomass composition of *Heterochlorella luteoviridis*. **Food Science and technology**, v. 37, n. Special Issue, p. 28–37, 2017.
MENEGOL, T.; GONÇALVES, C. F.; RODRIGUES, E.; RECH, R. Kinetic modeling of Heterochlorella luteoviridis in batch culture and optimization of a repeated-batch process: effect on biomass and concentration of bioactive compounds. **Unpublished article**, n. Under review, [s.d.]
MENEGOL, T.; RODRIGUES, E.; RECH, R. Continuous cultivation of Heterochlorella luteoviridis using CO2 from wine fermentation. **Unpublished article**, [s.d.]
MINHAS, A. K.; HODGSON, P.; BARROW, C. J.; ADHOLEYA, A. A review on the assessment of stress conditions for simultaneous production of microalgal lipids and carotenoids. **Frontiers in Microbiology**, v. 7, n. Artcile 546, p. 19p, 2016.
MISHRA, S. K.; SUH, W. I.; FAROOQ, W.; MOON, M.; SHRIVASTAV, A.; PARK, M. S.; YANG, J. W. Rapid quantification of microalgal lipids in aqueous medium by a simple colorimetric method. **Bioresource Technology**, v. 155, p. 330–333, 2014. Disponível em: <http://dx.doi.org/10.1016/j.biortech.2013.12.077>.
MOHAN, S. V.; DEVI, M. P.; SUBHASH, G. V.; CHANDRA, R. Algae Oils as Fuels. In: **Biofuels from Algae**. San Diego: Elsevier Ltd, 2014. p. 155–187.
MONOD, J. THE GROWTH OF BACTERIAL CULTURES. **Annual Reviews in Microbiology**, v. 3, p. 371–394, 1949.
NEUSTUPA, J.; NĚMCOVÁ, Y.; ELIÁŠ, M.; ŠKALOUD, P. *Kalinella bambusicola* gen. et sp. nov. (*Trebouxiophyceae, Chlorophyta*), a novel coccoid *Chlorella*-like subaerial alga from Southeast Asia. **Phycological Research**, v. 57, n. 3, p. 159–169, 2009.
OKUYAMA, H.; ORIKASA, Y.; NISHIDA, T. Significance of Antioxidative Functions of Eicosapentaenoic and Docosahexaenoic Acids in Marine Microorganisms. **APPLIED AND ENVIRONMENTAL MICROBIOLOGY**, v. 74, n. 3, p. 570–574, 2008.
PACKER, A.; LI, Y.; ANDERSEN, T.; HU, Q.; KUANG, Y.; SOMMERFELD, M. Bioresource Technology Growth and neutral lipid synthesis in green microalgae : A mathematical model. **Bioresource Technology**, v. 102, n. 1, p. 111–117, 2011.
PAES, C. R. P. S.; FARIA, G. R.; TINOCO, N. A. B.; CASTRO, D. J. F. A.; BARBARINO, E.; LOURENCO, S. O. Growth, nutrient uptake and chemical composition of *Chlorella* sp. and *Nannochloropsis oculata* under nitrogen starvation. **Latin American Journal of Aquatic Research**, v. 44, n. 2, p. 275–292, 2016.
PANCHA, I.; CHOKSHI, K.; GEORGE, B.; GHOSH, T.; PALIWAL, C.; MAURYA, R.; MISHRA, S. Nitrogen stress triggered biochemical and morphological changes in the microalgae *Scenedesmus* sp. CCNM 1077. **Bioresource Technology**, v. 156, p. 146–154, 2014.
PANCHA, I.; CHOKSHI, K.; GHOSH, T.; PALIWAL, C.; MAURYA, R.; MISHRA, S. Bicarbonate supplementation enhanced biofuel production potential as well as nutritional stress mitigation in the microalgae Scenedesmus sp. CCNM 1077. **Bioresource Technology**, v. 193, p. 315–323, 2015.

PEGG, C.; WOLF, M.; ALANAGREH, L.; PORTMAN, R.; BUCHHEIM, M. A. Morphological diversity masks phylogenetic similarity of *Ettlia* and *Haematococcus* (*Chlorophyceae*). **Phycologia**, v. 54, n. 4, p. 385–397, jul. 2015.
RENAUD, S. M.; THINH, L.-V.; LAMBRINIDIS, G.; PARRY, D. L. Effect of temperature on growth, chemical composition and fatty acid composition of tropical Australian microalgae grown in batch cultures. **Aquaculture**, v. 211, n. 1–4, p. 195–214, 2002.
RIBEIRO, R. L. L.; VARGAS, J. V. C.; MARIANO, A. B.; ORDONEZ, J. C. The experimental validation of a large-scale compact tubular microalgae photobioreactor model. **International Journal of Energy Research**, v. 41, n. 14, p. 2221–2235, 2017.
RODRIGUES, D. B.; FLORES, É. M. M.; BARIN, J. S.; MERCADANTE, A. Z.; JACOB-LOPES, E.; ZEPKA, L. Q. Production of carotenoids from microalgae cultivated using agroindustrial wastes. **Food Research International**, v. 65, n. PB, p. 144–148, 2014.
RUBIN, E. S. CO2 Capture and Transport. **Elements**, v. 4, n. 5, p. 311–317, 2008.
SACHDEVA, N.; KUMAR, G. D.; PRAKASH, R.; SHANKAR, A.; MANIKANDAN, B.; BASU, B.; KUMAR, D. Bioresource Technology Kinetic modeling of growth and lipid body induction in Chlorella pyrenoidosa under heterotrophic conditions. **Bioresource Technology**, v. 218, p. 934–943, 2016. Disponível em: <http://dx.doi.org/10.1016/j.biortech.2016.07.063>.
SAFI, C.; ZEBIB, B.; MERAH, O.; PONTALIER, P. Y.; VACA-GARCIA, C. Morphology, composition, production, processing and applications of Chlorella vulgaris: A review. **Renewable and Sustainable Energy Reviews**, v. 35, p. 265–278, 2014.
SAHU, A.; PANCHA, I.; JAIN, D.; PALIWAL, C.; GHOSH, T.; PATIDAR, S.; BHATTACHARYA, S.; MISHRA, S. Fatty acids as biomarkers of microalgae. **Phytochemistry**, 2013.
SCHMIDELL, W.; LIMA, U. de A.; AQUARONE, E.; BORZANI, W. **Biotecnologia Industrial - Vol.2 - Engenharia Bioquímica**. 1. ed. Brasil: Blucher, 2001.
SCHÜLER, L. M.; SCHULZE, P. S. C.; PEREIRA, H.; BARREIRA, L.; LEÓN, R.; VARELA, J. Trends and strategies to enhance triacylglycerols and high-value compounds in microalgae. **Algal Research**, v. 25, p. 263–273, 2017.
SHARMA, K. K.; SCHUHMANN, H.; SCHENK, P. M. High Lipid Induction in Microalgae for Biodiesel Production. **Energies**, v. 5, p. 1532–1553, 2012.
SIERRA, E.; ACIÉN, F. G.; FERNÁNDEZ, J. M.; GARCÍA, J. L.; GONZÁLEZ, C.; MOLINA, E. Characterization of a flat plate photobioreactor for the production of microalgae. **Chemical Engineering Journal**, v. 138, n. 1–3, p. 136–147, 2008.
SIMOPOULOS, A. P. The Importance of the Omega-6/Omega-3 Fatty Acid Ratio in Cardiovascular Disease and Other Chronic Diseases. **Experimental Biology and Medicine**, v. 233, n. 6, p. 674–688, 1 jun. 2008.
SIMOPOULOS, A. P. An increase in the Omega-6/Omega-3 fatty acid ratio increases the risk for obesity. **Nutrients**, v. 8, n. 3, p. 1–17, 2016.
SOARES, R. de P.; SECCHI, A. R. EMSO: A New Environment for Modelling, Simulation and Optimisation. **European Symposium on Computer Aided Process Engineering**, p. 947–952, 2003.
SOLIMENO, A.; SAMSÓ, R.; UGGETTI, E.; SIALVE, B.; STEYER, J. P.; GABARRÓ, A.; GARCÍA, J. New mechanistic model to simulate microalgae growth. **Algal Research**, v. 12, p. 350–358, 2015.
SOMOGYI, B.; FELFÖLDI, T.; SOLYMOSI, K.; FLIEGER, K.; MÁRIALIGETI, K.; BÖDDI, B.; VÖRÖS, L. One step closer to eliminating the nomenclatural problems of minute coccoid green algae: *Pseudochloris wilhelmii*, gen. et sp. nov. (*Trebouxiophyceae, Chlorophyta*). **European Journal of Phycology**, v. 48, n. 4, p. 427–436, nov. 2013.
SYDNEY, E. B.; STURM, W.; DE CARVALHO, J. C.; THOMAZ-SOCCOL, V.;

LARROCHE, C.; PANDEY, A.; SOCCOL, C. R. Potential carbon dioxide fixation by industrially important microalgae. **Bioresource Technology**, v. 101, n. 15, p. 5892–5896, 2010. Disponível em: <http://dx.doi.org/10.1016/j.biortech.2010.02.088>.
TAMURA, K.; NEI, M. Estimation of the number of base nucleotide substitutions in the control region of mitochondrial DNA in humans and chimpanzees. **Molecular Biology and Evolution**, v. 10, n. 3, p. 512–526, maio 1993.
TANG, H.; ABUNASSER, N.; GARCIA, M. E. D.; CHEN, M.; SIMON NG, K. Y.; SALLEY, S. O. Potential of microalgae oil from Dunaliella tertiolecta as a feedstock for biodiesel. **Applied Energy**, v. 88, n. 10, p. 3324–3330, 2011.
TANG, H.; CHEN, M.; SIMON NG, K. Y.; SALLEY, S. O. Continuous microalgae cultivation in a photobioreactor. **Biotechnology and Bioengineering**, v. 109, n. 10, p. 2468–2474, 2012.
TEVATIA, R. Bioresource Technology Kinetic modeling of photoautotropic growth and neutral lipid accumulation in terms of ammonium concentration in Chlamydomonas reinhardtii. v. 119, p. 419–424, 2012.
THAWECHAI, T.; CHEIRSILP, B.; LOUHASAKUL, Y.; BOONSAWANG, P.; PRASERTSAN, P. Mitigation of carbon dioxide by oleaginous microalgae for lipids and pigments production: Effect of light illumination and carbon dioxide feeding strategies. **Bioresource Technology**, v. 219, p. 139–149, 2016.
THOMPSON, J. D.; HIGGINS, D. G.; GIBSON, T. J. CLUSTAL W: Improving the sensitivity of progressive multiple sequence alignment through sequence weighting, position-specific gap penalties and weight matrix choice. **Nucleic Acids Research**, v. 22, n. 22, p. 4673–4680, nov. 1994.
TINOCO, N. A. B.; TEIXEIRA, C. M. L. L.; REZENDE, C. M. The Genus Dunaliella: Biotechnology and Applications. **Revista Virtual de Química**, v. 7, n. 4, p. 1421–1440, 2015.
ULMANN, L.; BLANCKAERT, V.; MIMOUNI, V.; ANDERSSON, M. X.; CHENAIS*, B. S. and B. **Microalgal Fatty Acids and Their Implication in Health and DiseaseMini-Reviews in Medicinal Chemistry**, 2017. .
URRETA, I.; IKARAN, Z.; JANICES, I.; IBAÑEZ, E.; CASTRO-PUYANA, M.; CASTAÑÓN, S.; SUÁREZ-ALVAREZ, S. Revalorization of *Neochloris oleoabundans* biomass as source of biodiesel by concurrent production of lipids and carotenoids. **Algal Research**, v. 5, n. 1, p. 16–22, 2014.
VAN WAGENEN, J.; MILLER, T. W.; HOBBS, S.; HOOK, P.; CROWE, B.; HUESEMANN, M. Effects of light and temperature on fatty acid production in *Nannochloropsis salina*. **Energies**, v. 5, n. 3, p. 731–740, 2012.
VATCHEVA, I.; DE JONG, H.; BERNARD, O.; MARS, N. J. I. Experiment selection for the discrimination of semi-quantitative models of dynamical systems. **Artificial Intelligence**, v. 170, n. 4–5, p. 472–506, 2006.
VAZ, B. S.; COSTA, J. A. V.; MORAIS, M. G.; DA SILVA VAZ, B.; COSTA, J. A. V.; DE MORAIS, M. G. CO2 Biofixation by the Cyanobacterium Spirulina sp. LEB 18 and the Green Alga Chlorella fusca LEB 111 Grown Using Gas Effluents and Solid Residues of Thermoelectric Origin. **Applied Biochemistry and Biotechnology**, v. 178, p. 418–429, 2015.
VOGELS, M.; ZOECKLER, R.; STASIW, D. M.; CERNY, L. C. P. F. Verhulst's ``notice sur la loi que la populations suit dans son accroissement'' from correspondence mathematique et physique. Ghent, vol. X, 1838. **Journal of Biological Physics**, v. 3, n. 4, p. 183–192, 1975.
WANG, B.; LI, Y.; WU, N.; LAN, C. Q. CO2 bio-mitigation using microalgae. **Applied Microbiology and Biotechnology**, v. 79, n. 5, p. 707–718, 2008.
WATANABE, S.; HIMIZU, A.; LEWIS, L. A.; FLOYD, G. L.; FUERST, P. A. *Pseudoneochloris marina* (*Chlorophyta*), a new coccoid Ulvophycean alga, and its

phylogenetic position inferred from morphological and molecular data. **Journal of Phycology**, v. 36, n. 3, p. 596–604, 2000.
WU, Z.; DUANGMANEE, P.; ZHAO, P.; MA, C. The effects of light, temperature, and nutrition on growth and pigment accumulation of three *Dunaliella salina* strains isolated from saline soil. **Jundishapur Journal of Microbiology**, v. 9, n. 1, p. 1–9, 2016.
XU, Y.; ISOM, L.; HANNA, M. A. Adding value to carbon dioxide from ethanol fermentations. **Bioresource Technology**, v. 101, n. 10, p. 3311–3319, 2010. Disponível em: <http://dx.doi.org/10.1016/j.biortech.2010.01.006>.
YANG, H.; XU, Z.; FAN, M.; GUPTA, R.; SLIMANE, R. B.; BLAND, A. E.; WRIGHT, I. Progress in carbon dioxide separation and capture: A review. **Journal of Environmental Sciences**, v. 20, p. 14–27, 2008.
YE, Z. W.; JIANG, J. G.; WU, G. H. Biosynthesis and regulation of carotenoids in *Dunaliella*: Progresses and prospects. **Biotechnology Advances**, v. 26, n. 4, p. 352–360, 2008.
YEN, H.; HSU, C.; CHEN, P. An integrated system of autotrophic Chlorella vulgaris cultivation using CO2 from the aerobic cultivation process of *Rhodotorula glutinis*. **Journal of the Taiwan Institute of Chemical Engineers**, v. 62, p. 158–161, 2016. Disponível em: <http://dx.doi.org/10.1016/j.jtice.2016.01.025>.
ZENG, X.; DANQUAH, M. K.; CHEN, X. D.; LU, Y. Microalgae bioengineering: From CO_2 fixation to biofuel production. **Renewable and Sustainable Energy Reviews**, v. 15, n. 6, p. 3252–3260, 2011.
ZHANG, X.-W.; SHI, X.-M.; CHEN, F. A kinetic model for lutein production by the green microalga Chlorella protothecoides in heterotrophic culture. **Journal of Industrial Microbiology & Biotechnology**, v. 23, p. 503–507, 1999.
ZHOU, W.; WANG, J.; CHEN, P.; JI, C.; KANG, Q.; LU, B.; LI, K.; LIU, J.; RUAN, R. Bio-mitigation of carbon dioxide using microalgal systems: Advances and perspectives. **Renewable and Sustainable Energy Reviews**, v. 76, n. March, p. 1163–1175, 2017.
ZHU, L. D.; LI, Z. H.; HILTUNEN, E. Strategies for Lipid Production Improvement in Microalgae as a Biodiesel Feedstock. **BioMed Research International**, v. 2016, p. 7–9, 2016.